AD 714482
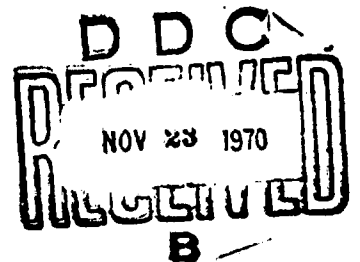
Spectrum of a Signal Reflected from a Time-Varying Random Surface

ALBERT H. NUTTALL
Office of the Associate Technical Director for Research

BENJAMIN F. CRON
Ocean Sciences Division

DDC

NOV 23 1970

RECEIVED

B

25 August 1970

NAVAL UNDERWATER SYSTEMS CENTER

New London Laboratory

113

REVIEWED AND APPROVED: 25 August 1970

W. A. Von Winkle

W. A. Von Winkle
Associate Technical Director
for Research
New London Laboratory

Correspondence concerning this report should be addressed as follows:

Officer in Charge
New London Laboratory
Naval Underwater Systems Center
New London, Connecticut 06320

ABSTRACT

The power density spectrum of the received acoustic waveform after reflection off the time-varying random sea surface is evaluated at an arbitrary observation point in the farfield. For a monochromatic transmitted signal and a narrow-band Gaussian surface-height variation, the received acoustic spectrum is shown to consist of an impulse at the transmitted acoustic frequency plus sidelobes centered at frequencies separated from the transmitted frequency by multiples of the surface center frequency. The powers in the coherent component and scattered sideband components of the received pressure waveform are evaluated in terms of the surface roughness and spatial-temporal correlation function of the surface. For the special case of elliptical contours of iso-correlation at zero time delay, the sideband powers and scattering strengths are evaluated in terms of two fundamental parameters that include the geometry of the experiment, the incident acoustic frequency, the root mean square (rms) surface height, and the surface correlation distances.

The rms bandwidths of the sideband scatter components are evaluated for small surface roughness and shown to be approximately proportional to the square root of the sideband number. Numerous examples of sideband scattering strengths for a variety of spatial correlation functions, including exponential and Gaussian decay as special cases, are given.

ADMINISTRATIVE INFORMATION

TABLE OF CONTENTS

TABLE OF CONTENTS (Cont'd)

LIST OF TABLES

LIST OF ILLUSTRATIONS

LIST OF ILLUSTRATIONS (Cont'd)

GLOSSARY[*]

Q	Location of acoustic source
A	Location of observation point
O	Origin of coordinates
R_o	Distance from origin to observation point
$\vec{u}_Q, \vec{u}_A$	Unit vectors from origin in direction of source and receiver, respectively
$\vec{i}, \vec{j}, \vec{k}$	Unit vectors in x,y,z directions, respectively
a_Q, b_Q, c_Q	Direction cosines of source
a_A, b_A, c_A	Direction cosines of receiver
a, b, c	Sums of direction cosines
t	Time
x, y	Position
$\zeta(x,y,t)$	Surface height at position x,y at time t
f	Frequency
f_a	Acoustic frequency
$p(t)$	Received pressure waveform
λ_a	Acoustic wavelength
k_a	Acoustic wave number
B	Geometric scale factor (See Appendix A)
$P_i(x,y)$	Incident pressure field
$s(t)$	General transmitted signal pressure waveform
$S(f)$	Voltage density spectrum of s(t)
$r(t)$	Received pressure waveform
v	Propagation velocity
$H(f_a; t)$	Instantaneous transfer function of surface
$p_c(t)$	Coherent component of received presure waveform
f_ζ	Characteristic function of surface
q_1, q_2	Probability density functions of surface heights
F	Auxiliary function, Eq. (9)
$p_s(t)$	Scatter component of received pressure waveform
J	Autocorrelation function of incident illumination
S	Scattering strength
h, θ	Amplitude and phase of surface-height variation
f_s	Center frequency of surface-height variation
m	Order of sideband
A_m	Complex amplitude of mth sideband component
σ^2	Mean square surface height
R_p	Correlation function of received pressure
R_s	Correlation function of scatter pressure

[*]In order of appearance.

GLOSSARY (Cont'd)

ρ	Normalized spatial-temporal correlation function of surface
β	Surface roughness parameter, Eq. (42)
G_s	Spectrum of scatter component
$\underline{\rho}$	Complex envelope of ρ
ζ_{kl}	Kronecker delta ($= 1$ if $k = 1$; 0 otherwise)
T_m	Spectral shape of mth sideband
S_m	Scattering strength of mth sideband
ρ_1	Special form of spatial-temporal correlation, Eq. (52)
L_x, L_y, L	Correlation distances
ρ_2	Auxiliary function, Eq. (54)
a	Surface correlation parameter, Eq. (58)
U_m	Auxiliary function proportional to scattering strength in specular direction, Eq. (60)
V_m	Auxiliary function proportional to scattering strength in nonspecular directions, Eq. (62)
$\underline{g}$	Low-pass spectrum (See Appendix D)
B_s	Rms bandwidth of surface-height spectrum.
B_m	Rms bandwidth of mth sideband
$\hat{A}^2$	Directional wave spectrum
g	Acceleration of gravity
A^2	Directional wave spectrum (polar form)
Φ	Surface-height spectrum
A_2^2	Special form of directional wave spectrum, Eq. (87)
R, Q	Parameters of the spatial correlation decay (See Section 4.3)
$\hat{\Phi}$	Dimensionless auxiliary function proportional to surface-height spectrum, Eq. (96)
x	Dimensionless parameter proportional to frequency, Eq. (97)
$x(t)$	Stationary single-sided process (See Appendix B)
$x_r(t), x_i(t)$	Real and imaginary parts of $x(t)$, respectively
$\mathcal{H}$	Hilbert transform
I_s	Average scatter intensity (See Appendix C)
Ω	Solid angle of receiver
σ_s	Scattering coefficient or scattering cross section (See Appendix C)
I_{scat}	Average scatter intensity
$I_{.nc}$	Average incident intensity
A_{eff}	Effective area of insonification
$g(u, v, f)$	Normalized cross-spectrum (See Appendix D)
g_+, ρ_+	Auxiliary single-sided functions (See Appendix D)
ρ_H	Hilbert transform of ρ
q	Auxiliary variable ($= Q/R$; see Appendix E)
L	Limit of integration (See Appendix F)
E	Error of integration (See Appendix F)

x

GLOSSARY (Cont'd)

overbar	Ensemble average
*	Conjugate
rms	Root mean square

SPECTRUM OF A SIGNAL REFLECTED FROM A TIME-VARYING RANDOM SURFACE

1. INTRODUCTION

The purpose of this study is to determine the spectrum of an acoustic signal reflected from a time-varying random surface. Of the many scientists who have investigated scattering from such a surface, we will mention only a few. Rayleigh considered a sinusoidal fixed surface and solved for the reflected pressure for a given incident monochromatic wave. Eckart's classic work [1] on scattering from a random surface employed the Kirchoff method; i.e., he assumed that the surface could be represented by the tangent plane to the surface at each point of incidence. Starting with the Helmholtz equation, Beckmann and Spizzichino [2] also used the Kirchoff approximation, but, in their derivation, they differentiated with respect to the normal to the surface instead of the vertical axis, and used an integration by parts to eliminate edge effects. Thus, they obtained a different geometric factor from that of Eckart [1] for the reflected pressure. LaCasce and Tamarkin [3] performed experimental studies on the reflection off a fixed sinusoidal pressure-release surface. Horton and Muir [4] also performed experimental studies on the scattering from a rough random surface, compared their results with a modified version of the Eckart theory, and found good agreement. Wagner [5] considered a Gaussian surface, and using the parameters of root-mean-square (rms) height and correlation of surface heights, and treating the incident waves as rays, determined the amount of shadowing as a function of the grazing angle of the incident acoustic wave. From these results, a correction value for the shadowing effect was made by Wagner [5] to the Eckart [1] and Beckmann and Spizzichino [2] theories. Marsh [6] also utilized the Rayleigh method and considered the signal reflected from a random surface to consist of an infinite set of plane waves. By applying boundary conditions on the surface, he solved for the scattering coefficient of the surface reflection.

The number of investigations of a time-varying random surface is considerably less than that of a fixed surface. Of these, we will mention

only the works of Roderick and Cron [7] and Parkins [8]. Roderick and Cron considered a sinusoidal traveling surface wave, where, for a single-frequency incident acoustic wave, the frequency of the reflection in the specular direction is the same as the incident frequency, and the frequencies in the nonspecular directions are equal to the incident frequency plus multiples of the surface frequency. They compared the theoretical predictions of the amplitudes of these components with experiment. Parkins considered a time-varying random surface, a joint Gaussian distribution of heights, and a Neumann-Pierson surface-height spectrum. For both small and large surface roughness, he obtained the scattered acoustic spectrum.

In our work, we start with the assumptions used by others:

● the Kirchoff method [2, p. 20] — the method of physical optics — is used,

● the insonified area is in the farfield (Fraunhofer region) of the source,

● the observation point is in the farfield of the insonified area,

● the surface is pressure-release,

● no shadowing or multiple reflections occur,

● a directional source is used, and

● the surface particle velocity is small compared with the speed of sound.

Starting with the Helmholtz integral and a given incident single-frequency acoustic source, we obtain the (complex) pressure at the observation point. The surface height is designated a function of position x, y, and time t; the first- and second-order probability distributions of height are assumed independent of absolute position and time and dependent only on the differences in the x and y coordinates and time. That is, the surface is assumed homogeneous and stationary. The autocorrelation function of the received acoustic complex pressure is obtained by using these properties. The Fourier transform of the autocorrelation function then yields the received acoustic power spectrum.

2

The equation for the power spectrum is then specialized to the case of a joint Gaussian distribution of surface heights and a narrow-band, surface-height spectrum at a point; for this case, the spatial-temporal correlation function of the surface can be represented as a sinusoidal oscillation in time-delay with a slowly varying amplitude and phase. It is then assumed that the iso-values of the surface-correlation function is an ellipse; for this case, it is shown that the received acoustic spectrum consists of a series of spectral lobes or sidebands, each separated from the incident acoustic frequency by multiples of the center frequency of the surface variation, plus an impulse at the incident acoustic frequency. The relative powers in these sideband components are evaluated in terms of two fundamental parameters: the first is the surface-roughness parameter, and the second is related to the correlation distances of the surface (the horizontal separation for which the surface correlation falls to e^{-1} of its origin value). The powers in the sidebands are numerically evaluated and plotted versus these two parameters, for both specular and nonspecular directions, for a variety of spatial correlation functions, including exponential and Gaussian decay as special cases.

2. REFLECTION FROM A GENERAL TIME-VARYING SURFACE

2.1 RECEIVED PRESSURE WAVEFORM REFLECTED FROM A TIME-VARYING SURFACE

The geometry of the scattering experiment is depicted in Fig. 1.
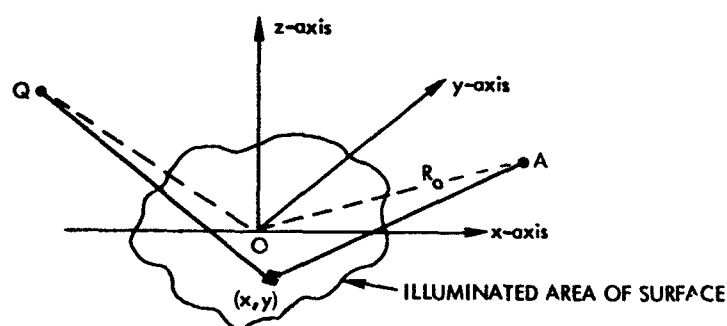
Fig. 1 - Scattering Geometry

The source of acoustic radiation is at Q, and the observation point is at A. The symbol O is an origin of coordinates. Let the unit vectors in the x, y, z directions be $\vec{i}, \vec{j}, \vec{k}$, respectively, and let $\vec{u}_Q$ and $\vec{u}_A$ be unit vectors from O in the directions of source Q and receiver A, respectively. Then,

$$
\begin{aligned}
\vec{u}_Q &= a_Q \vec{i} + b_Q \vec{j} + c_Q \vec{k} \quad, \\
\vec{u}_A &= a_A \vec{i} + b_A \vec{j} + c_A \vec{k} \quad,
\end{aligned}
\tag{1}
$$

where (a_Q, b_Q, c_Q) and (a_A, b_A, c_A) are the direction cosines of the source and receiver, respectively.

Let the sums of direction cosines be denoted by

$$
\begin{aligned}
a &= a_Q + a_A \quad, \\
b &= b_Q + b_A \quad, \\
c &= c_Q + c_A \quad.
\end{aligned}
\tag{2}
$$

The specular direction corresponds to $a = b = 0$; i.e., $a_A = -a_Q$, $b_A = -b_Q$, and $c_A = c_Q$. It is the direction in which all the reflected energy would occur for a mirror-like surface.

The height of the reflecting surface at position x, y fluctuates with time and is denoted by $\zeta(x, y, t)$. The average surface height corresponds to $\zeta = 0$. Under the assumptions given in Section 1, the (complex) received pressure at A, for a single-frequency excitation $\exp(i2\pi f_a t)$ at Q, is given by [8, Eqs. (1) and (10)[1]; 1, Eqs. (1) and (6)[2]; 4, Eq. (9); 9, Eqs. (6.9) and (6.24)]

$$
p(t) = -i \exp[i(2\pi f_a t - k_a R_o)] \frac{B}{\lambda_a R_o} \iint dx\, dy\, \hat{p}_i(x, y) \cdot
$$
$$
\exp[i k_a (ax + by + c\zeta(x, y, t))] \quad,
\tag{3}
$$

where[3]

      f_a = acoustic frequency,

      λ_a = acoustic wavelength,

---

[1]The factor ϕ^+ is missing in (10) of Ref. 8.

[2]The exponent inside the integral in (6) of Ref. 1 should be negative; see also Ref. 4, footnote 6.

[3]Strictly, the argument t in ζ should be replaced by the retarded time taken by a signal to travel from a reflecting point (x,y) to A. However, for a slowly fluctuating surface that does not change much in the time taken for sound to propagate across the illuminated region, a good approximation is $t - R_o/v$, where v is the propagation velocity. The delay R_o/v has been dropped in ζ in (3) for notational simplicity. Also integrals without limits are over the range of nonzero integrand.

4

k_a = acoustic wave number $(2\pi/\lambda_a)$,

R_o – distance from origin O to observation point A,

$\hat{p}_i(x,y)$ – spatially dependent component of the incident pressure field on the reflecting surface (without the phase factor due to propagation over the distance from Q to O), and

B – real scale factor depending only on the geometry of the experiment.(See Appendix A for further details on this factor.)

(Since some authors assume an excitation of the form $\exp(i2\pi f_a t)$, differences in sign with (3) will occur in those references).

For a general signal s(t) transmitted, with voltage density spectrum S(f), the received pressure waveform r(t) is given by

$$r(t) = \int df_a \, p(t; f_a) \, S(f_a)$$

$$= \int df_a \, \exp(i2\pi f_a t) \, H(f_a; t) \, S(f_a) \quad , \tag{4a}$$

where

$$H(f_a; t) \equiv -i \, \exp(-i k_a R_o) \, \frac{B}{\lambda_a R_o} \iint dx \, dy \, \hat{p}_i(x \, y) \cdot$$

$$\exp[i k_a (ax + by + c \, \zeta(x, y, t))] \quad . \tag{4b}$$

We have indicated explicitly the dependence of received pressure p on acoustic frequency f_a ($\hat{p}_i$ is also dependent on f_a) and used (3). The representation in (4a) shows that the surface can be viewed as a linear time-varying filter on transmitted acoustic waveforms with instantaneous transfer function $H(f_a; t)$ given by (4b).

For a real sinusoidal acoustic signal transmitted,

$$s(t) = \cos(2\pi f_a t) = \text{Re}\{\exp(i2\pi f_a t)\} \quad , \tag{5}$$

the real received pressure is given by $\text{Re}\{p(t)\}$. The power in the real received signals is

$$\overline{\text{Re}^2\{p(t)\}} = \frac{1}{4}\overline{[p(t) + p^*(t)]^2} = \frac{1}{2}\overline{|p(t)|^2} \quad , \tag{6}$$

where we have used the fact that $\overline{p^2(t)} = 0$; this follows from (3) upon noting that if ζ is stationary, then p(t) is stationary, narrow-band, and centered around frequency f_a and has its spectral content confined to positive frequencies. (See Appendix B.) Under the reasonable assumption that surface height $\zeta(x, y, t)$ varies slowly with time, as compared with $\exp(i2\pi f_a t)$,[4] p(t) is narrowband. Thus, attention can be focused on

---

[4] For example, surface-height variations typically have spectral content in the neighborhood of fractions of Hertz, whereas acoustic frequencies are of the order of tens of Hertz (and greater).

complex pressure p(t) and appropriate real parts or factors of 1/2 applied later when necessary.

2.2 COHERENT AND SCATTER COMPONENTS FOR A RANDOM SURFACE

The received pressure for a single-frequency excitation is given by (3). The coherent component [2, Section 7.3] of this waveform is defined as its mean value (ensemble average over all possible surface states):

$$p_c(t) \equiv \overline{p(t)} = -i \exp[i(2\pi f_a t - k_a R_o)] \frac{B}{\lambda_a R_o} \iint dx\, dy\, \hat{p}_i(x,y) \cdot$$
$$\exp[ik_a(ax + by)]\, f_\zeta(k_a c) \quad , \tag{7}$$

where

$$f_\zeta(k_a c) \equiv \overline{\exp[ik_a c\, \zeta(x,y,t)]}$$
$$= \int d\zeta \exp(ik_a c\zeta)\, q_1(\zeta) \tag{8}$$

is the first-order characteristic function (CF) of the surface wave height. Since we are assuming a homogeneous stationary surface, q_1 is the first-order probability density function (PDF) of the surface wave height and is independent of absolute position x, y and time t. The first-order CF contains all first-order statistical information about the surface wave-height variation since it is a Fourier transform of the first-order PDF.

If we define the double integral in (7) as P,

$$\iint dx\, dy\, \hat{p}_i(x,y) \exp[ik_a(ax + by)] = P(k_a a, k_a b) \quad , \tag{9}$$

the coherent component is given by

$$p_c(t) = -i \exp[i(2\pi f_a t - k_a R_o)] \frac{B}{\lambda_a R_o} P(k_a a, k_a b)\, f_\zeta(k_a c) \quad \tag{10}$$

This is a general relation for the received coherent component of pressure for any surface statistics, degree of roughness, and observation point.

Since the effective extents of the incident illumination on the surface are much larger than the acoustic wavelength, P takes on appreciable values only when $a \cong 0$, $b \cong 0$, which corresponds to the specular direction. (This follows upon noting that P in (9) is a double Fourier transform of the incident pressure $\hat{p}_i$.) Therefore, the coherent component is appreciable only near the specular direction.

6

For a perfectly smooth surface, $\zeta = 0$, and the first-order CF equals unity. As the surface roughness increases, the magnitude of the CF decreases, thereby causing the amplitude of the coherent component to decrease. The coherent component is not identically zero for a rough surface; however, it is negligible for a very rough surface.

From (10), since the only dependence of $p_c(t)$ on time is via the term $\exp(i2\pi f_a t)$, the spectrum of the coherent component must be an impulse at frequency f_a, just like the transmitted signal spectrum. However, the amplitude and phase shift of the coherent component depend on the physical locations of the transmission and observation points and the degree of surface roughness.

The scatter component of the received pressure is defined as the remainder

$$p_s(t) \equiv p(t) - p_c(t) = p(t) - \overline{p(t)} \quad , \tag{11}$$

which has zero mean. In order to evaluate the mean-square value[5] of the scatter component, we note that

$$\overline{|p_s(t)|^2} = \overline{|p(t)|^2} - \overline{|p_c(t)|^2} = \overline{|p(t)|^2} - \left|\overline{p(t)}\right|^2 \quad . \tag{12}$$

That is, the mean square value of the scatter component p_s is equal to the mean square value of the total received pressure p less the squared magnitude of the coherent component p_c. Using (3), we obtain

$$\overline{|p(t)|^2} = \left(\frac{B}{\lambda_a R_o}\right)^2 \iiiint dx_1\, dy_1\, dx_2\, dy_2\, \hat{p}_i(x_1, y_1)\, \hat{p}_i^*(x_2, y_2) \cdot \tag{13}$$

$$\exp[ik_a a(x_1 - x_2) + ik_a b(y_1 - y_2)]\, f_\zeta(k_a c, -k_a c; x_1 - x_2, y_1 - y_2, 0) \quad ,$$

where

$$f_\zeta(k_a c, -k_a c; u, v, \tau) = \overline{\exp[ik_a c\zeta(x, y, t) - ik_a c\zeta(x-u, y-v, t-\tau)]}$$

$$= \iint d\zeta_1\, d\zeta_2\, \exp(ik_a c\zeta_1 - ik_a c\zeta_2)\, q_2(\zeta_1, \zeta_2; u, v, \tau) \tag{14}$$

is the second-order CF of the surface wave heights. Since the surface is homogeneous and stationary, q_2 is the second-order PDF of surface wave heights and depends only on differences in position and time. If we let $u = x_1 - x_2$, $v = y_1 - y_2$ in (13), there follows

$$\overline{|p(t)|^2} = \left(\frac{B}{\lambda_a R_o}\right)^2 \iint du\, dv\, J(u, v)\, \exp[ik_a(au + bv)]\, f_\zeta(k_a c, -k_a c; u, v, 0) \quad , \tag{15}$$

---

[5] Mean magnitude-squared value, more precisely.

where J is the autocorrelation of the illumination $\hat{p}_i$ incident on the surface:

$$J(u,v) = \iint dx\,dy\, \hat{p}_i(x,y)\, \hat{p}_i^*(x-u, y-v) \quad . \tag{16}$$

Before forming $\overline{|p_s(t)|^2}$ from (12), we first note from (9) that we can express

$$|P(k_a a, k_a b)|^2 = \iint du\,dv\, J(u,v)\, \exp[i k_a(au+bv)] \quad . \tag{17}$$

Therefore, using (12), (15), (10), and (17), we obtain

$$\overline{|P_s(t)|^2} = \overline{|p(t)|^2} - |P_c(t)|^2$$

$$= \left(\frac{B}{\lambda_a R_o}\right)^2 \iint du\,dv\, J(u,v)\, \exp[i k_a(au+bv)] \cdot \tag{18}$$

$$\left[f_\zeta(k_a c, -k_a c; u, v, 0) - |f_\zeta(k_a c)|^2 \right] .$$

This is a general relation for the mean-square value of the received scatter component in terms of the autocorrelation function J of the incident pressure $\hat{p}_i$ on the reflecting surface and on the first- and second-order CF's of the surface-height variations ζ. No assumptions about the degree of surface roughness have been made.

We will now make the reasonable assumption that the effective extents on the surface of the incident illumination $\hat{p}_i$ are much larger than the distances at which the surface heights are statistically dependent on each other. Mathematically, this is equivalent to assuming that the bracketed difference of CF's in (18) decays to zero in u and v much sooner than $J(u,v)$ does. (The difference in CF's goes to zero as $|u|, |v| \to \infty$ because then

$$f_\zeta(k_a c, -k_a c; u, v, \tau) \longrightarrow |f_\zeta(k_a c)|^2 .) \tag{19}$$

The double integral in (18) then is virtually unchanged if $J(u,v)$ is replaced by its origin value, yielding

$$\overline{|p_s(t)|^2} = \left(\frac{B}{\lambda_a R_o}\right)^2 J(0,0) \iint du\,dv\, \exp[i k_a(au+bv)] \cdot \tag{20}$$

$$[f_\zeta(k_a c, -k_a c; u, v, 0) - |f_\zeta(k_a c)|^2] \quad .$$

This double Fourier transform on space variables u and v is as far as the analysis can be carried without further assumptions on wave-height statistics. The surface statistics needed in these quantitative measures of the coherent and scattered components are contained entirely

in the first- and second-order surface height CF's. Arbitrary surface roughness is allowed.

As the surface roughness decreases, the difference in CF's in (18) and (19) goes to zero (because $\zeta \to 0$). In this case, the scattered component disappears, as indeed it must for a smooth surface.

In Appendix C, the scattering strength[6] S of the surface, defined as the ratio

$$\frac{\text{average scattered intensity at receiver due to unit scattering area, referred to unit distance}}{\text{average incident intensity on surface}} , \tag{21}$$

is shown to be given by

$$S = \frac{\overline{|P_s(t)|^2} \ R_o^2}{c_Q J(0,0)}. \tag{22}$$

If we substitute (20) into (22), the above equation becomes

$$S = \frac{B^2}{c_Q} \frac{1}{\lambda_a^2} \iint du\, dv\, \exp[i k_a (au + bv)] \cdot$$
$$[f_\zeta(k_a c, -k_a c; u, v, 0) - |f_\zeta(k_a c)|^2] \ . \tag{23}$$

This is a dimensionless quantity. The dimensionless factor B^2/c_Q depends solely on the geometry of the experiment.

For a surface of very slight roughness, i.e.,

$$k_a c \max|\zeta(x, y, t)| \ll 1 \ , \tag{24}$$

we can approximate the exponential in (3) as

$$\exp[i k_a c\ \zeta(x, y, t)] \cong 1 + i k_a c\ \zeta(x, y, t) \ . \tag{25}$$

Then, (3) becomes

$$p(t) \cong -i \exp[i(2\pi f_a t - k_a R_o)] \frac{B}{\lambda_a R_o} [P(k_a a, k_a b)$$
$$+ i k_a c \iint dx\, dy\, \hat{p}_i(x, y) \exp[i k_a (ax + by)]\ \zeta(x, y, t)] \ . \tag{26}$$

---

[6]The term "scattering strength" is used in this report as an intensity ratio and is not converted to decibels.

The first term of (26) is the coherent component, and the second term of (26) is the scatter component. This equation for the coherent component is a special case of (10), where CF $f_\zeta(k_a c)$ is approximately unity. Thus, the general results (10) and (18) can be reduced to special cases, including very slight roughness (or very rough surfaces), as desired, by appropriate choice of CF's. Also (23) is a general relation for the scattering strength, which is applicable to any degree of roughness and surface statistics.

3. REFLECTION FROM A NARROW-BAND, TIME-VARYING SURFACE

In this section, we restrict consideration to the case where the surface-height variation at each point of space is a narrow-band function of time [10, pp. 347-348 and Section 8.5]; this is the case, for example, when the sea surface is characterized as swell [10, Section 1.2].

3.1 NARROW-BAND COMPONENTS OF RECEIVED PRESSURE WAVEFORM

The surface height for this case of narrow-band variation can be represented as

$$\zeta(x, y, t) = h(x, y, t) \cos[2\pi f_s t + \theta(x, y, t)] \quad , \tag{27}$$

where, for fixed position x, y, the amplitude h and phase θ vary slowly with time t in comparison with $\cos(2\pi f_s t)$. The center frequency of the surface-height variation is f_s. If we substitute (27) into (3) for the received pressure and use the expansion [11, 8.5114]

$$\exp[ik_a c\, h\, \cos(2\pi f_s t + \theta)]$$
$$= \sum_{m=-\infty}^{\infty} i^m J_m(k_a ch) \exp[im(2\pi f_s t + \theta)] \quad , \tag{28}$$

the received pressure can be represented as

$$p(t) = \sum_{m=-\infty}^{\infty} A_m(t) \exp[i2\pi(f_a + mf_s)t] \quad , \tag{29}$$

where

$$A_m(t) \equiv -i \exp(-ik_a R_o) \frac{B}{\lambda_a R_o} i^m \iint dx\, dy\, \hat{p}_i(x, y) J_m[k_a ch(x, y, t)] \cdot \tag{30}$$

$$\exp[ik_a(ax + by) + im\, \theta(x, y, t)] \quad .$$

10

Since h and θ vary slowly with time, so also does $A_m(t)$. However, if $k_a ch_{max} \gg 1$ or $m \gg 1$, the rate of variation of $A_m(t)$ is much faster than that of h or θ. This may be seen by noting that Bessel function $J_m(x)$ is an oscillatory function of x; thus, $J_m[k_a ch]$ can go through many cycles of variation while h goes through but one, if $k_a ch_{max} \gg 1$. Also, if $m \gg 1$, $\exp(im\theta)$ varies much faster than θ. The upshot is that $A_m(t)$ of (30) will contain a considerably higher frequency content than either h or θ if either of the above conditions are satisfied.

Equation (29) expresses the received pressure waveform as a sum of narrow-band components (if $k_a ch_{max}$ and m are not much larger than unity), with the mth component being centered at frequency $f_a + mf_s$. That is, the received pressure has spectral lobes displaced from the transmitted acoustic frequency f_a by multiples of the surface center frequency f_s. In addition, there is the coherent component at f_a. This behavior is depicted in Fig. 2.
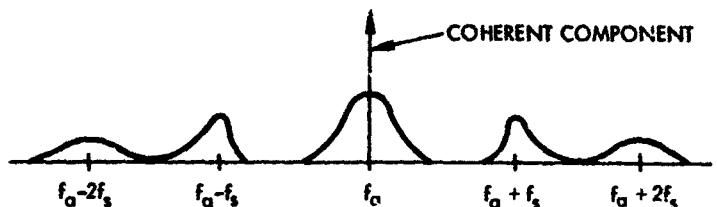
Fig. 2 - Received Acoustic Spectrum

As a special case of (30), consider a traveling sinusoidal surface of fixed amplitude:

$$h(x, y, t) = h ,$$
$$\theta(x, y, t) = c_1 x + c_2 y + c_3 . \tag{31}$$

c_1 and c_2 are related to the direction of travel of the surface wave and its velocity of propagation, and c_3 is the phase at $x = y = 0$. Then, using (9), (30) becomes

$$A_m(t) = -i \exp(-ik_a R_o) \frac{B}{\lambda_a R_o} i^m J_m(k_a ch) \exp(imc_3) P(k_a a + mc_1, k_a b + mc_2) , \tag{32}$$

which is independent of time. This case has been investigated previously [7, Appendix].

11

Now if the surface is actually random, the quantities h and c_3, above, could be considered as random variables, with the PDF for c_3 uniform over a 2π interval. In this case, the mean (ensemble average) of the mth complex amplitude $A_m(t)$ in (32) is zero for $m \neq 0$; thus, there are no coherent components in any of the sidebands. For $m = 0$, an assumption on the PDF of h is necessary to evaluate the ensemble average[7] $\overline{J_m(k_a ch)}$. For example, for a Rayleigh PDF of surface heights,

$$\frac{h}{\sigma^2} \exp\left(-\frac{h^2}{2\sigma^2}\right), \ h > 0 \ . \tag{33}$$

where σ is the rms wave height, the mean value of $A_0(t)$ $[11, 6.631\ 4]$ is

$$\overline{A_0(t)} = -i \exp(-i k_a R_0) \frac{B}{\lambda_a R_o} P(k_a a, k_a b) \exp(-\tfrac{1}{2} k_a^2 c^2 \sigma^2) \ . \tag{34}$$

However, (34) coupled with (29) is seen to be but a special case of (10) when ζ is first-order Gaussian:

$$f_\zeta(k_a c) = \exp(-\tfrac{1}{2} k_a^2 c^2 \sigma^2) \ . \tag{35}$$

Thus, the approach given in Subsection 2.2 is a very powerful one for evaluating the coherent component, and includes numerous special cases. Nevertheless, (29) and (30) are useful for lending insight into the spectral behavior of the received pressure waveform for a narrow-band, surface-height variation. They could be used as the starting point for the theory to be developed in the next subsection, but a more compact approach has been utilized there.

3.2 SPECTRA AND POWER OF INDIVIDUAL NARROW-BAND COMPONENTS

The received pressure waveform $p(t)$ was given in (3) and the coherent component (the mean of the received pressure) in (10). We now wish to evaluate the correlation function of p, and then the spectrum, for a narrow-band, surface-height variation. The correlation function R_p of p is, by a simple generalization of (13) through (15),

$$R_p(\tau) = \overline{p(t)\, p^*(t-\tau)}$$
$$= \left(\frac{B}{\lambda_a R_o}\right)^2 \exp(i 2\pi f_a \tau) \iint du\, dv\, J(u, v) \exp[i k_a (au + bv)] f_\zeta(k_a c, -k_a c; u, v, \tau)$$

[7] Since the surface process and, therefore, the received acoustic process are not ergodic in this case, this average is not equal to the time average over individual member functions.

$$\overline{= \overline{p(t)} \ \overline{p^*(t-\tau)}} + \left(\frac{B}{\lambda_a R_o}\right)^2 \exp(i2\pi f_a \tau) \iint du\, dv\, J(u,v)\, \exp[ik_a(au+bv)] \cdot$$

$$[f_\zeta(k_a c, -k_a c; u, v, \tau) - |f_\zeta(k_a c)|^2] \quad , \tag{36}$$

where we have used (10) and (17). We define the covariance function of p as the correlation function of the ac component (i. e., scatter component) of p:

$$R_s(\tau) = \overline{p_s(t) \, p_s^*(t-\tau)}$$

$$= \overline{[p(t) - \overline{p(t)}] [p^*(t-\tau) - \overline{p^*(t-\tau)}]}$$

$$= \left(\frac{B}{\lambda_a R_o}\right)^2 \exp(i2\pi f_a \tau) \iint du\, dv\, J(u,v)\, \exp[ik_a(au+bv)] \cdot \tag{37}$$

$$[f_\zeta(k_a c, -k_a c; u, v, \tau) - |f_\zeta(k_a c)|^2] \quad .$$

Equation (37), a general relation for the correlation function of the scatter component, reduces to the mean-square pressure of (18) for $\tau = 0$.

Again we make the assumption that the effective extents on the surface of the incident illumination $\hat{p}_i$ are much larger than the distances at which the surface heights are statistically dependent on each other, and get the approximation (See (18) through (20)) for the correlation of the scatter component:

$$R_s(\tau) = \left(\frac{B}{\lambda_a R_o}\right)^2 \exp(i2\pi f_a \tau)\, J(0,0) \iint du\, dv\, \exp[ik_a(au+bv)] \cdot \tag{38}$$
$$[f_\zeta(k_a c, -k_a c; u, v, \tau) - |f_\zeta(k_a c)|^2] \quad .$$

At this point, we make an assumption about the statistics of the surface heights, namely, that the second-order PDF of surface heights is joint Gaussian [10, pp. 343-345]. Then [12, Eq. (8-23)],

$$f_\zeta(k_a c, -k_a c; u, v, \tau) = \exp[-k_a^2 c^2 \sigma^2 \{1 - \rho(u,v,\tau)\}] \quad , \tag{39}$$

where σ is the rms wave height and ρ is the normalized spatial-temporal correlation function of surface heights, assumed homogeneous and stationary:

$$\sigma^2 \rho(u, v, \tau) = \overline{\zeta(x, y, t)\, \zeta(x-u, y-v, t-\tau)} \quad . \tag{ }$$

If we substitute (39) into (38) and use (19), there follows for the correlation function of the scatter component

$$R_s(\tau) = \left(\frac{B}{\lambda_a R_c}\right)^2 \exp(i2\pi f_a \tau) \, J(0,0) \, \exp(-\beta^2) \iint du \, dv \, \exp[i k_a (au + bv)] \cdot$$

$$[\exp\{\beta^2 \rho(u, v, \tau)\} - 1] \quad , \tag{41}$$

where we have defined the surface roughness parameter [2, p. 82, Eq. (10)]

$$\beta = k_a c \sigma \quad . \tag{42}$$

The mean-square value of the scatter component for the Gaussian surface is given by substituting $\tau = 0$ into (41); then only knowledge about $\rho(u, v, 0)$, the normalized correlation between two separated surface heights at the same instant of time, is required.

Thus far, the surface correlation function $\rho(u, v, \tau)$ has been general. The spectrum G_s of the scatter component is given by the Fourier transform of (41),

$$G_s(f) = \int d\tau \exp(-i2\pi f \tau) \, R_s(\tau) \quad , \tag{43}$$

and generally can be numerically evaluated by a Fast Fourier Transform, (FFT). Thus, the received scatter-pressure spectrum could be evaluated from (41) and (43) for any degree of surface roughness, with no assumptions about narrow-band surface variation and narrow-band components of the received pressure. However, a double integral and an FFT is involved.

The approach taken in this report is to specialize to the case of a narrow-band, surface-height spectrum. Then, ρ takes the form (See Appendix D)

$$\rho(u, v, \tau) = \text{Re} \{ \underline{\rho}(u, v, \tau) \exp(i2\pi f_s \tau) \}$$

$$= |\underline{\rho}(u, v, \tau)| \, \cos[2\pi f_s \tau + \arg\{\underline{\rho}(u, v, \tau)\}] \quad , \tag{44}$$

where $\underline{\rho}(u, v, \tau)$ is the complex envelope of $\rho(u, v, \tau)$, and varies slowly with τ as compared to $\exp(i2\pi f_s \tau)$.

Upon substitution of (44) into (41), and using the expansion [11, 8.511 4 and 8.406 3]

$$\exp(x \cos \phi) = \sum_{m=-\infty}^{\infty} I_m(x) \exp(im\phi) \quad , \tag{45}$$

14

we get

$$R_s(\tau) = \left(\frac{B}{\lambda_a R_o}\right)^2 \exp(i2\pi f_a \tau) \, J(0,0) \, \exp(-\beta^2) \sum_{m=-\infty}^{\infty} \iint du \, dv$$

$$\exp[ik_a(au+bv)]\left[I_m(\beta^2|\varrho(u,v,\tau)|) - \delta_{om}\right]\exp(i2\pi m f_s \tau + i \, m \, \arg\{\varrho(u,v,\tau)\}) \quad , \quad (46)$$

where δ_{om} is the Kronecker delta.

The spectrum of the scatter component is obtained by Fourier transforming (46):

$$G_s(f) = \left(\frac{B}{\lambda_a R_o}\right)^2 J(0,0) \sum_{m=-\infty}^{\infty} T_m(f-f_a-mf_s) \quad , \quad (47)$$

where

$$T_m(f) = \int d\tau \exp(-i2\pi f \tau) \, \exp(-\beta^2) \iint du \, dv \exp[ik_a(au+bv)]$$

$$\left[I_m(\beta^2|\varrho(u,v,\tau)|) - \delta_{om}\right]\exp(i \, m \, \arg\{\varrho(u,v,\tau)\}) \quad . \quad (48)$$

Thus, the scatter spectrum is composed of spectral lobes, or sidebands, centered at frequencies equal to the acoustic frequency f_a plus multiples of the surface center frequency f_s, as anticipated by (29) and (30) and shown in Fig. 2. The mth order sideband is defined as that spectral lobe centered at frequency $f_a + mf_s$. The zeroth order sideband is centered at f_a, but is spread in frequency; it is distinct from the coherent component of the received pressure, which has a delta function at frequency f_a.

For a given surface spatial-temporal correlation function ρ, observation point (a, b, c), and surface roughness β, (48) can be numerically evaluated (by a double integral and FFT) for the spectrum of the mth sideband component of the received scatter pressure. The total power in the mth sideband is obtained by integrating the mth term in (47) over all frequencies, and is denoted by

$$\overline{|P_{sm}(t)|^2} = \left(\frac{B}{\lambda_a R_o}\right)^2 J(0,0) \, \exp(-\beta^2) \iint du \, dv \exp[ik_a(au+bv)]$$

$$\left[I_m(\beta^2|\varrho(u,v,0)|) - \delta_{om}\right]\exp(i \, m \, \arg\{\varrho(u,v,0)\}) \quad . \quad (49)$$

The scattering strength of the mth sideband is defined in a manner similar to (C-12) in Appendix C as

$$S_m = \frac{\overline{|P_{sm}(t)|^2}\, R_o^2}{c_Q\, J(0,0)} = \frac{B^2}{c_Q}\, \frac{1}{\lambda_s^2}\, \exp(-\beta^2) \iint du\, dv\, \exp[i k_s (au + bv)] \cdot$$

$$\left[I_m(\beta^2 |\varrho(u,v,0)|) - \delta_{om} \right] \exp(i m \arg\{\varrho(u,v,0)\}) \quad .$$

(50)

The scattering strength S_m depends on the spatial-temporal correlation function $\varrho(u,v,r)$ at zero time delay ($r = 0$).

3.3 SPECIAL FORM OF SURFACE CORRELATION

Thus far, the spatial-temporal surface correlation function $\rho(v,v,r)$ has been general, except for the narrow-band assumption. We now wish to specialize to a particular form. Note first that if z is purely real, but perhaps negative,

$$I_m(|z|) \exp(i m \arg\{z\}) = I_m(z) \quad .$$

(51)

Now consider that correlation function ρ has the form

$$\rho(u,v,r) = \rho_1 \left(\sqrt{\left(\frac{u}{L_x}\right)^2 + \left(\frac{v}{L_y}\right)^2}, r \right)$$

(52)

That is, for a fixed delay r, contours of iso-correlation values are elliptical.[8] (There is no need to consider a rotated ellipse if the x, y axes are aligned with local surface directional properties.) Distances L_x and L_y are the (correlation) distances in the x and y directions, respectively, at which the correlation is down to a specified fraction (e.g., 1/e) of its peak value.

Several important special cases of surface correlation can be subsumed by (52). For example, if the correlation distances L_x and L_y are equal, the surface is isotropic. However, if one of the correlation distance is infinite, the surface correlation function is one-dimensional; i.e., it depends on only one of the variables u, v. Further specialization of the "one-dimensional" surface-correlation function would be a periodic "one-dimensional" surface-correlation function, and as a particular case of the latter, a sinusoidal surface-correlation

---

[8] See for example, Ref. 13, p. 81, where experimental results of this form have been obtained.

16

function. Thus (52) is particularly useful for detailed investigation because it retains a great deal of generality and is a reasonable approximation to many practical situations.

Using (D-2) and (52), we note that

$$\rho(u, v, -\tau) = \rho(u, v, \tau) \quad . \tag{53}$$

That is, surface correlation ρ is even in τ for any u, v, under assumption (52). Employing (D-15) through (D-17), we have for this case of (52),

$$\rho(u, v, 0) = \rho_1 \left(\sqrt{\left(\frac{u}{L_x}\right)^2 + \left(\frac{v}{L_y}\right)^2}, 0 \right) \equiv \rho_2 \left(\sqrt{\left(\frac{u}{L_x}\right)^2 + \left(\frac{v}{L_y}\right)^2} \right) . \tag{54}$$

If we combine (50), (51), and (54), the mth order scattering strength is

$$S_m = \frac{B^2}{c_Q} \frac{1}{\lambda_a^2} \exp(-\beta^2) \iint du\, dv \exp[i k_a(au + bv)] \cdot$$

$$\left[I_m \left(\beta^2 \rho_2 \left(\sqrt{\left(\frac{u}{L_x}\right)^2 + \left(\frac{v}{L_y}\right)^2} \right) \right) - \delta_{om} \right] . \tag{55}$$

Since $I_{-m}(x) = I_m(x)$, the scattering strengths of the pair of symmetrically located sidebands at $f_a - mf_s$ and $f_a + mf_s$ are equal, under the assumption (52); this is not true for general ρ. When we let

$$u = L_x\, r \cos\theta \quad ,$$
$$v = L_y\, r \sin\theta \quad , \tag{56}$$

in (55) and perform the integration on θ, the scattering strength becomes

$$S_m = \frac{B^2}{c_Q} \frac{L_x L_y}{\lambda_a^2} 2\pi \exp(-\beta^2) \int_0^\infty dr\, r\, J_0(ar) \left[I_m(\beta^2 \rho_2(r)) - \delta_{om} \right] , \tag{57}$$

where

$$a \equiv k_a \sqrt{a^2 L_x^2 + b^2 L_y^2} \quad . \tag{58}$$

Recollect from (42) that

$$\beta = k_a c \sigma \quad . \tag{59a}$$

The fundamental parameters a and β are dimensionless and are basic measures of surface behavior in the horizontal and vertical directions, respectively. The former is related to the correlation distance of the surface, whereas the latter depends on the surface roughness.

The quantity a in (58) can take values in the range from zero to very large values compared with unity. For example, in the specular direction, $a = b = 0$ and $a = 0$. However, for other directions, if the ratio of correlation distance to acoustic wavelength is much larger than unity, a takes on large values. Of course, a can not become arbitrarily large by letting the correlation distances increase, because they have been assumed less than the illuminated extents. (See text following (18).) The quantity β in (59) can take values in the range from zero to values of the order of 10 without violating the conditions stated in the paragraph following (30). Thus, for a smooth surface, $\beta = 0$, whereas, for a rough surface, β can take on very large values. But, in this latter case, the sideband components in Fig. 2 of the received scatter pressure would spread out significantly in frequency and overlap each other. These sidebands can not be separated at the receiver by a filter, and the scattering strength S_m would lose its meaning. It would be necessary to resort to the general case given in (41) and (43) for the received scatter spectrum to find how much power lies in a particular spectral band.

The scatter correlation function for the elliptical spatial correlation case is obtained by substituting (52) into (41):

$$R_s(\tau) = 2\pi L_x L_y \left(\frac{B}{\lambda_a R_o}\right)^2 \exp(i2\pi f_a \tau) \, J(0,0) \exp(-\beta^2) \cdot$$
$$\int_0^\infty dr \, r \, J_0(ar) \, [\exp\{\beta^2 \rho_1(r, \tau)\} - 1] \quad \tag{59b}$$

However, for our purposes in this report, in order to retain physical significance and interpretation for scattering strength S_m, we consider a and β upper-limited to values of the order of 10.

For the specular direction, (57) becomes (See Appendix A)

$$S_m = c_Q (k_a L_x)(k_a L_y) U_m(\beta) \quad , \tag{60}$$

where

$$U_m(\beta) \equiv (2\pi)^{-1} \exp(-\beta^2) \int_0^\infty dr \, r \left[I_m(\beta^2 \rho_2(r)) - \delta_{om}\right] \quad . \tag{61}$$

The function $U_m(\beta)$ in (61) depends on surface roughness β and the form of the spatial correlation function ρ_2. In Section 5, plots of $U_m(\beta)$ versus β for several forms of spatial correlation ρ_2 are given, including exponential and Gaussian spatial correlation and

18

exponential and Gaussian modulation of a sinusoid or Bessel function for the spatial correlation The factor preceding $U_m(\beta)$ in (60) is held constant for these plots; thus, the geometry, acoustic frequency, and correlation distances are considered fixed. Each plot, therefore, measures the dependence of the mth scattering strength S_m on surface roughness β as the rms wave height σ is varied.

For directions other than specular, $\alpha \neq 0$, and a change of variable in (57) yields

$$S_m = \frac{B^2}{c_Q \left(a^2\frac{L_x}{L_y} + b^2\frac{L_y}{L_x}\right)} V_m(\alpha, \beta) \quad , \tag{62}$$

where

$$V_m(\alpha, \beta) \equiv (2\pi)^{-1} \exp(-\beta^2) \int_0^\infty ds\ s\ J_o(s) \left[I_m(\beta^2 \rho_2(s/\alpha)) - \delta_{om}\right] \quad . \tag{63}$$

The function $V_m(\alpha, \beta)$ in (63) depends on α, β, and the form of the spatial correlation function ρ_2. If the factor preceding V_m in (62) is held constant, the geometry and the ratio of correlation distances must be considered fixed. Then, the function V_m measures the dependence of scattering strength on α as the correlation distances L_x and L_y are varied (although their ratio is fixed) and on β as the rms wave height σ is varied. Plots of $V_m(\alpha, \beta)$ versus α and β for several forms of ρ_2 are also presented in Section 5.

For the particular surface correlation function form assumed in (52), the general expression for the correlation function of the received scatter pressure waveform given in (41) takes a special form. It is, using (56),

$$R_s(\tau) = B^2(k_a L_x)(k_a L_y)\frac{J(0,0)}{R_o^2}\exp(i2\pi f_a \tau)(2\pi)^{-1}\exp(-\beta^2)\int_0^\infty dr\ r \quad \cdot$$
$$\tag{64}$$
$$J_o(\alpha r)[\exp\{\beta^2 \rho_1(r,\tau)\} - 1] \quad .$$

Thus, only a single integral need be evaluated in order to obtain the scatter correlation function. The scatter spectrum follows from (43). Arbitrary surface roughness is allowed. The scattering strength for the total scatter power is, using (C-12) and (54),

$$S = \frac{R_s(0) R_o^2}{c_Q J(0,0)} = \frac{B^2}{c_Q} (k_a L_x)(k_a L_y)(2\pi)^{-1} \exp(-\beta^2) \int_0^\infty dr \, r \cdot$$

$$J_o(ar)[\exp\{\beta^2 \rho_2(r)\} - 1] \quad . \tag{65}$$

Again, a single integral must be evaluated for the scattering strength, and arbitrary surface roughness is allowed.

3.4 NARROW-BAND SIDEBAND SPECTRA FOR SMALL ROUGHNESS

The spectrum of the received scatter pressure was represented as a sum of narrow-band lobes in (47) and (48) for general surface roughness β and narrow-band correlation ρ. (See Fig. 2.) For small β, a useful approximation to (48) can be made: first note [11, 8.445] that

$$I_m(x) - \delta_{om} \cong \left\{ \begin{array}{ll} \dfrac{x^2}{4}, & m = 0 \\[2ex] \dfrac{(x/2)^m}{m!}, & m \geq 1 \end{array} \right\} \quad \text{for } x \ll 1 \quad . \tag{66}$$

When we employ this approximation in (48) and use (D-7), there follows

$$T_o(f) \cong \frac{1}{4}\beta^4 \exp(-\beta^2) \iint du \, dv \exp[i k_a(au+bv)] \int dw \, \underline{g}(u, v, w) \, \underline{g}^*(u, v, w-f) \quad ,$$

$$T_1(f) \cong \frac{1}{2}\beta^2 \exp(-\beta^2) \iint du \, dv \exp[i k_a(au+bv)] \, \underline{g}(u, v, f) \quad , \tag{67}$$

$$T_2(f) \cong \frac{1}{8}\beta^4 \exp(-\beta^2) \iint du \, dv \exp[i k_a(au+bv)] \int dw \, \underline{g}(u, v, w) \, \underline{g}(u, v, f-w) \quad .$$

The largest term is $T_1(f)$, which is proportional to β^2 and to the double Fourier transform of the low-pass spectrum $\underline{g}$ of the surface correlation. $T_1(f)$ is not simply proportional to $\underline{g}(0, 0, f)$, the low-pass spectrum at a point of the surface-height variation. $T_o(f)$ is proportional to β^4 and is related to the autocorrelation of the low-pass spectrum $\underline{g}$. $T_2(f)$ is proportional to β^4 and related to the convolution of the low-pass spectrum $\underline{g}$.

For the special case when the spatial-temporal surface correlation function is separable in space and time variables,

20

$$\rho(u, v, \tau) = \rho_3(u, v) \; \rho_4(\tau) \quad , \tag{68}$$

$\underline{g}(u, v. f)$ is also separable,

$$\underline{g}(u, v, f) = \rho_3(u, v) \; \underline{g}_4(f) \quad , \tag{69}$$

and the frequency-dependent terms of (67) are given by

$$\int dw \; \underline{g}_4(w) \; \underline{g}_4^*(w - f) \quad , \tag{70a}$$

$$\underline{g}_4(f) \quad , \tag{70b}$$

$$\int dw \; \underline{g}_4(w) \; \underline{g}_4(f - w) \quad , \tag{70c}$$

respectively. Since, from (69),

$$\underline{g}(0, 0, f) = \underline{g}_4(f) \quad , \tag{71}$$

$\underline{g}_4(f)$ is proportional to the surface-height spectrum at a point and, therefore, is real. Equation (70) states that the zeroth-order scatter sideband spectrum $T_o(f)$ is directly proportional to the autocorrelation of the wave-height spectrum and is even about $f = 0$ (which corresponds to $f = f_a$ in the received acoustic spectrum). Also, the first-order sideband spectrum is directly proportional to the wave-height spectrum, and the second-order sideband spectrum is proportional to the convolution of the wave-height spectrum and need not be even about $f = 0$ (which corresponds to $f = f_a + 2f_s$ in the received acoustic spectrum).

The mth order sideband $T_m(f)$ is proportional to β^{2m} for small β and $|m| \geq 1$. This sideband involves higher order convolutions of the low-pass spectrum, thereby causing significant spreading in frequency. This is consistent with the observations made in the text following (30).

3.5 RMS BANDWIDTH OF SIDEBANDS FOR SMALL ROUGHNESS

It is of interest to know quantitatively the amount of frequency spreading that each sideband undergoes. One simple measure of this spreading, short of evaluating the actual sideband spectrum, is the rms bandwidth of each sideband. We start by defining the rms bandwidth B_s of the surface-height spectrum $\underline{g}$ for the special case of (68) according to

$$B_s^2 = \frac{\int df\, f^2\, \underline{g}(0,0,f)}{\int df\, \underline{g}(0,0,f)} = \frac{\int df\, f^2\, \underline{g}_4(f)}{\int df\, \underline{g}_4(f)} = \int df\, f^2\, \underline{g}_4(f) \quad , \tag{72}$$

where we have used Appendix D and the fact that

$$\rho_3(0,0) = \rho_4(0) = 1, \tag{73}$$

since $\rho(0,0,0) = 1$.

For small roughness, the spectra of the zeroth and first- and second-order sidebands are given in (70). From (70b), it follows immediately, using (72), that the rms bandwidth B_1 of the first-order sideband is equal to B_s, the rms surface-spectrum bandwidth. The zeroth order rms bandwidth B_0 is available from (70a) as

$$B_0^2 = \frac{\int df\, f^2 \int dw\, \underline{g}_4(w)\, \underline{g}_4(w-f)}{\int df \int dw\, \underline{g}_4(w)\, \underline{g}_4(w-f)} = 2B_s^2 \quad , \tag{74}$$

utilizing the fact that

$$\int df\, f\, \underline{g}_4(f) = 0 \quad , \tag{75}$$

from (D-5), (D-6), and (69). Similarly, it may be shown, in general, that the rms bandwidth of the mth order sideband is given by

$$B_m = \left\{ \begin{array}{ll} \sqrt{2}\, B_s, & m = 0 \\ \sqrt{|m|}\, B_s, & m \neq 0 \end{array} \right\} \quad , \tag{76}$$

if $\beta \ll 1$. Thus, the zeroth and second-order sidebands are $\sqrt{2}$ wider than the surface spectrum, and the higher order bandwidths increase as the square root of the order number. For the small roughness case, the correlation distances or direction cosines do not enter into this relation.

4. RELATION OF SURFACE CORRELATION FUNCTION TO DIRECTIONAL WAVE SPECTRUM

The results in the previous section require specific forms for the spatial-temporal surface correlation ρ for their numerical evaluation. In this section, we shall use the relation between the surface correlation

22

function ρ and the directional wave spectrum for a wind-generated sea composed entirely of gravity waves, and specialize to several cases of interest.

4.1 GENERAL RELATIONS

For a homogeneous surface, the spatial-temporal surface correlation function $\rho(u, v, \tau)$ can be expressed in terms of the directional wave spectrum $\widehat{A}^2(\mu, \nu)$ [13, Part 8; 10, Chapter 8]:

$$\sigma^2 \rho(u, v, \tau) = \iint d\mu \, d\nu \, \widehat{A}^2(\mu, \nu) \cos[u\mu + v\nu - g^{\frac{1}{2}}(\mu^2 + \nu^2)^{\frac{1}{4}} \tau] \quad , \tag{77}$$

where g is the acceleration of gravity and μ and ν are the wave numbers in rectangular coordinates. In particular, the temporal correlation of the surface-height variation at a point is given by

$$\sigma^2 \rho(0, 0, \tau) = \iint d\mu \, d\nu \, \widehat{A}^2(\mu, \nu) \cos[g^{\frac{1}{2}}(\mu^2 + \nu^2)^{\frac{1}{4}} \tau] \quad . \tag{78}$$

An alternate representation of the directional wave spectrum in terms of the polar form $A^2(\mu, \nu)$ is often used:

$$\widehat{A}^2(\mu, \nu) = \frac{g^{\frac{1}{2}} A^2 (g^{\frac{1}{2}}(\mu^2 + \nu^2)^{\frac{1}{4}}, \tan^{-1}\nu/\mu)}{2(\mu^2 + \nu^2)^{\frac{3}{4}}} \quad . \tag{79}$$

If we substitute (79) into (78) and make the substitutions $\mu = (2\pi f)^2 \cos\theta/g$, $\nu = (2\pi f)^2 \sin\theta/g$, the surface-height temporal correlation becomes

$$\sigma^2 \rho(0, 0, \tau) = 2\pi \int_0^\infty df \cos(2\pi f\tau) \int_{-\pi}^\pi d\theta \, A^2(2\pi f, \theta) \quad . \tag{80}$$

The (double-sided) surface-height spectrum (at a point) is denoted by $\Phi(f)$ and is the Fourier transform of (80):

$$\Phi(f) = \int d\tau \exp(-i2\pi f\tau) \, \sigma^2 \rho(0, 0, \tau) = \pi \int_{-\pi}^\pi d\theta \, A^2(2\pi|f|, \theta)$$

$$= (2\pi)^4 \, g^{-2} \, |f|^3 \int_{-\pi}^\pi d\theta \, \widehat{A}^2\left(\frac{4\pi^2 f^2 \cos\theta}{g}, \frac{4\pi^2 f^2 \sin\theta}{g}\right) \quad . \tag{81}$$

The last form follows from (79).

4.2 ELLIPTICAL SURFACE CORRELATION

The results above are for general directional wave spectra. Here we will consider a special case of particular interest. We assume first that the directional wave spectrum $\widehat{A}^2$ possesses 180° symmetry:

$$\hat{A}^2(-\mu, -\nu) = \hat{A}^2(\mu, \nu) \quad . \tag{82}$$

This is done for mathematical tractability, rather than for any underlying physical reason. Then, from (77), $\rho(u, v, \tau)$ is even in τ for all u, v:

$$\rho(u, v, -\tau) = \rho(u, v, \tau) \quad . \tag{83}$$

When we use (D-15) through (D-17) and (77), there follows

$$\varrho(u, v, 0) = \rho(u, v, 0) = \iint d\mu \, d\nu \, \sigma^{-2} \, \hat{A}^2(\mu, \nu) \cos(\nu \mu + \nu \nu) \quad . \tag{84}$$

But this relation can be inverted by a double Fourier transform to obtain the directional wave spectrum $\hat{A}^2(\mu, \nu)$ in terms of $\varrho(u, v, 0)$:

$$\sigma^{-2} \hat{A}^2(\mu, \nu) = (2\pi)^{-2} \iint du \, dv \exp[-i(\mu u + \nu v)] \, \rho(u, v, 0) \quad . \tag{85}$$

We have used the symmetry of $\hat{A}^2$ in obtaining (85).

For the elliptical correlation form assumed in (52), we had in (54)

$$\varrho(u, v, 0) = \rho_2 \left(\sqrt{\left(\frac{u}{L_x}\right)^2 + \left(\frac{v}{L_y}\right)^2} \right). \tag{86}$$

If we substitute (86) into (85), the directional wave spectrum takes the form

$$\hat{A}^2(\mu, \nu) = \sigma^2 L_x L_y (2\pi)^{-1} \int_0^\infty d\tau \, \tau \, \rho_2(\tau) \, J_0 \left(\sqrt{(L_x \mu)^2 + (L_y \nu)^2} \, \tau \right)$$

$$\equiv A_2^2 \left(\sqrt{(L_x \mu)^2 + (L_y \nu)^2} \right). \tag{87}$$

Thus, the directional wave spectrum is also elliptical if the surface correlation is elliptical at zero delay. (An isotropic surface is a special case of (87).) Equation (87) may be expressed compactly as

$$A_2^2(\eta) = \sigma^2 L_x L_y (2\pi)^{-1} \int_0^\infty d\tau \, \tau \, \rho_2(\tau) \, J_0(\eta \tau) \quad . \tag{88}$$

For any particular form of spatial correlation ρ_2, (88) can be evaluated numerically; then, (87) yields the directional wave spectrum.

Conversely, if the directional wave spectrum $\hat{A}^2$ is elliptical, so also is $\varrho(u, v, 0)$. The exact relation is obtained by setting

24

$$\hat{\Lambda}^2(\mu, \nu) = A_2^2 \left(\sqrt{(L_x \mu)^2 + (L_y \nu)^2} \right) \tag{89}$$

in (84). There follows

$$\varrho(u, v, 0) = (\sigma^2 L_x L_y)^{-1} 2\pi \int\limits_0^\infty d\eta \, \eta \, A_2^2(\eta) \, J_o \left(\sqrt{\left(\frac{u}{L_x}\right)^2 + \left(\frac{v}{L_y}\right)^2} \, \eta \right)$$
$$\equiv \rho_2 \left(\sqrt{\left(\frac{u}{L_x}\right)^2 + \left(\frac{v}{L_y}\right)^2} \right), \tag{90}$$

or more compactly,

$$\rho_2(r) = (\sigma^2 L_x L_y)^{-1} 2\pi \int\limits_0^\infty d\eta \, \eta \, A_2^2(\eta) \, J_o(r\eta) \ . \tag{91}$$

Equations (88) and (91) are a Hankel-transform pair of order zero [14, p. 136]. Specification of either ρ_2 or A_2^2 determines the other.

The surface-height spectrum $\Phi(f)$ for the elliptical surface correlation is obtained by substituting (89) into (81):

$$\Phi(f) = (2\pi)^4 \, g^{-2} \, |f|^3 \int\limits_{-\pi}^\pi d\theta \, A_2^2 \left(\sqrt{(L_x \cos\theta)^2 + (L_y \sin\theta)^2} \, \frac{4\pi^2 f^2}{g} \right) \ . \tag{92}$$

For the special case of an isotropic surface, $L_x = L_y = L$, (92) becomes

$$\Phi(f) = (2\pi)^5 \, g^{-2} \, |f|^3 \, A_2^2 \left(\frac{4\pi^2 f^2 L}{g} \right) \tag{93a}$$

and (91) takes the more familiar form

$$\sigma^2 \rho_2(r) = \int\limits_0^\infty df [2\Phi(f)] \, J_o \left(\frac{4\pi^2 f^2 L r}{g} \right) \ . \tag{93b}$$

Here, $2\Phi(f)$ is the equivalent single-sided surface-height spectrum.

4.3 EXAMPLES

Four examples of the elliptical surface correlation function given in (86) will be considered. The first is exponential decay of a cosinusoidal spatial variation:

$$\rho_2(r) = \exp(-Rr)\cos(Qr), \quad r \geq 0 \quad . \tag{94}$$

For Q equal to zero, simple exponential decay of the spatial correlation is realized. R is of the order of unity. When we substitute (94) into (88), it follows that [11, 6.623 2]

$$A_2^2(\eta) = \sigma^2 L_x L_y (2\pi)^{-1} R^{-2} \ \mathrm{Re}\left\{\frac{1+iQ/R}{[(1+iQ/R)^2 + (\eta/R)^2]^{3/2}}\right\} \quad . \tag{95}$$

The surface-height spectrum for the elliptical surface correlation then requires the numerical evaluation of (92). For an isotropic surface, $L_x = L_y = L$, substitution of (95) into (93a) yields for the surface-height spectrum

$$\Phi(f) = 2\pi\sigma^2 \sqrt{\frac{L}{gR}}\,\hat{\Phi}(x) \quad , \tag{96}$$

where the dimensionless parameter x is defined as

$$x = 2\pi f \sqrt{\frac{L}{gR}} \quad , \tag{97}$$

and the dimensionless function $\hat{\Phi}$ is defined as

$$\hat{\Phi}(x) = |x|^3 \ \mathrm{Re}\left\{\frac{1+iQ/R}{[(1+iQ/R)^2 + x^4]^{3/2}}\right\} \quad . \tag{98}$$

A plot of the frequency-dependent term $\hat{\Phi}$ is given in Fig. 3 for several values of $Q/R \leq 1$. As $x \to 0+$, the Re component of (98) approaches

$$\frac{1-(Q/R)^2}{[1+(Q/R)^2]^2} \quad . \tag{99}$$

Since the surface-height spectrum can not be negative, it is necessary (but not sufficient) that $Q/R \leq 1$ in order for (94) to be a valid form of spatial correlation. The spectrum of (96) decays as $|f|^{-3}$ for large frequencies.

Since Q was upper-limited to a value of unity in the above example, the surface-height spectrum can not be made arbitrarily narrow. It is, therefore, of interest to demonstrate that arbitrarily narrow spectra are possible through a slightly modified spatial correlation, namely, exponential decay of a Bessel function:
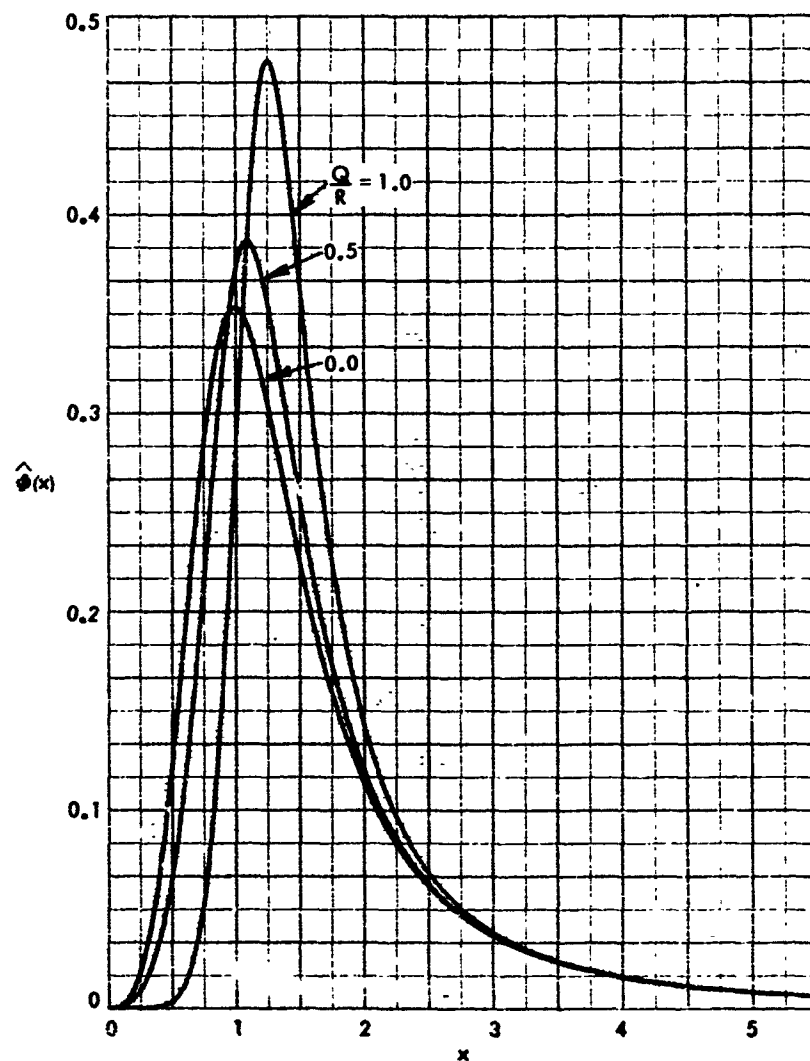
26

Fig. 3 - Surface-Height Spectrum for Exponentially Modulated Cosine Spatial Correlation

$$\rho_2(r) = \exp(-Rr)\, J_o(Qr),\ r \geq 0 \ .\tag{100}$$

This function also oscillates with r, but decays slightly faster than (94) because the envelope of $J_o(t)$ decays as $t^{-\frac{1}{2}}$ for large t. If we substitute (100) into (88), there follows [15, pp. 314-316, Eqs. (11), (14), and (19)]

$$A_2^2(\eta) = \sigma^2 L_x L_y (2\pi)^{-1} \int_o^\infty dr\, r \exp(-Rr)\, J_o(Qr)\, J_o(\eta r)$$

$$= \frac{\sigma^2 L_x L_y}{\pi^2}\ \frac{1}{R^2}\ \left[1 + \left(\frac{\eta}{R} - \frac{Q}{R}\right)^2\right]^{-1} \left[1 + \left(\frac{\eta}{R} + \frac{Q}{R}\right)^2\right]^{-\frac{1}{2}} E(\cdot)\ ,\tag{101}$$

where $E(\cdot)$ is a complete elliptic integral of the second kind with modulus [16, Chapter 17; see especially p. 590]

$$k = \left\{ 4\frac{Q}{R}\frac{\eta}{R}\left[1 + \left(\frac{\eta}{R} + \frac{Q}{R}\right)^2\right]^{-1} \right\}^{\frac{1}{2}}\ ,\tag{102}$$

or parameter

$$m = 4\frac{Q}{R}\frac{\eta}{R}\left[1 + \left(\frac{\eta}{R} + \frac{Q}{R}\right)^2\right]^{-1}\ .\tag{103}$$

The surface-height spectrum follows upon substitution of (101) into (92) for the elliptical surface correlation case. Since $A_2^2(\eta)$ of (101) is positive for all choices of Q and R [16, p. 609; m of (103) is always less than unity], the surface-height spectrum $\Phi(f)$ of (92) is nonnegative; therefore, we consider the spatial correlation form in (100) for arbitrary values of Q and R.

Rather than evaluate (92) numerically, we restrict attention here to the isotropic surface and use (93a) to obtain the surface-height spectrum:

$$\Phi(f) = 2\pi\sigma^2 \sqrt{\frac{L}{gR}}\, \widehat{\Phi}(x)\ ,\tag{104}$$

where

$$x \equiv 2\pi f \sqrt{\frac{L}{gR}}\tag{105}$$

and

$$\widehat{\Phi}(x) \equiv \frac{2}{\pi}|x|^3 \left[1 + \left(x^2 - \frac{Q}{R}\right)^2\right]^{-1} \left[1 + \left(x^2 + \frac{Q}{R}\right)^2\right]^{-\frac{1}{2}} E(\cdot)\ .\tag{106}$$

28

The parameter m of the complete elliptic integral is given by

$$m = 4\frac{Q}{R}x^2 \left[1 + \left(x^2 + \frac{Q}{R}\right)^2\right]^{-1} \ . \tag{107}$$

The frequency-dependent function $\hat{\Phi}(x)$ is plotted versus x in Fig. 4 for several values of Q/R. The spectrum decays as $|f|^{-3}$ for large frequencies. The narrow-band character of the surface-height spectrum for large Q/R is evident.

The third example of spatial surface correlation is Gaussian decay of a cosine[9]:

$$\rho_2(r) = \exp(-R^2 r^2)\cos(Qr), \ r \geq 0 \ . \tag{108}$$

Substituting (108) into (88), we obtain

$$A_2^2(\eta) = \sigma^2 L_x L_y (2\pi)^{-1} R^{-2} \int_0^\infty dt\, t \exp(-t^2) \cos\left(\frac{Q}{R}t\right) J_o\left(\frac{\eta}{R}t\right) \ . \tag{109}$$

The surface-height spectrum for an isotropic surface follows upon substituting (109) into (93a):

$$\Phi(f) = 2\pi\sigma^2 \sqrt{\frac{L}{gR}} \ \hat{\Phi}(x) \ , \tag{110}$$

where

$$x = 2\pi f \sqrt{\frac{L}{gR}} \tag{111}$$

and

$$\hat{\Phi}(x) = |x|^3 \int_0^\infty dt\, t \exp(-t^2) \cos\left(\frac{Q}{R}t\right) J_o(x^2 t) \ . \tag{112}$$

This function is plotted in Fig. 5 for several values of Q/R. (The method for evaluating (112) is given in Appendix E. For $Q/R > 1.848$, $\hat{\Phi}(x)$ goes negative at the origin, thereby invalidating (108) in that range.)

The fourth example of surface correlation to be considered is Gaussian decay of a Bessel function:

$$\rho_2(r) = \exp(-R^2 r^2) J_o(Qr), \ r \geq 0 \ . \tag{113}$$

Q equal to zero corresponds to Gaussian spatial decay of the correlation. When we substitute (113) into (88), there follows [11, 6.633 2]

---

[9] This is a form treated by Lysanov (Ref. 17) and suggested by Schulkin (Ref. 18, p. 42).
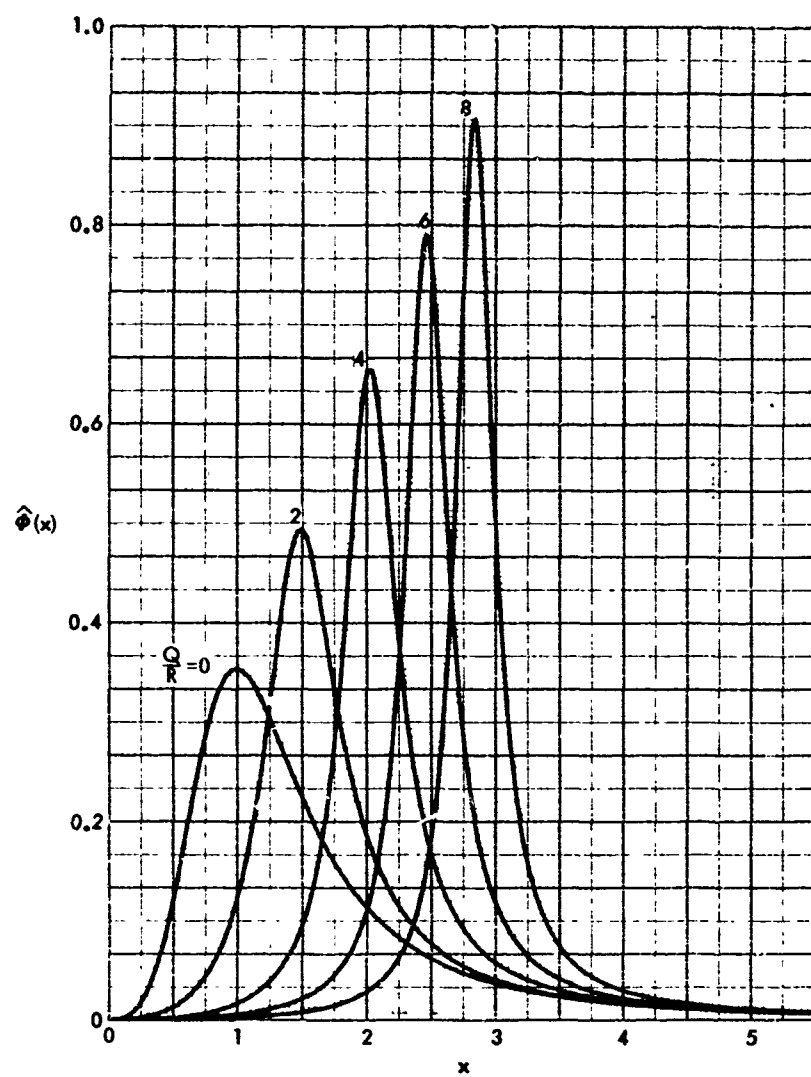
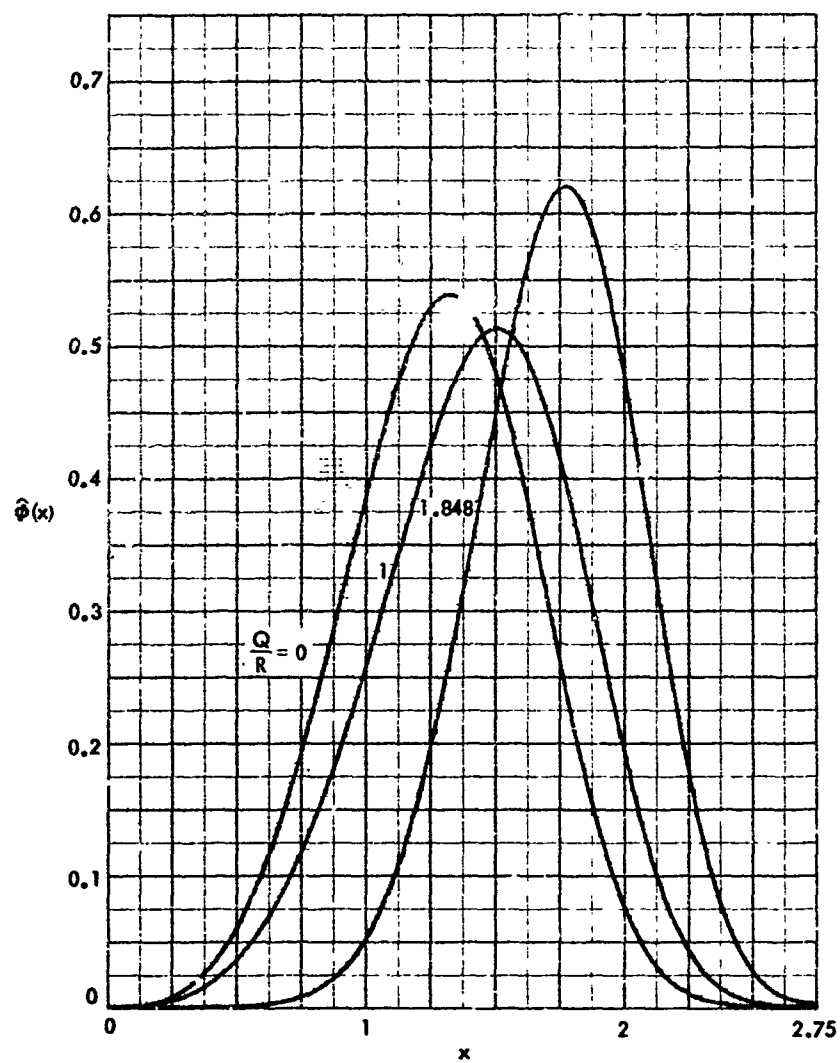Fig. 4 - Surface-Height Spectrum for Exponentially Modulated Bessel Function Spatial Correlation

Fig. 5 - Surface-Height Spectrum Gaussianly Modulated Cosine Spatial Correlation

$$A_2^2(\eta) = \sigma^2 L_x L_y (4\pi)^{-1} \frac{1}{R^2} \exp\left(-\frac{Q^2+\eta^2}{4R^2}\right) I_o\left(\frac{Q\eta}{2R^2}\right). \tag{114}$$

The surface-height spectrum follows upon substituting (114) into (92) for the elliptical surface correlation case. Since $A_2^2(\eta)$ of (114) is positive for all choices of Q and R, the surface-height spectrum $\Phi(f)$ of (92) is nonnegative; therefore, we consider the spatial correlation form in (113) for all Q and R.

The exponential and Bessel function in (114) can be expressed as

$$\exp\left(-\left(\frac{\eta-Q}{2R}\right)^2\right) \exp\left(-\frac{Q\eta}{2R^2}\right) I_o\left(\frac{Q\eta}{2R^2}\right). \tag{115}$$

Since the function $\exp(-t) I_o(t)$ is weakly dependent on t, it is seen that $A_2^2(\eta)$ possesses a peak approximately at $\eta = Q$ of width proportional to R. The integral of (92) for $\Phi(f)$ tends to smooth this peak. However, the isotropic surface-height spectrum of (93) does not involve this smoothing and is a peaked spectrum; a measure of the peakedness is the "quality" ratio of center frequency to bandwidth, and is related to the ratio Q/R for this example.

The surface-height spectrum for an isotropic surface is obtained by substituting (114) into (93a), and is given by

$$\Phi(f) = 2\pi\sigma^2 \sqrt{\frac{L}{gR}} \hat{\Phi}(x) , \tag{116}$$

where

$$x \equiv 2\pi f \sqrt{\frac{L}{gR}} \tag{117}$$

and

$$\hat{\Phi}(x) \equiv \tfrac{1}{2}|x|^3 \exp\left[-\tfrac{1}{4}\left(\frac{Q}{R}\right)^2 - \tfrac{1}{4}x^4\right] I_o\left(\tfrac{1}{2}\frac{Q}{R}x^2\right) . \tag{118}$$

The frequency-dependent term $\hat{\Phi}$ is plotted versus the dimensionless parameter x in Fig. 6 for several values of Q/R. The spectrum decays as $\exp(-cf^4)$ for large frequencies.

The narrow-band character of the surface-height spectrum is evident from Figs. 4 and 6 when the ratio Q/R is large compared to unity.
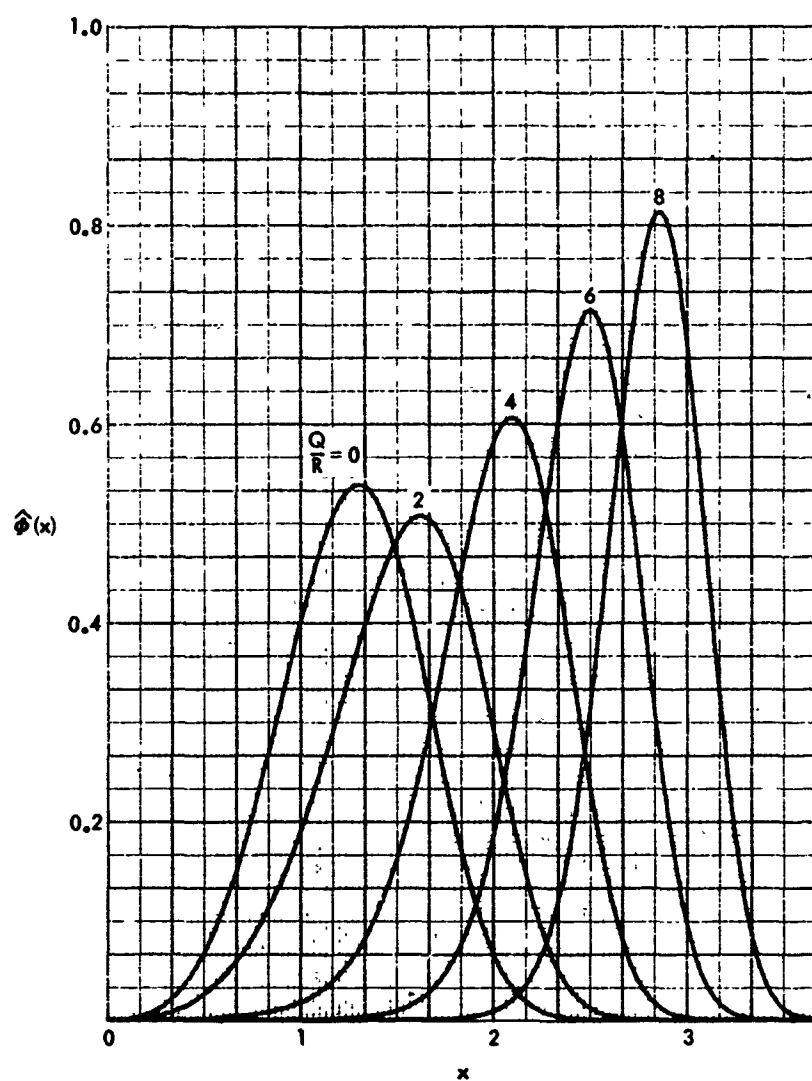
32

Fig. 6 - Surface-Height Spectrum for Gaussianly Modulated Bessel Function Spatial Correlation

5 SCATTERING STRENGTHS OF SIDEBAND COMPONENTS

For the case of a narrow-band surface-height spectrum, the scattered acoustic spectrum at a receiving point may be obtained from (47) and (48). The general form of the received acoustic spectrum was shown in Fig. 2 to consist of a series of spectral lobes or sidebands, each separated from the incident acoustic frequency f_a by multiples of the center frequency f_s of the surface variation, plus an impulse at the acoustic frequency f_a. This impulse is the coherent component.

The total acoustic power in each spectral lobe, or equivalently the scattering strength, may be obtained from (60) and (61) for the specular direction, and from (62) and (63) for the nonspecular direction. In this section, we will evaluate $U_m(\beta)$ and $V_m(a, \beta)$, as given by (61) and (63), respectively. As mentioned in Subsection 3.4, if the factor preceding $U_m(\beta)$ is held constant, the geometry, acoustic frequency, and correlation distances are considered fixed. The plot of $U_m(\beta)$, therefore, measures the dependence of the mth scattering strength on the surface rms wave height σ through the roughness parameter β. $V_m(a, \beta)$ measures the dependence of the mth scattering strength on the correlation distances L_x and L_y (although their ratio is fixed) through a, and on the rms wave height σ through β. (Integrals (61) and (63) were numerically evaluated by Simpson's Rule; the error analysis is contained in Appendix F.)

In Figs. 7 through 9, $U_m(\beta)$ is plotted versus β for $m = 0, 1, 2, 3, 4$ for an exponentially modulated Bessel function spatial correlation,

$$\rho_2(r) = \exp(-r) \, J_0(Qr) \quad , \tag{119}$$

for values of $Q = 8, 4, 0$. In Figs. 10 through 12, a similar set of curves is plotted, the only difference being that the spatial correlation is a Gaussianly modulated Bessel function:

$$\rho_2(r) = \exp(-r^2) \, J_0(Qr) \quad . \tag{120}$$

To better explain these figures, let us concentrate temporarily on Fig. 12; here $Q = 0$, meaning the spatial correlation is Gaussian. $U_1(\beta)$ corresponds to the scattering strength in the first sideband (either above or below the acoustic frequency f_a). Since $a = 0$, we are considering only the specular direction. $\beta = 0$ corresponds to a flat surface; for this value of β, there is no scattered power in the
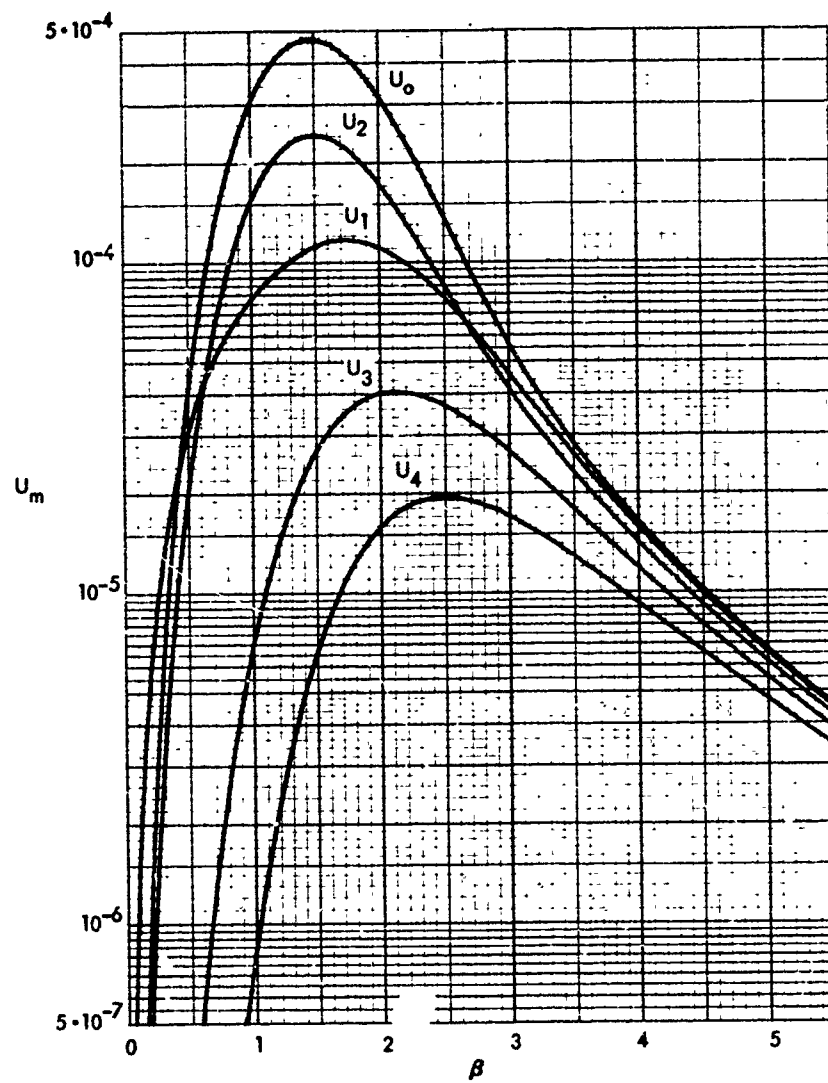
34

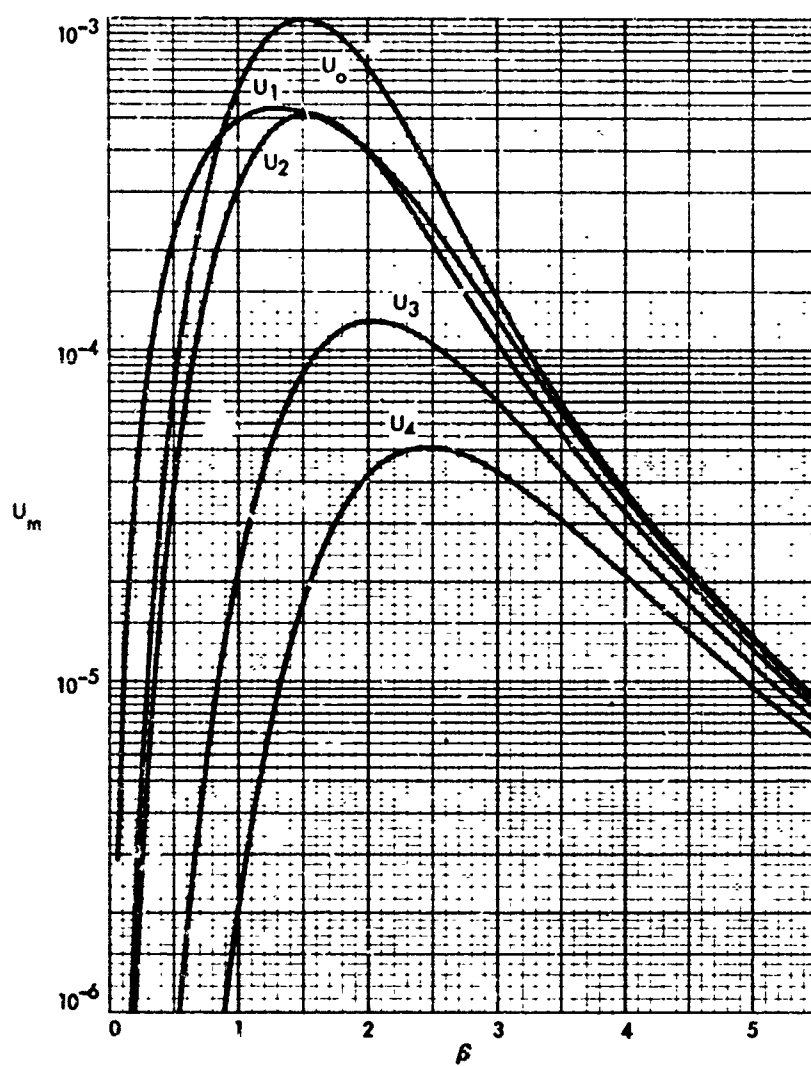Fig. 7 - U_m for Exponentially Modulated Bessel Function Spatial Correlation, $Q = 8$

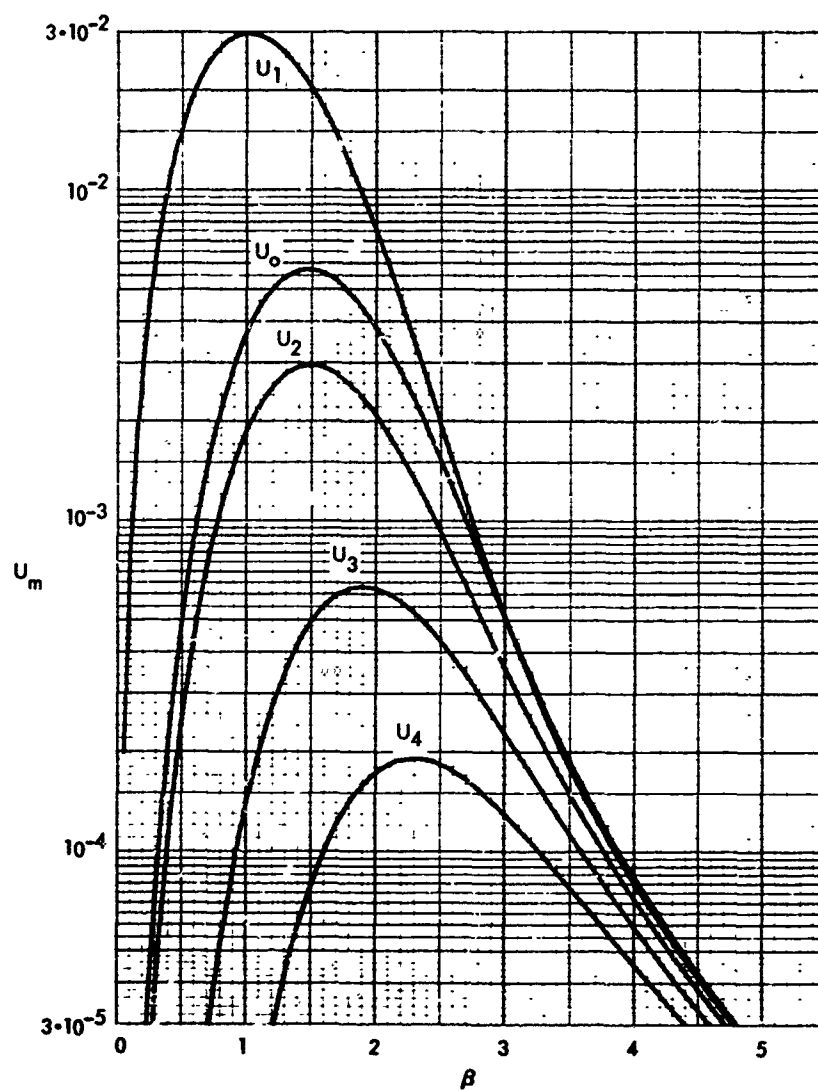Fig. 8 - U_m for Exponentially Modulated Bessel Function Spatial Correlation, $Q = 4$

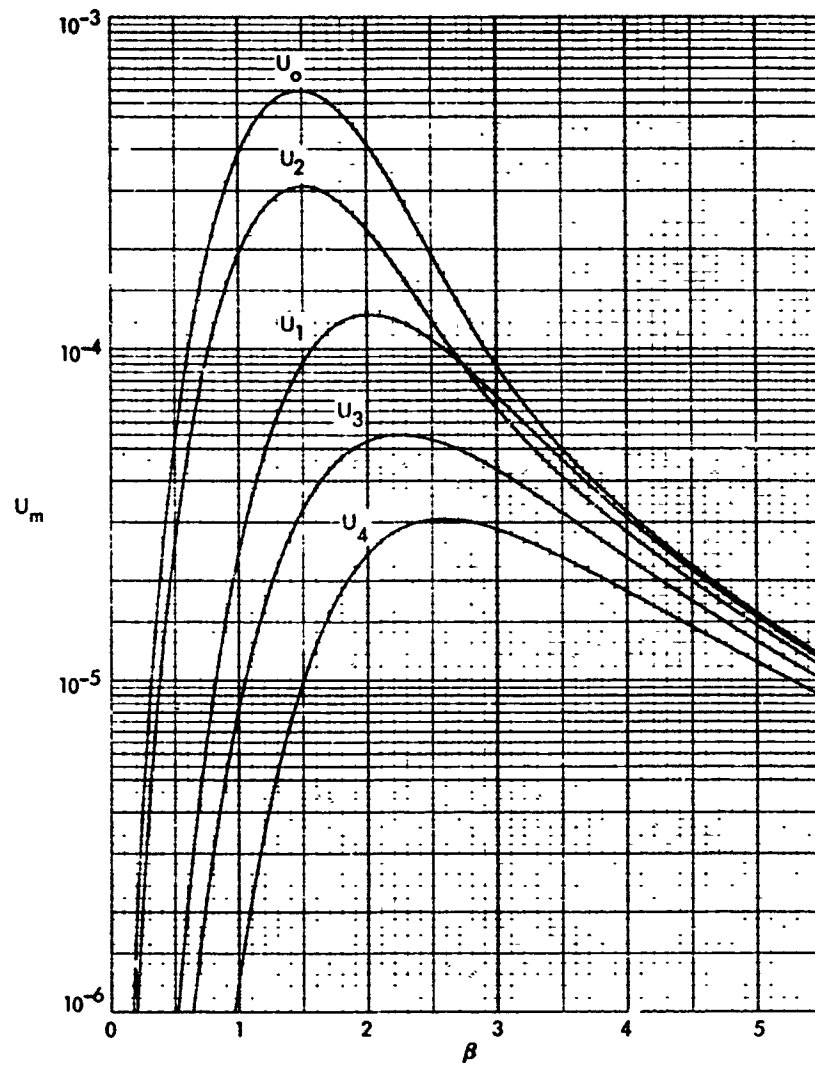Fig. 9 - U_m for Exponential Spatial Correlation

Fig. 10 - U_m for Gaussianly Modulated Bessel Function Spatial Correlation, $Q = 8$
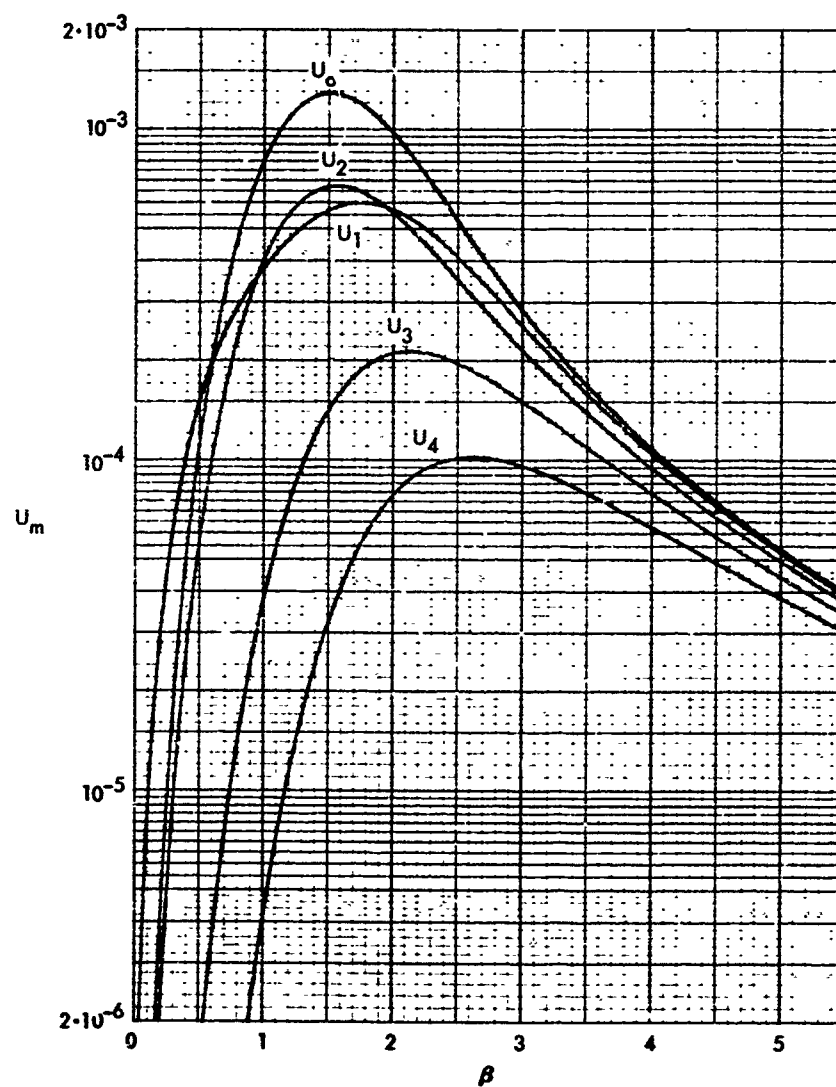
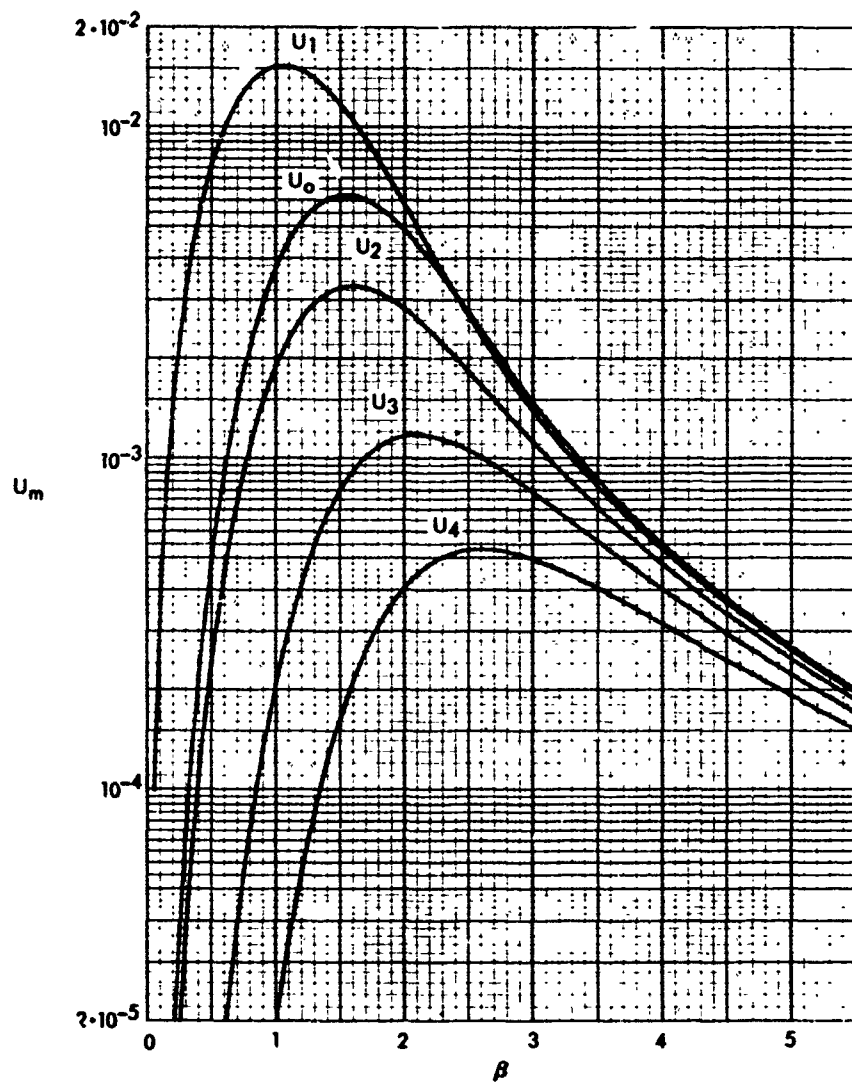Fig. 11 - U_m for Gaussianly Modulated Bessel Function Spatial Correlation, $Q = 4$

Fig. 12 - U_m for Gaussian Spatial Correlation

sidebands since all the reflected power appears in the coherent component. As β increases, there is less power in the coherent component, and more scattered power appears in the sidebands. The power in the first sideband reaches a maximum value when the surface roughness parameter β is approximately unity, and decreases thereafter. For these larger values of β, the surface is rougher, and more of the scattered power will appear in higher-order sidebands in directions other than specular. We have plotted the zeroth through fourth-order sideband scattering strength factors $U_m(\beta)$ in Figs. 7 through 12. All the curves initially increase as β increases from zero, reach a maximum, and then decrease. For large β, there is little difference in power between the various sidebands.

For $Q = 4$, or 8, the gross features of the sideband powers are similar to those for $Q = 0$, whether the modulation is exponential or Gaussian. However, whereas for $Q = 0$, $U_1(\beta)$ is larger than $U_0(\beta)$ for a large range of β, the reverse is true for $Q = 4$ and 8. For larger Q, the zeroth and second-order sidebands contain most of the scattered power in the specular direction. As Q increases, the power in each sideband, for a given roughness β, decreases. The reason for this is that the total scattered power in the specular direction decreases with increasing Q, since the correlation distance decreases. (This latter effect is due to the factor $J_0(Qr)$ in (119) and (120), which decays with r in addition to the exponential terms.)

For small β, the power in the first sideband is proportional to β^2, and the powers in the zeroth and second-order sidebands behave as β^4 (See (67)). This is not apparent in Fig. 10 for the Gaussian modulated case for $Q = 8$, because the effect occurs at smaller β values than plotted.

The major difference between the exponentially modulated and Gaussianly modulated curves occurs at larger values of β. Here the sideband powers are much larger for the Gaussian case than for the exponential case. This is true for all Q and all orders of sidebands plotted.

In Figs. 13 through 27, three-dimensional plots of $V_m(\alpha, \beta)$ versus α and β are given for $m = 0, 1, 2, 3, 4$ and for an exponentially modulated Bessel function spatial correlation (See (119)) for values of

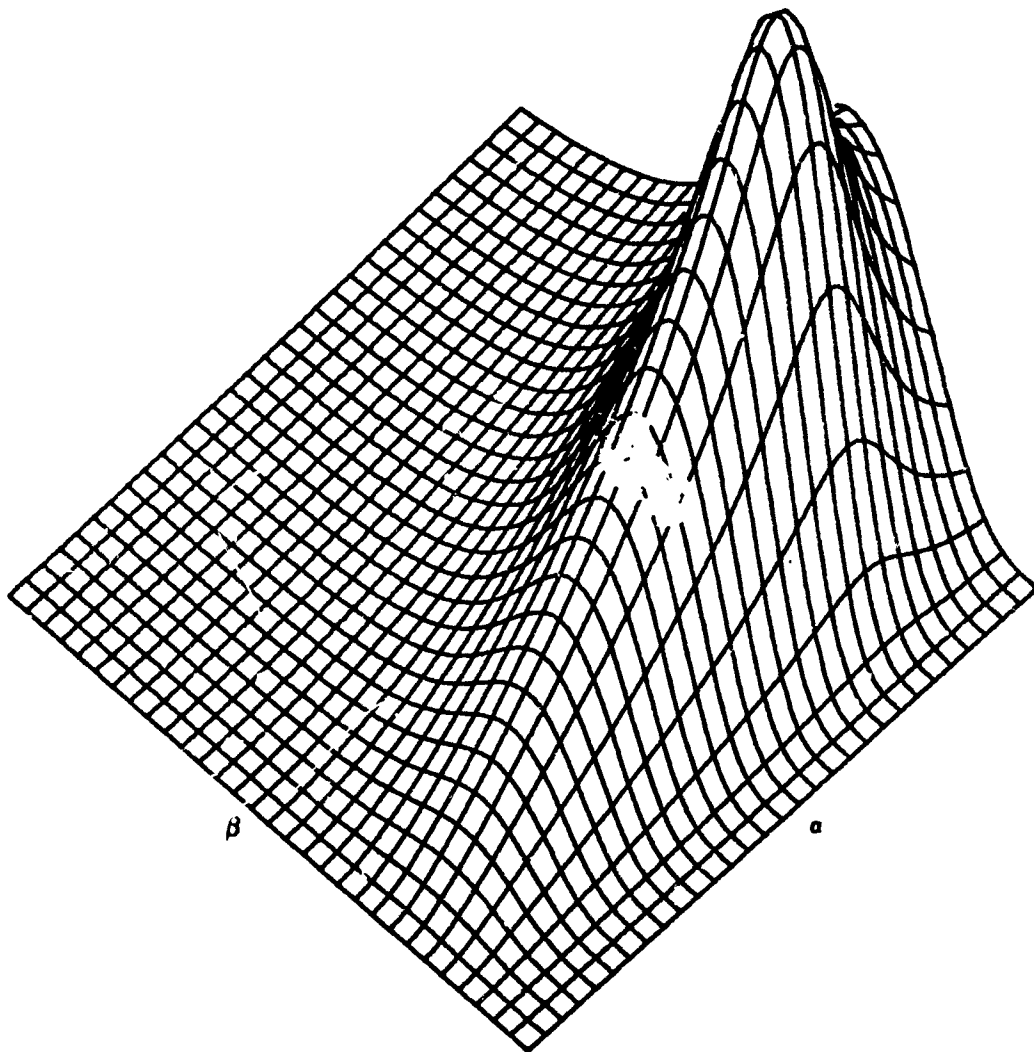Fig. 13 - V_0 for Exponentially Modulated Bessel Function Spatial Correlation, $Q = 8$

$\left(V_0 = .268 \cdot 10^{-1} \text{ at } \alpha = 15 \; 1/3, \; \beta = 1.6\right)$

42

Fig. 14 - V_1 for Exponentially Modulated Bessel Function Spatial Correlation, $Q = 8$

$\left(V_1 = .763 \cdot 10^{-1} \text{ at } \alpha = 8, \beta = 1.0\right)$

Fig. 15 - V_2 for Exponentially Modulated Bessel Function Spatial Correlation, $Q = 8$
$(V_2 = .144 \cdot 10^{-1}$ at $\alpha = 15\ 1/3,\ \beta = 1.6)$

44

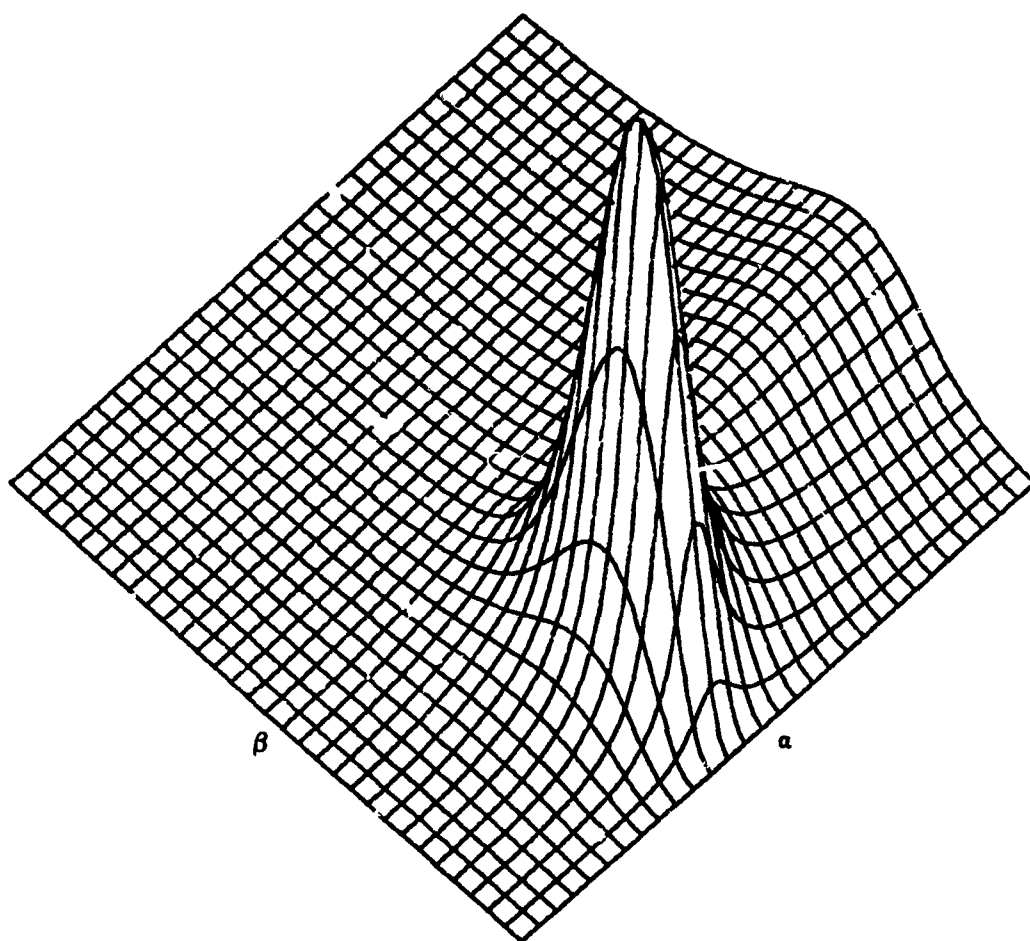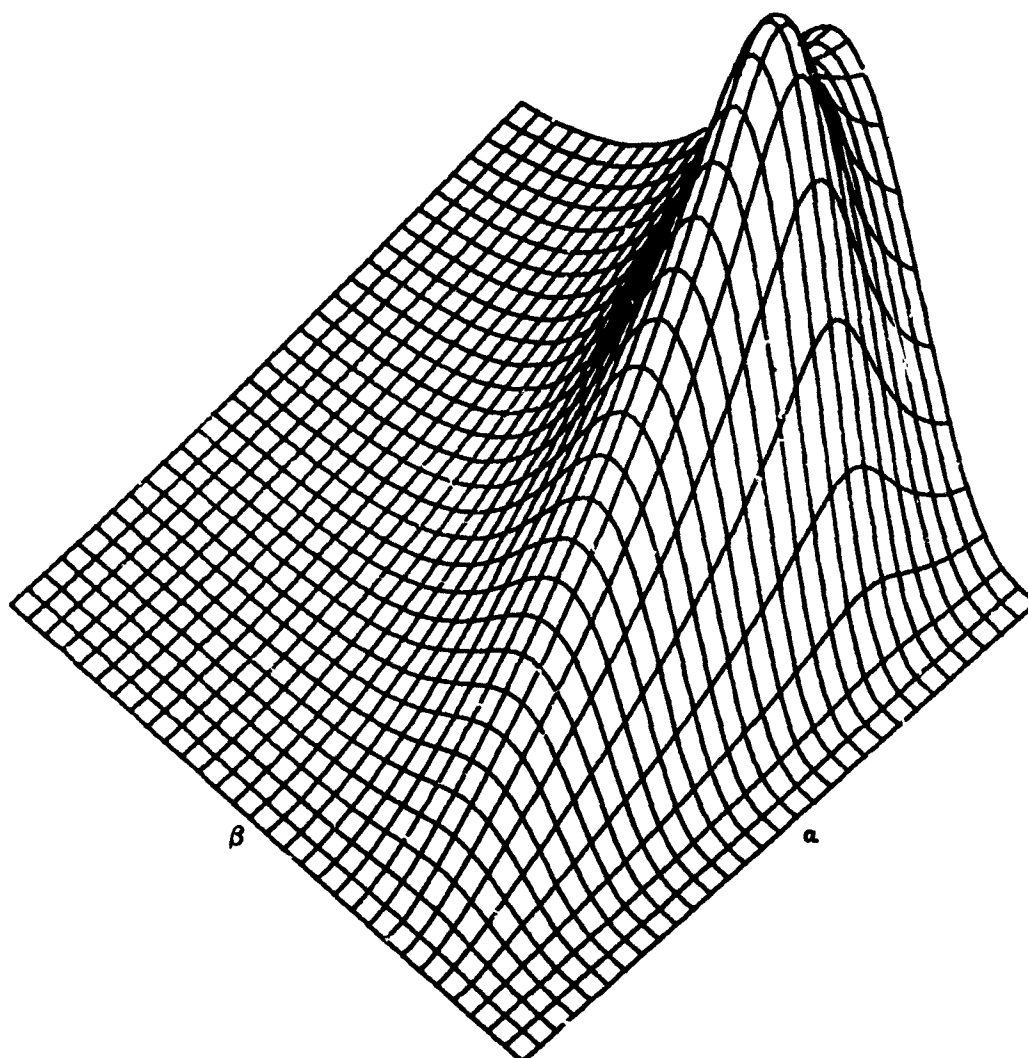Fig. 16 - V_3 for Exponentially Modulated Bessel Function Spatial Correlation, $Q = 8$

$\left(V_3 = .678 \cdot 10^{-2} \text{ at } \alpha = 20, \beta = 2.4\right)$

Fig. 17 – V_4 for Exponentially Modulated Bessel Function Spatial Correlation, $Q = 8$

$(V_4 = .392 \cdot 10^{-2}$ at $\alpha = 20$, $\beta = 2.9)$
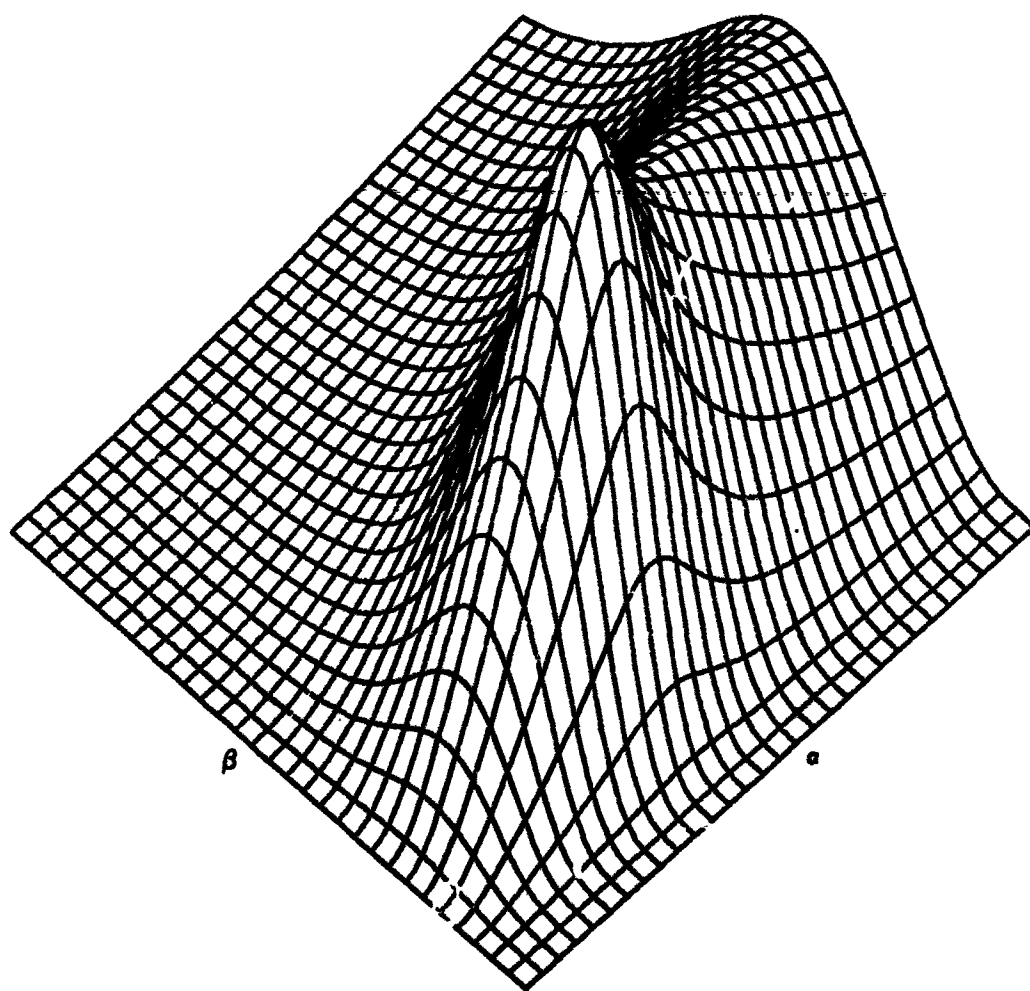
Fig. 18 - V_0 for Exponentially Modulated Bessel Function Spatial Correlation, $Q = 4$

$\left(V_0 = .196 \cdot 10^{-1} \text{ at } \alpha = 72/3, \beta = 1.6\right)$
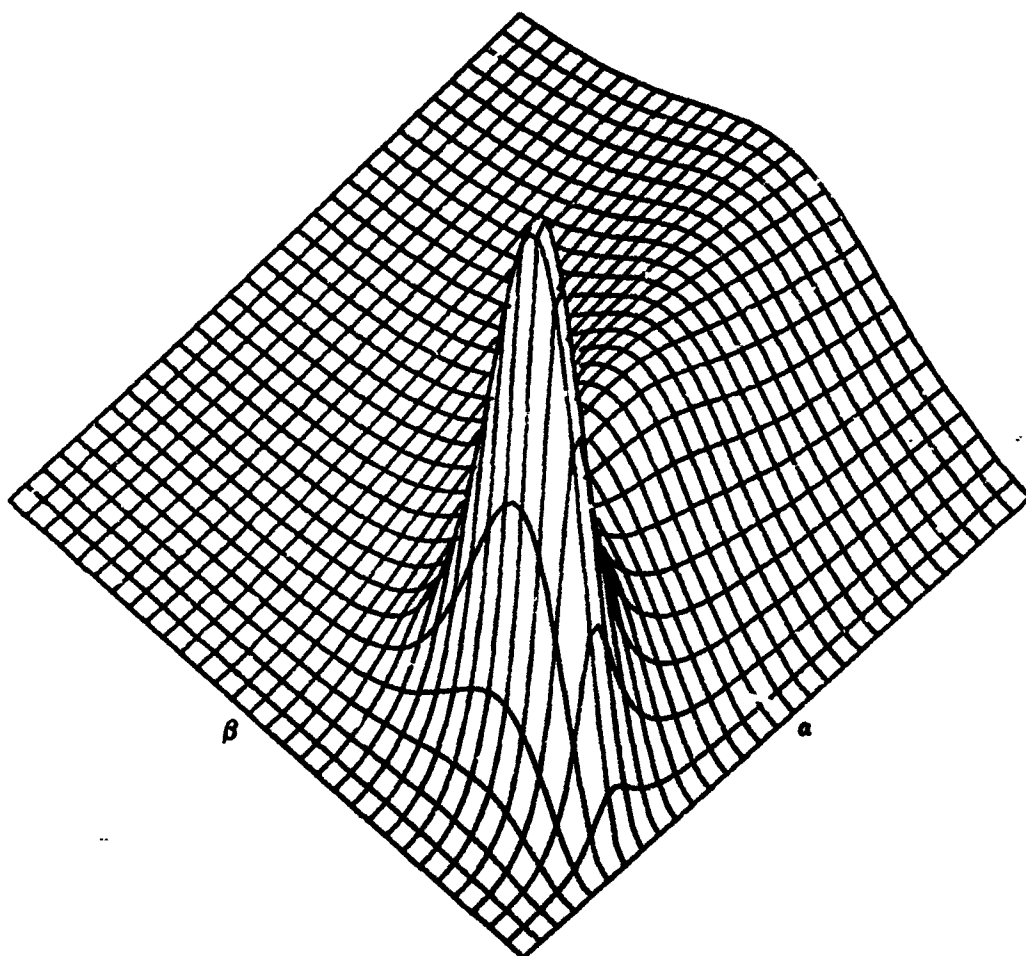
Fig. 19 - V_1 for Exponentially Modulated Bessel Function Spatial Correlation, $Q = 4$
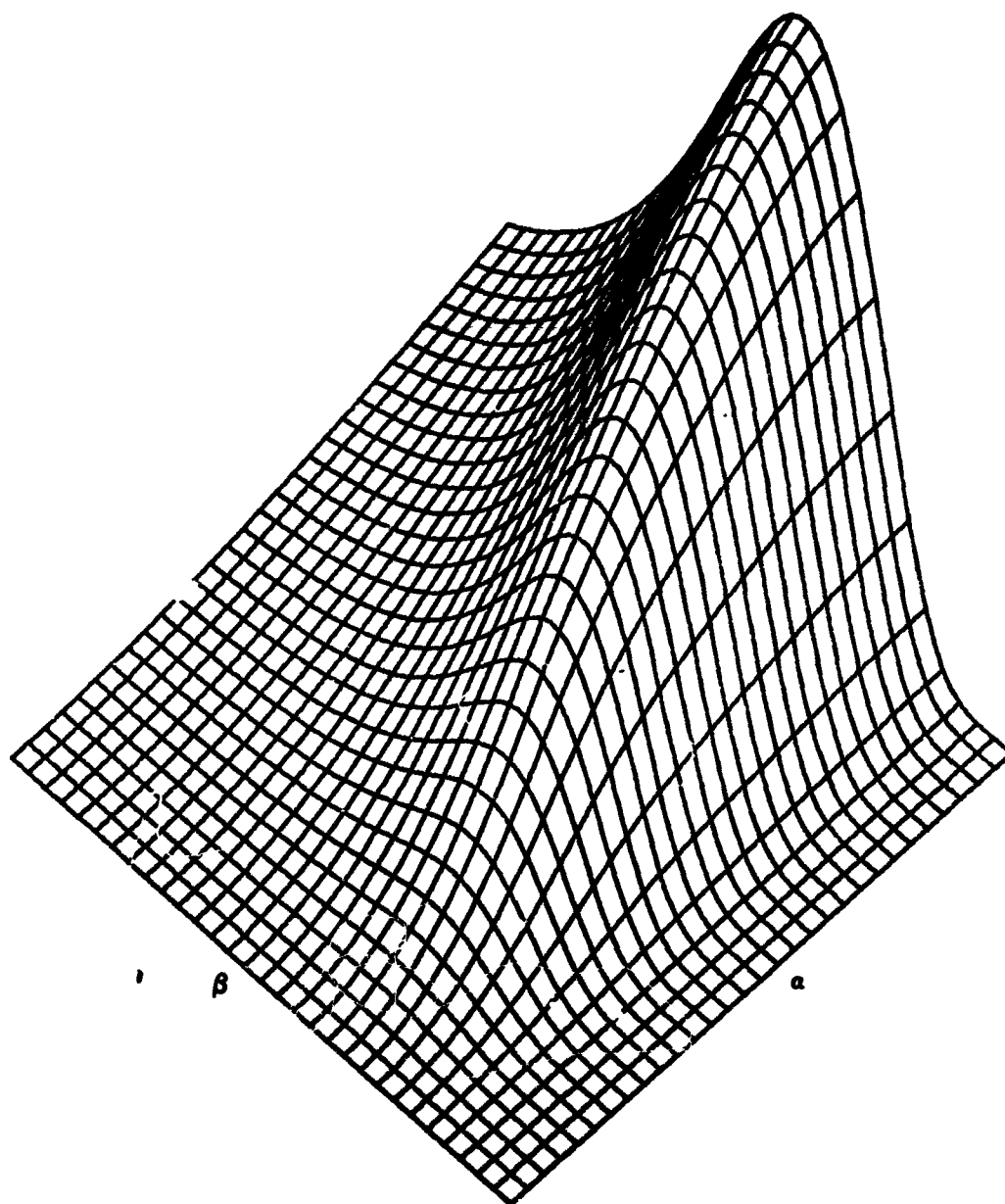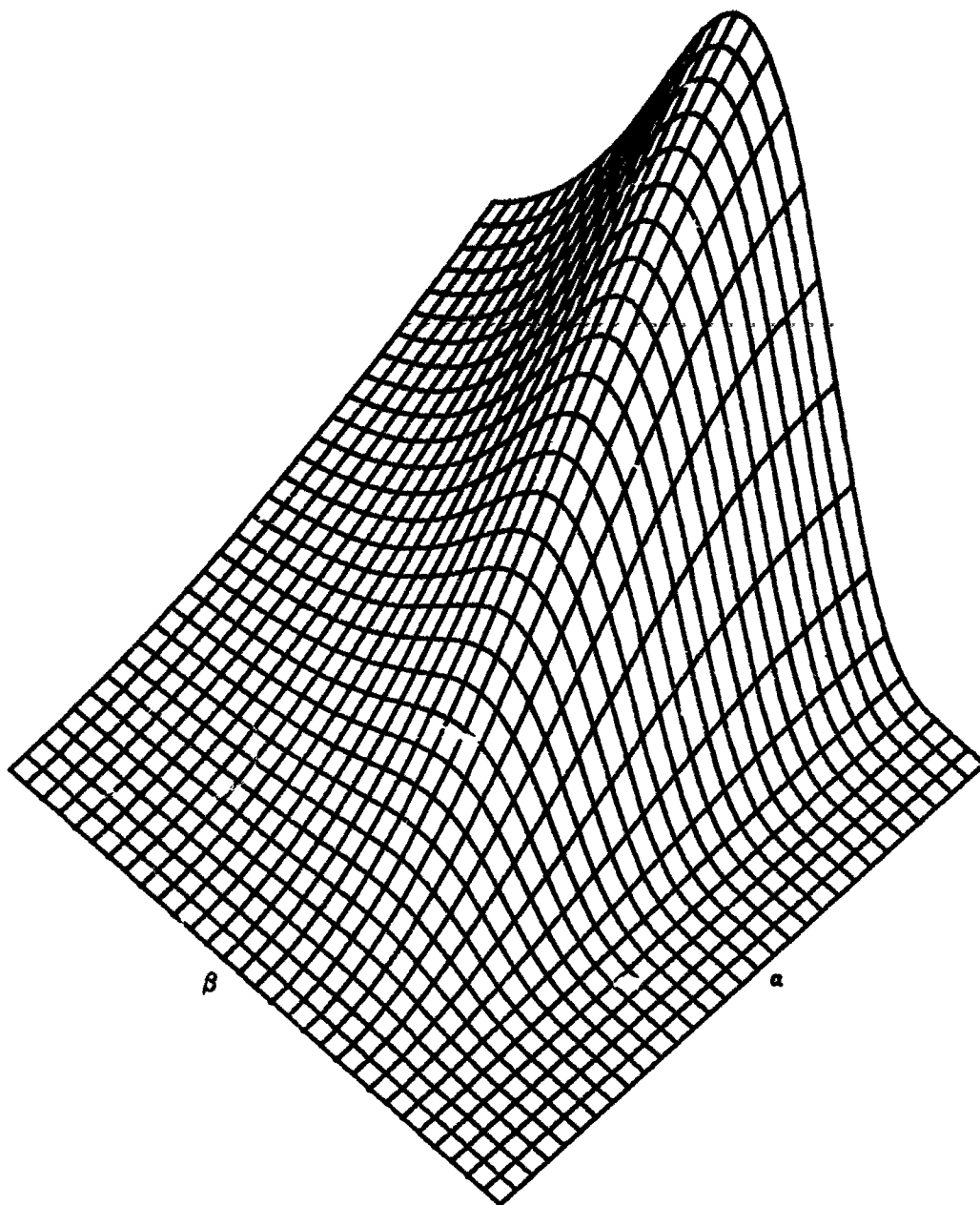$(V_1 = .395 \cdot 10^{-1}$ at $\alpha = 4\,1/3, \beta = 1.0)$
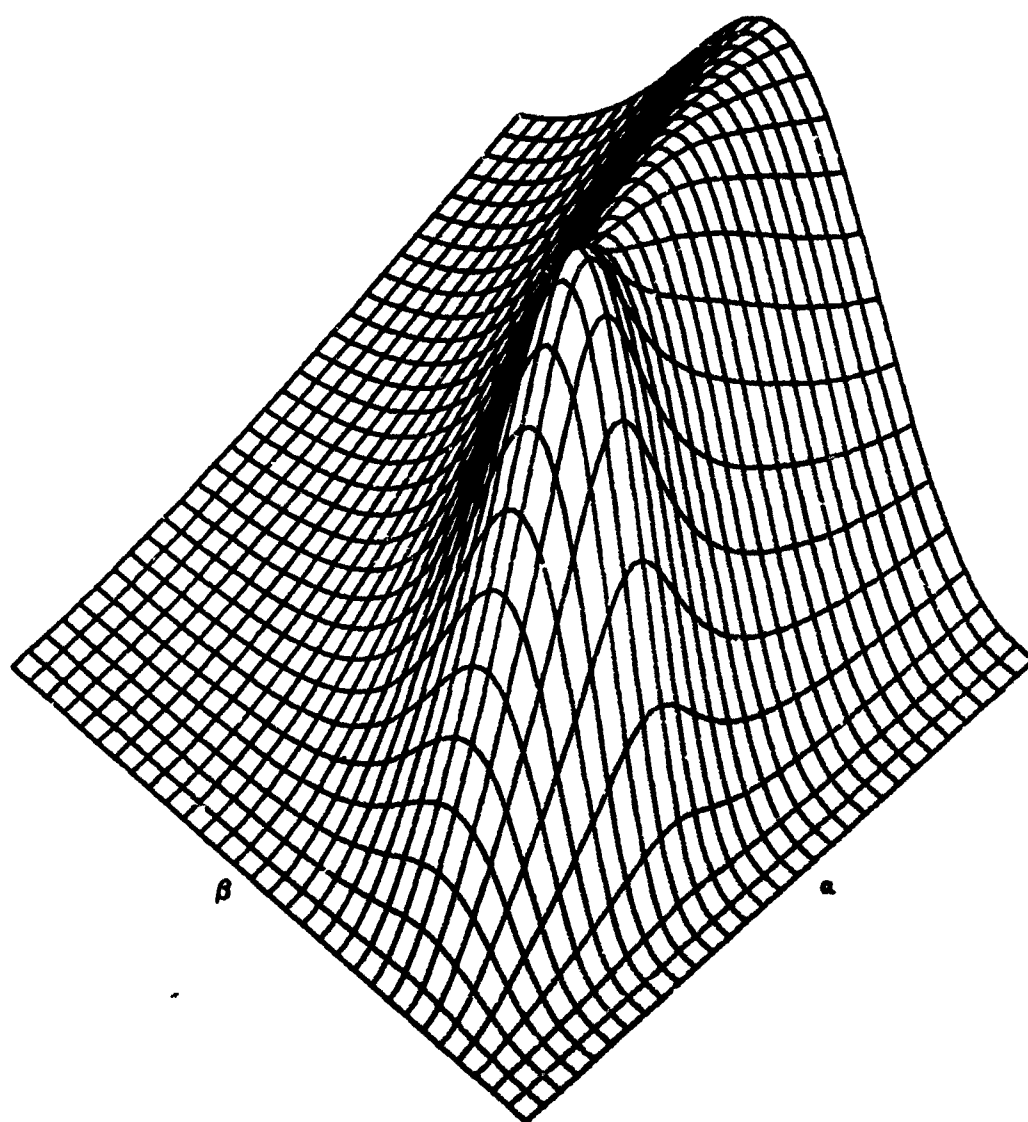
Fig. 20 - V_2 for Exponentially Modulated Bessel Function Spatial Correlation, $Q = 4$
$\left(V_2 = .106 \cdot 10^{-1} \text{ at } \alpha = 8, \beta = 1.7\right)$
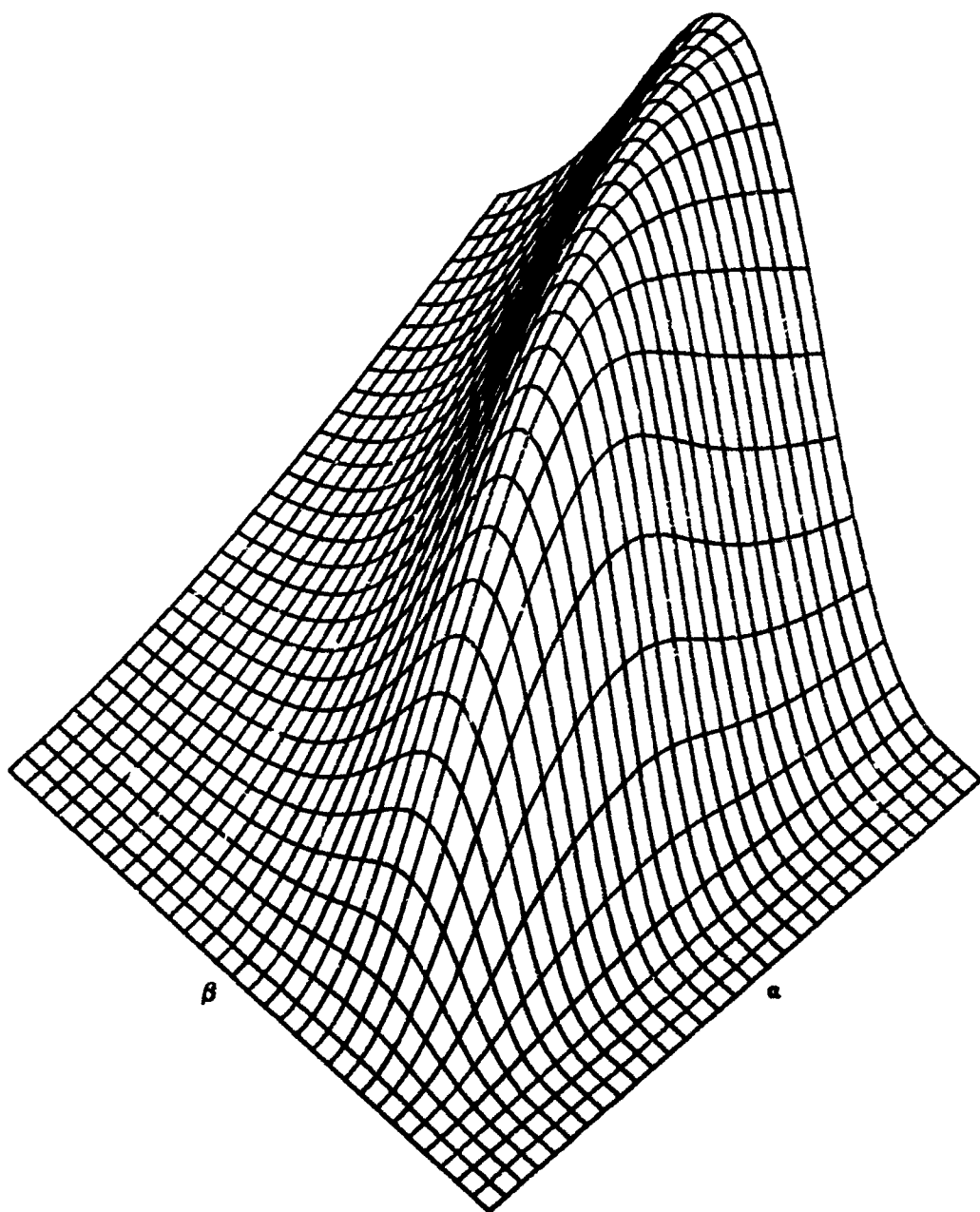
Fig. 21 - V_3 for Exponentially Modulated Bessel Function Spatial Correlation, $Q = 4$
$$\left(V_3 = .601 \cdot 10^{-2} \text{ at } \alpha = 17, \beta = 2.9\right)$$
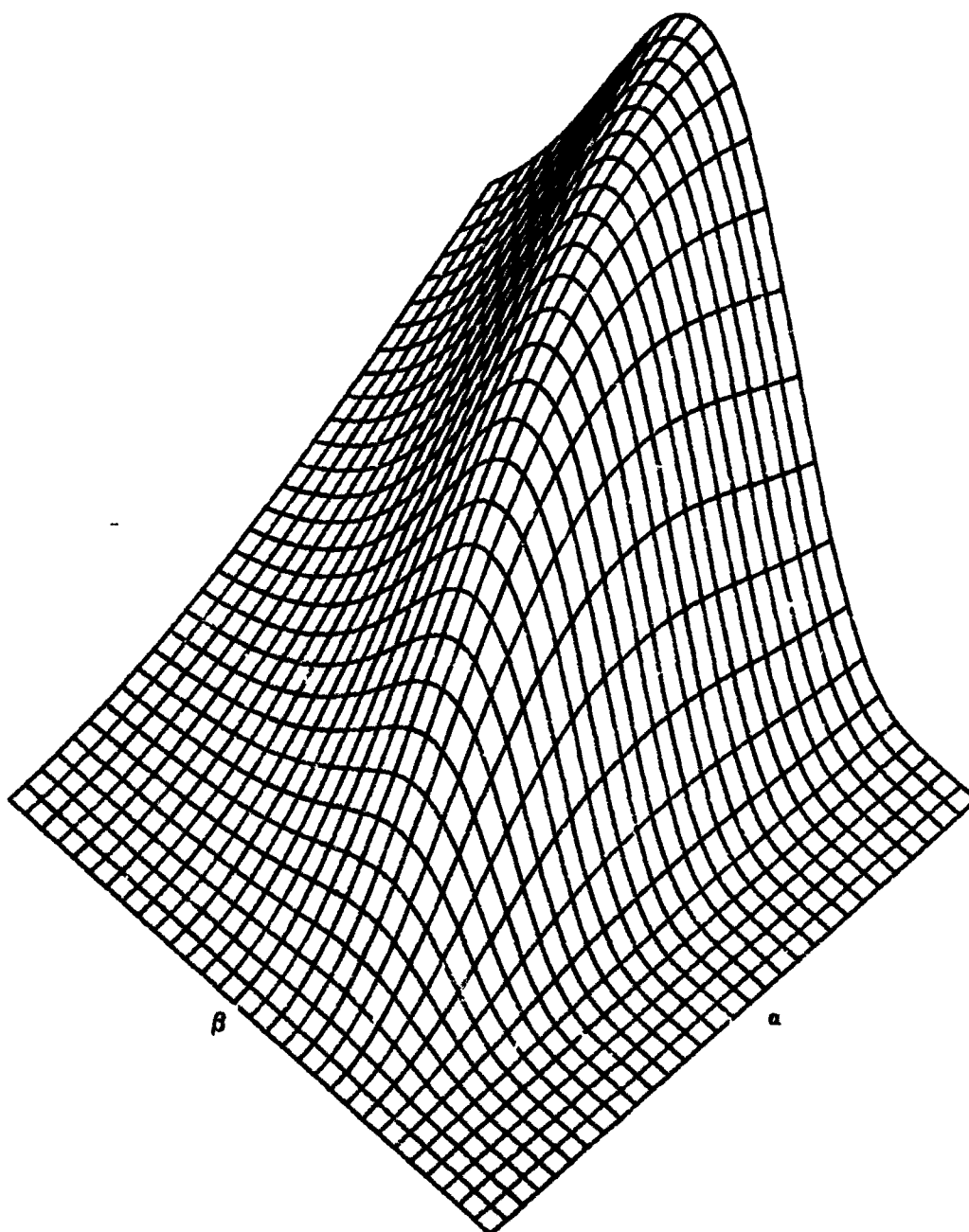
Fig. 22 - V_4 for Exponentially Modulated Bessel Function Spatial Correlation, $C = 4$
$$\left(V_4 - .425 \cdot 10^{-2} \text{ at } a - 20, \beta - 3.4\right)$$
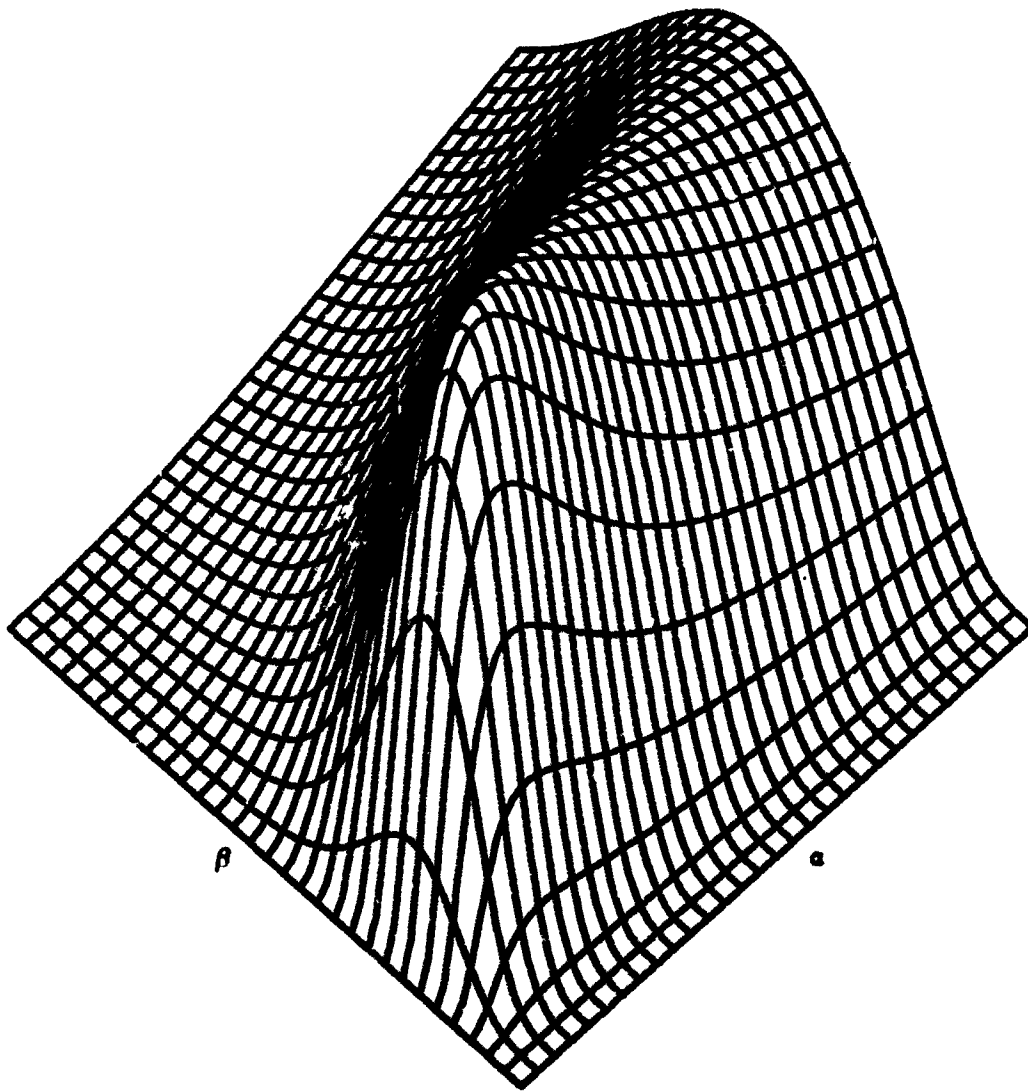
Fig. 23 - V_0 for Exponential Spatial Correlation
$\left(V_0 = .106 \cdot 10^{-1} \text{ at } \alpha = 4, \beta = 1.7 \right)$
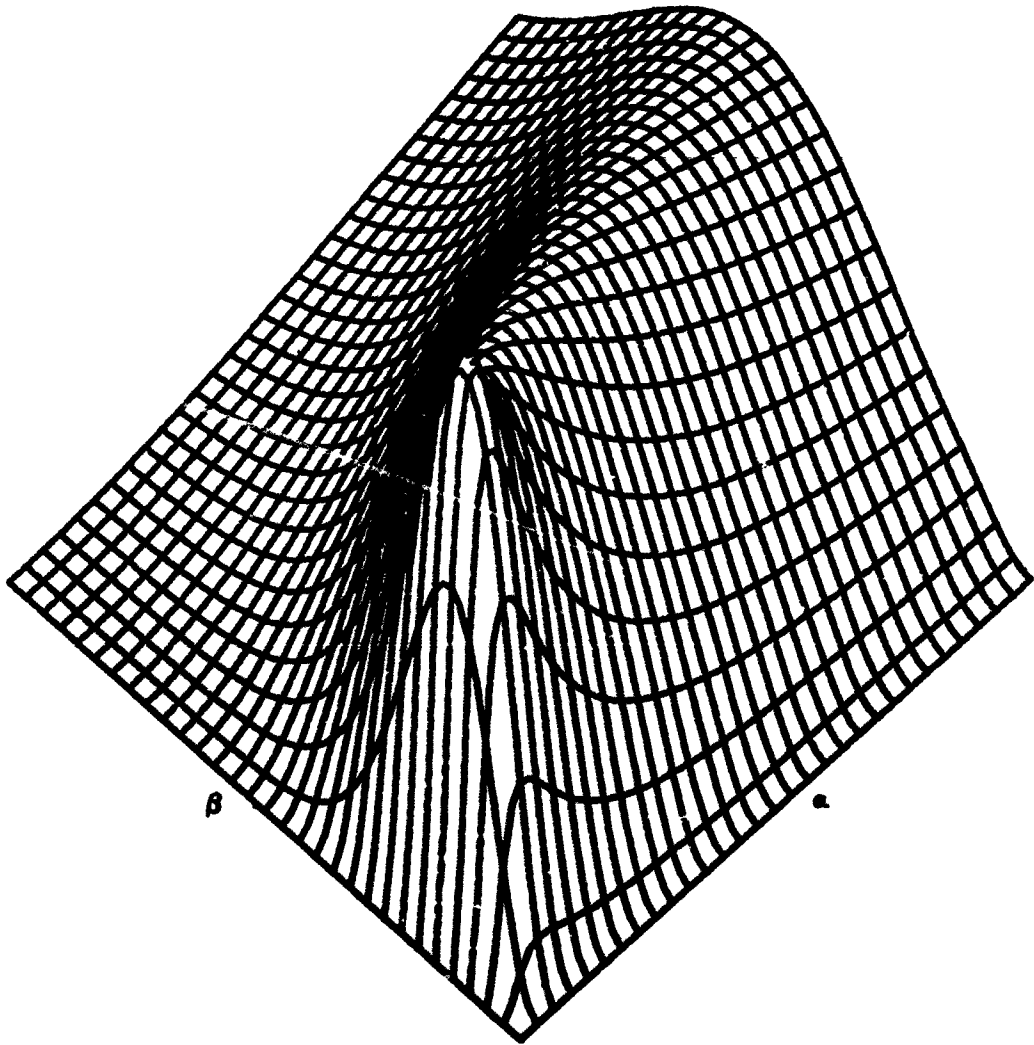
Fig. 24 - V_1 for Exponential Spatial Correlation

$$\left(V_1 = .120 \cdot 10^{-1} \text{ at } \alpha = 1\ 2/3,\ \beta = 1.1\right)$$
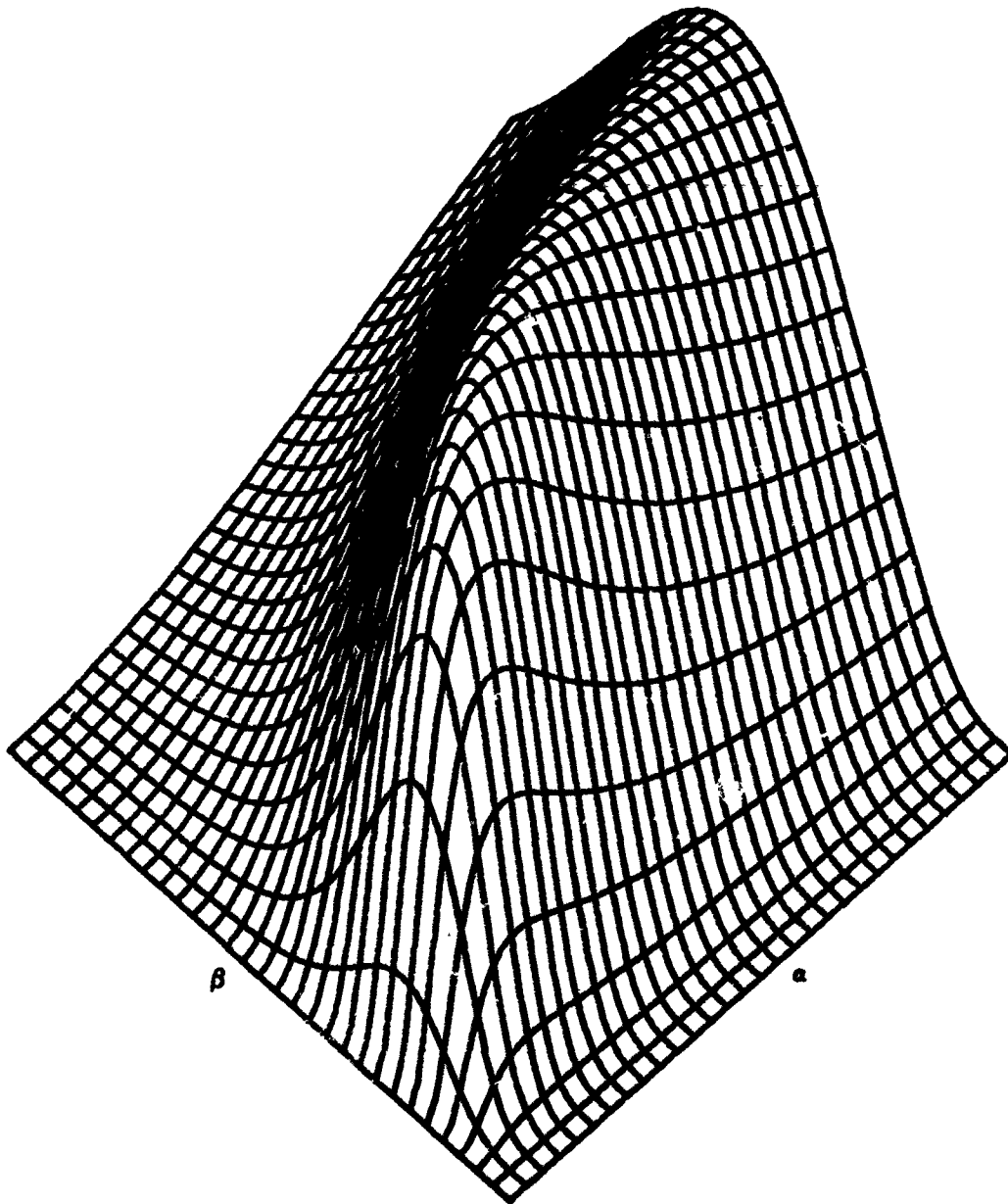
Fig. 25 - V_2 for Exponential Spatial Correlation

$\left(V_2 = .643 \cdot 10^{-2} \text{ at } \alpha = 6\ 2/3, \beta = 2.2\right)$
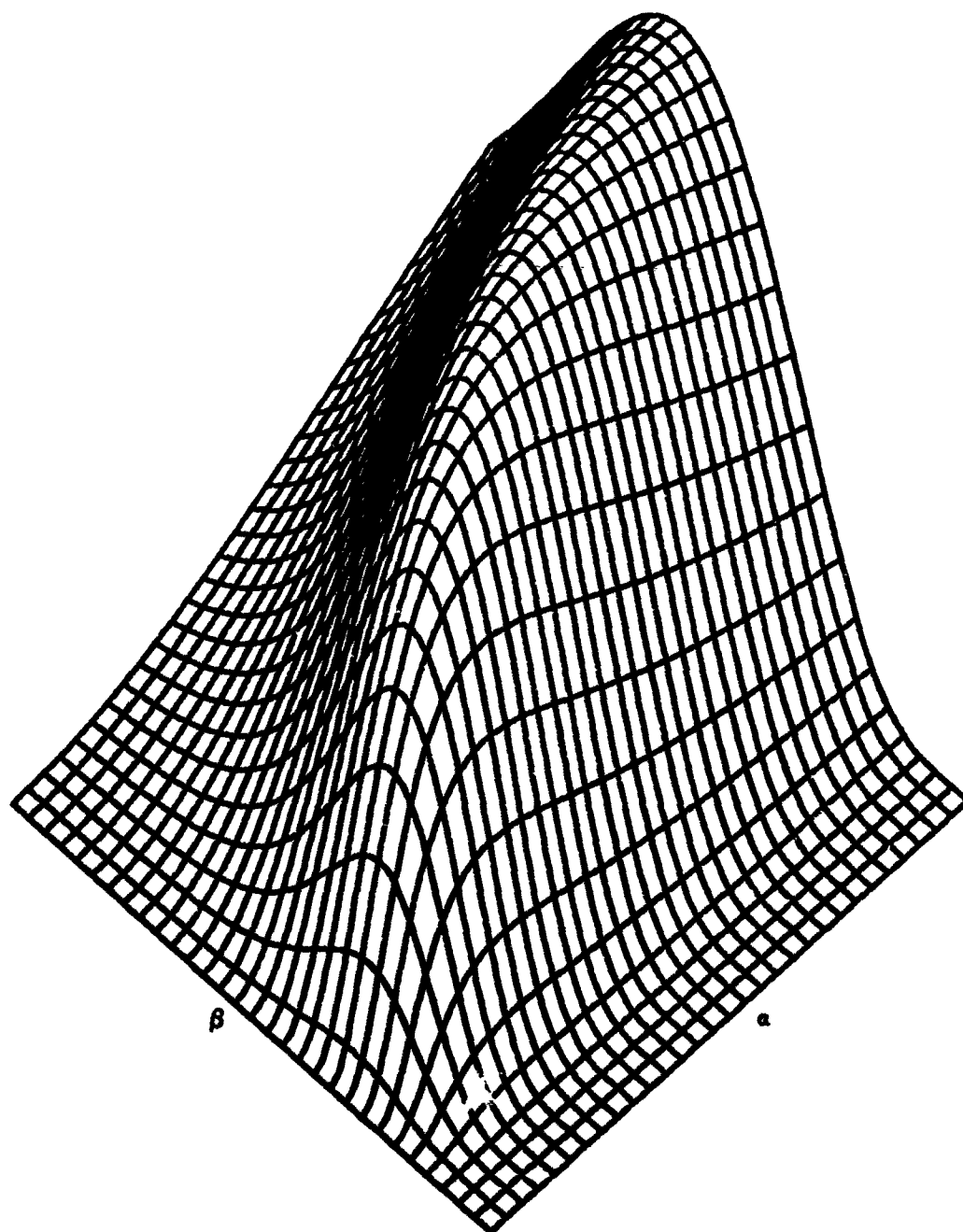
Fig. 26 - V_3 for Exponential Spatial Correlation
$\left(V_3 = .460 \cdot 10^{-2} \text{ at } \alpha = 14\ 1/3,\ \beta = 3.2\right)$

55

Fig. 27 - V_4 for Exponential Spatial Correlation

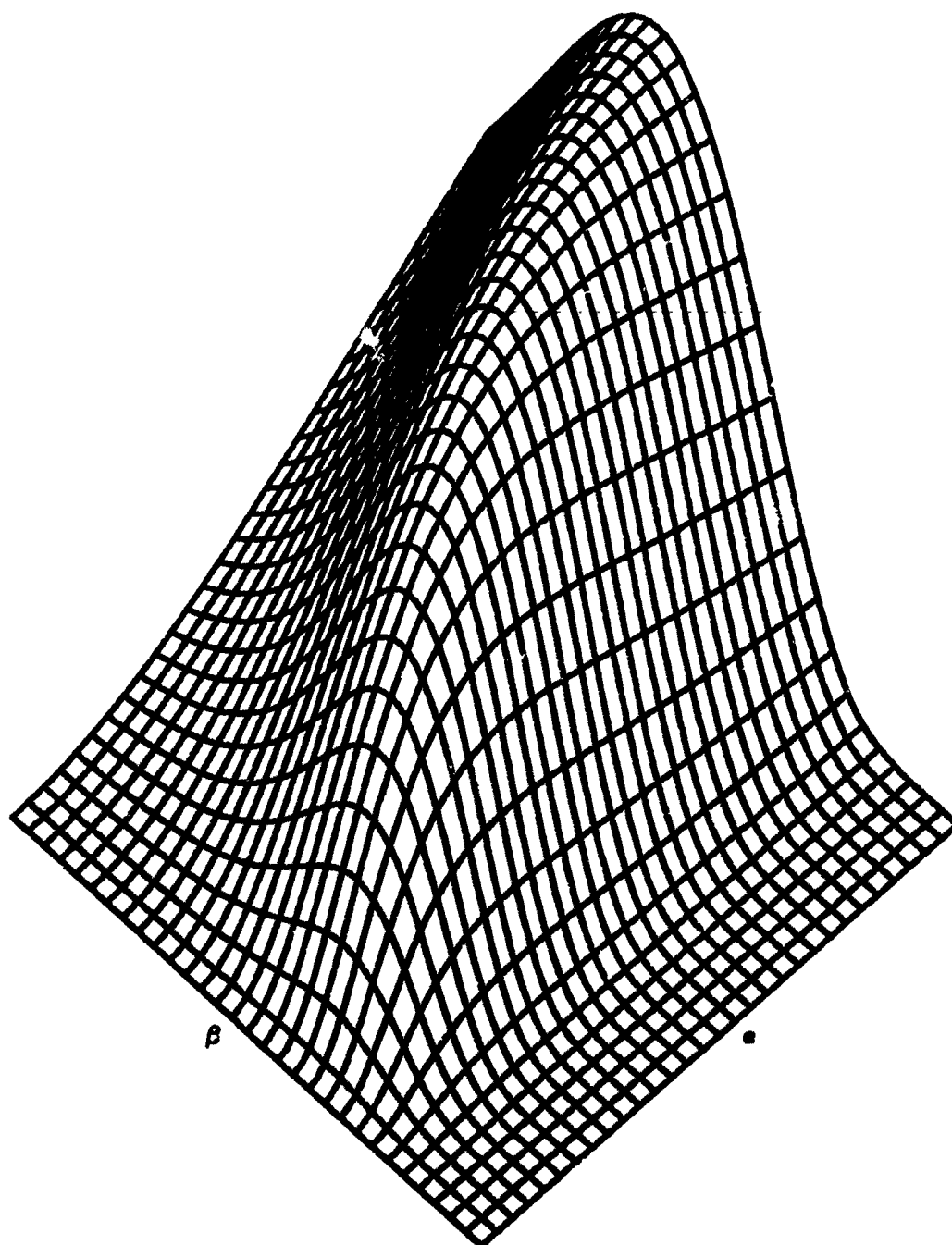$\left(V_4 = .352 \cdot 10^{-2} \text{ at } \alpha = 20, \beta = 3.9\right)$

$Q = 8, 4, 0$. In Figs. 28 through 42, a similar set of curves is plotted; the only difference is that the spatial correlation is a Gaussianly modulated Bessel function of the form of (120). These functions were computed for $\alpha = 0(1/3)20$ and $\beta = 0(.1)6$. The maximum·values attained by $V_m(\alpha, \beta)$ at this grid structure are presented in Table 1 and are noted on each plot. (These values are not necessarily the maximum values of $V_m(\alpha, \beta)$, but simply the maximum values at the sample points investigated.) Since the plots are isometric, values of $V_m(\alpha, \beta)$ at other values of α, β can be obtained by measuring the vertical distance above the α, β plane and scaling according to the values given.

To explain the detailed behavior of these plots, it is helpful to consider β as a measure of the surface vertical roughness, and α as a measure of the surface horizontal roughness. As β increases, the surface becomes rougher in the vertical direction; also as α decreases, i.e., the correlation distances decrease, the surface becomes rougher in the horizontal direction. For a given α, the behavior of $V_m(\alpha, \beta)$ with β is similar to that observed in Figs. 7 through 12.

For $\beta = 0$, $V_m(\alpha, \beta)$ is zero for all α since the surface is flat and there is no scattered power. As β increases, the scattered power increases, reaching a maximum. As β increases still further, the curve decreases, indicating that more of the scattered power appears in higher order sidebands. Note from the plots that for a given surface spatial correlation and a given Q, the location (α, β), at which $V_m(\alpha, \beta)$ reaches a maximum value, increases as m increases; i.e., the peak location recedes from the origin.

For a given β (fixed roughness) and a large α (large correlation distances), the surface is very planar, resulting in most of the reflected power appearing in the specular direction. As α decreases from large values, the surface becomes less planar, more power is scattered in the nonspecular direction, and V_m increases. However, as α decreases still further, the surface becomes rougher in the horizontal direction, and more of the scattered power appears in the higher order sidebands, so that each particular $V_m(\alpha, \beta)$ decreases with α in this range. The ratio β/α is a measure of the average slope of the surface; as this ratio increases, more of the scattered

Table 1

APPROXIMATE LOCATIONS OF MAXIMUM
VALUES OF $V_m (\alpha, \beta)$

Fig. No.	α	β	$V_m (\alpha, \beta)$
13	15 1/3	1.6	$.268 \cdot 10^{-1}$
14	8	1.0	$.763 \cdot 10^{-1}$
15	15 1/3	1.6	$.144 \cdot 10^{-1}$
16	20	2.4	$.678 \cdot 10^{-2}$
17	20	2.9	$.392 \cdot 10^{-2}$
18	7 2/3	1.6	$.196 \cdot 10^{-1}$
19	4 1/3	1.0	$.395 \cdot 10^{-1}$
20	8	1.7	$.106 \cdot 10^{-1}$
21	17	2.9	$.601 \cdot 10^{-2}$
22	20	3.4	$.425 \cdot 10^{-2}$
23	4	1.7	$.106 \cdot 10^{-1}$
24	1 2 3	1.1	$.120 \cdot 10^{-1}$
25	6 2 3	2.2	$.643 \cdot 10^{-2}$
26	14 1 3	3.2	$.460 \cdot 10^{-2}$
27	20	3.9	$.352 \cdot 10^{-2}$
28	15	1.6	$.325 \cdot 10^{-1}$
29	8 1/3	1.0	$.705 \cdot 10^{-1}$
30	15 1/3	1.7	$.177 \cdot 10^{-1}$
31	20	2.7	$.890 \cdot 10^{-2}$
32	20	3.1	$.570 \cdot 10^{-2}$
33	7 2/3	1.6	$.249 \cdot 10^{-1}$
34	4 2/3	1.1	$.398 \cdot 10^{-1}$
35	8	1.8	$.141 \cdot 10^{-1}$
36	13 1/3	3.1	$.903 \cdot 10^{-2}$
37	18	4.1	$.690 \cdot 10^{-2}$
38	3	1.7	$.210 \cdot 10^{-1}$
39	2	1.1	$.237 \cdot 10^{-1}$
40	4	2.2	$.125 \cdot 10^{-1}$
41	6 1/3	3.3	$.886 \cdot 10^{-2}$
42	8	4.1	$.683 \cdot 10^{-2}$

Fig. 28 - V_0 for Gaussianly Modulated Bessel Function Spatial Correlation, $Q = 8$
$\left(V_0 = .325 \cdot 10^{-1} \text{ at } \alpha = 15, \beta = 1.6\right)$
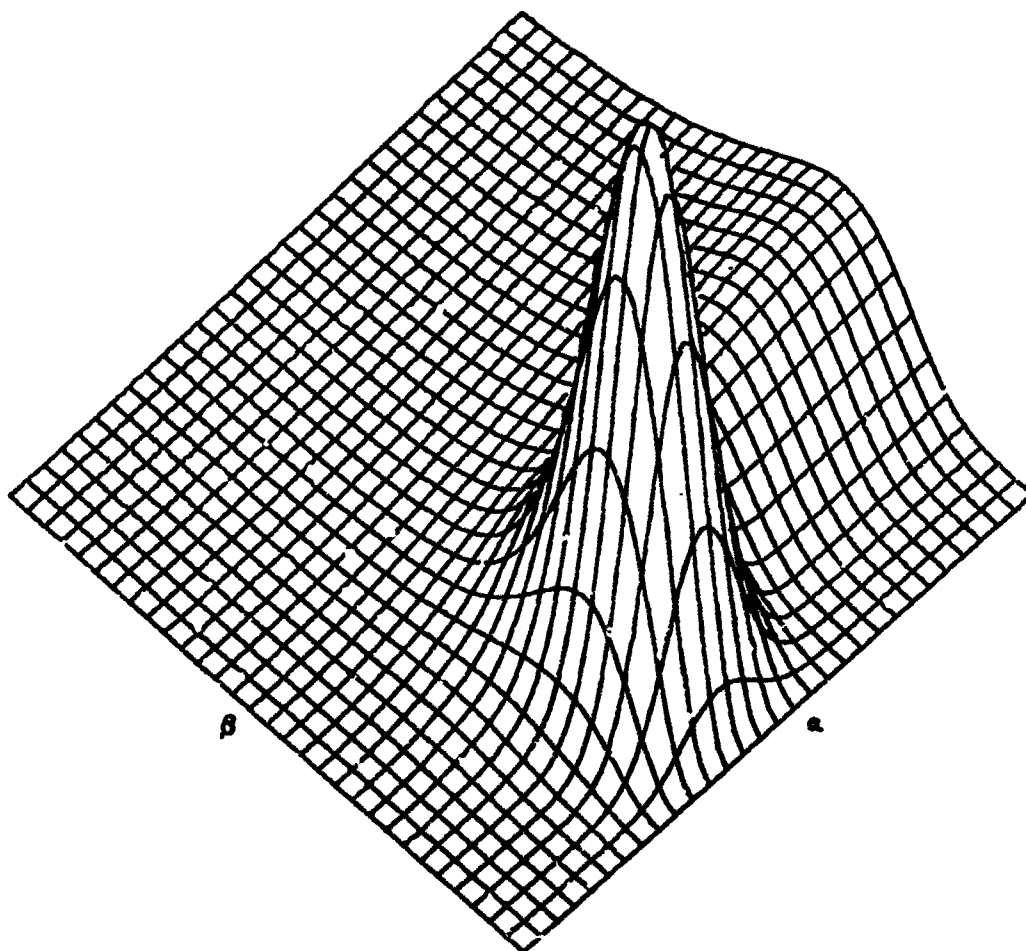
Fig. 29 - V_1 for Gaussianly Modulated Bessel Function Spatial Correlation, $Q = 8$
$\left(V_1 = .705 \cdot 10^{-1} \text{ at } \alpha = 8\ 1/3, \beta = 1.0\right)$

60
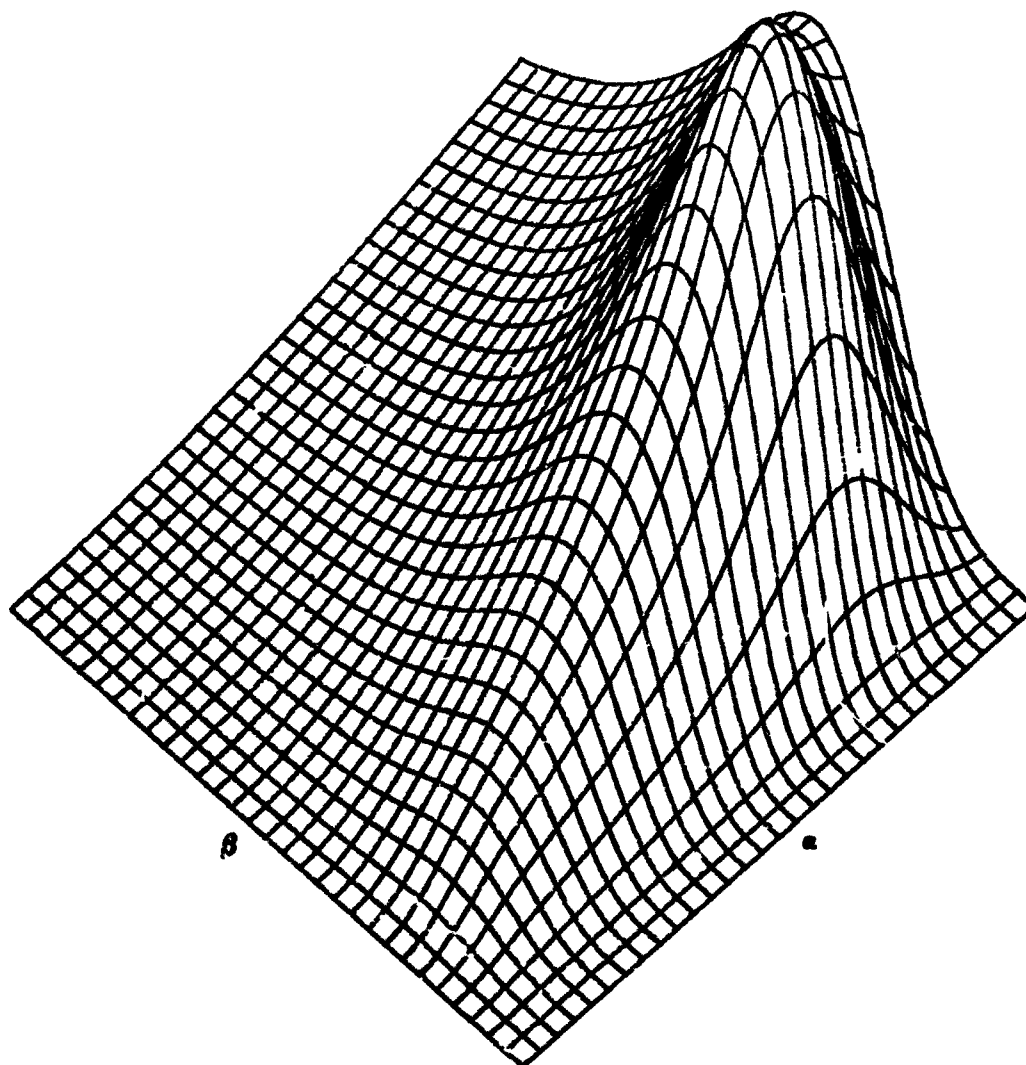
Fig. 30 - V_2 for Gaussianly Modulated Bessel Function Spatial Correlation, $Q = 8$
$\left(V_2 = .177 \cdot 10^{-1} \text{ at } \alpha = 15\,1/3, \beta = 1.7\right)$
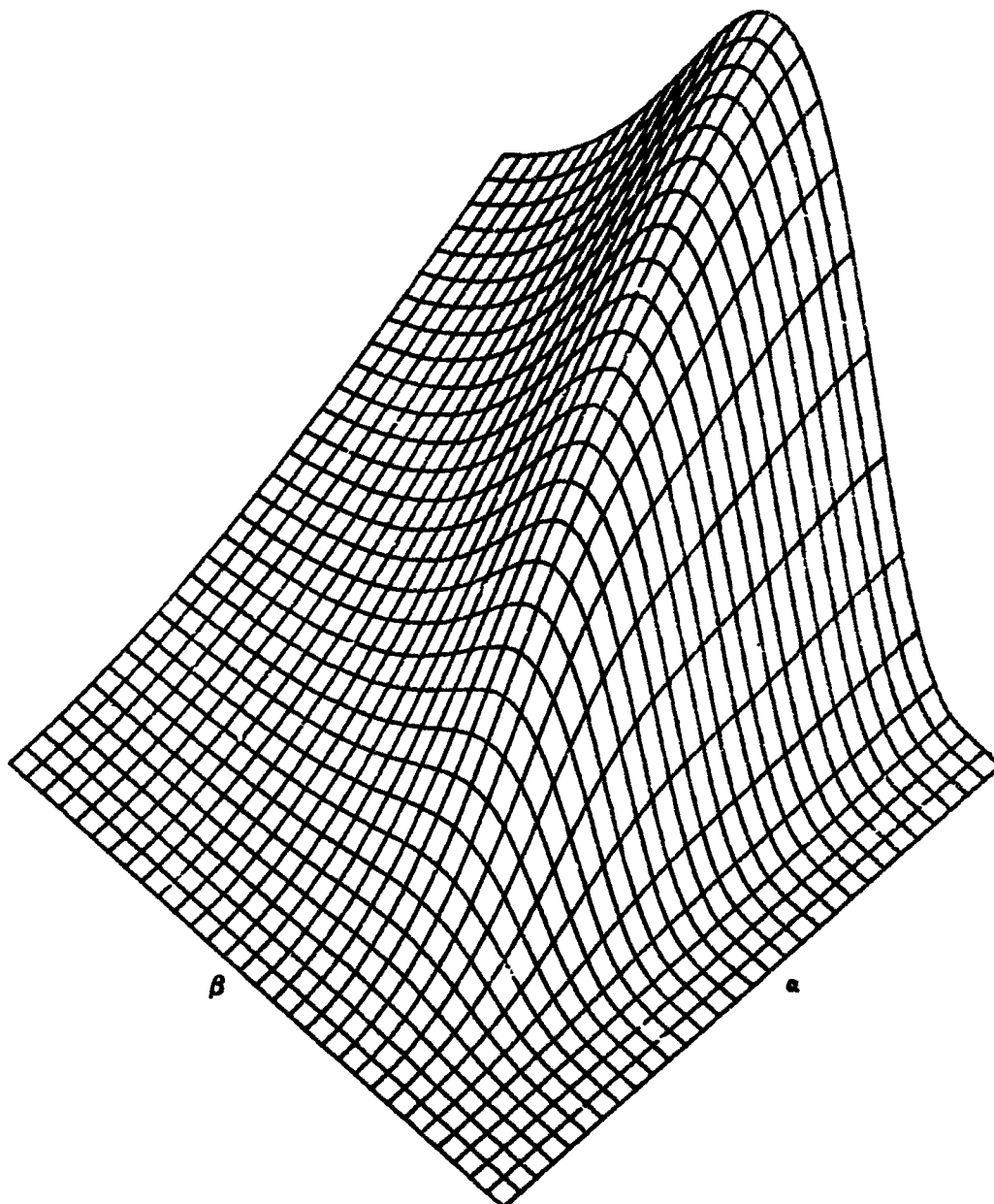
Fig. 31 - V_3 for Gaussianly Modulated Bessel Function Spatial Correlation, $Q = 8$

$\left(V_3 = .890 \cdot 10^{-2} \text{ at } \alpha = 20, \beta = 2.7\right)$
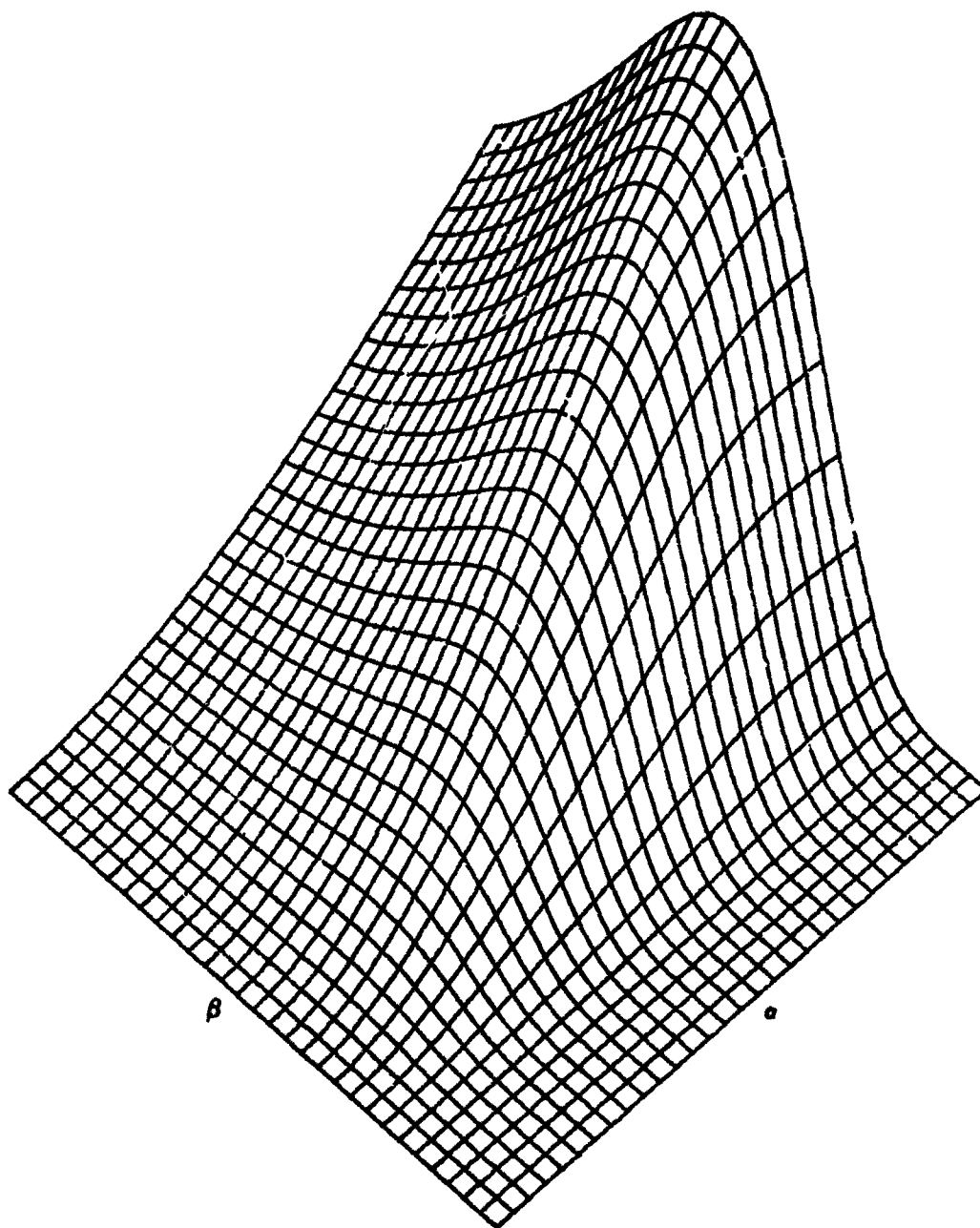
Fig. 32 - V_4 for Gaussianly Modulated Bessel Function Spatial Correlation, $Q = 8$

$\left(V_4 = .570 \cdot 10^{-2} \text{ at } \alpha = 20, \beta = 3.1\right)$
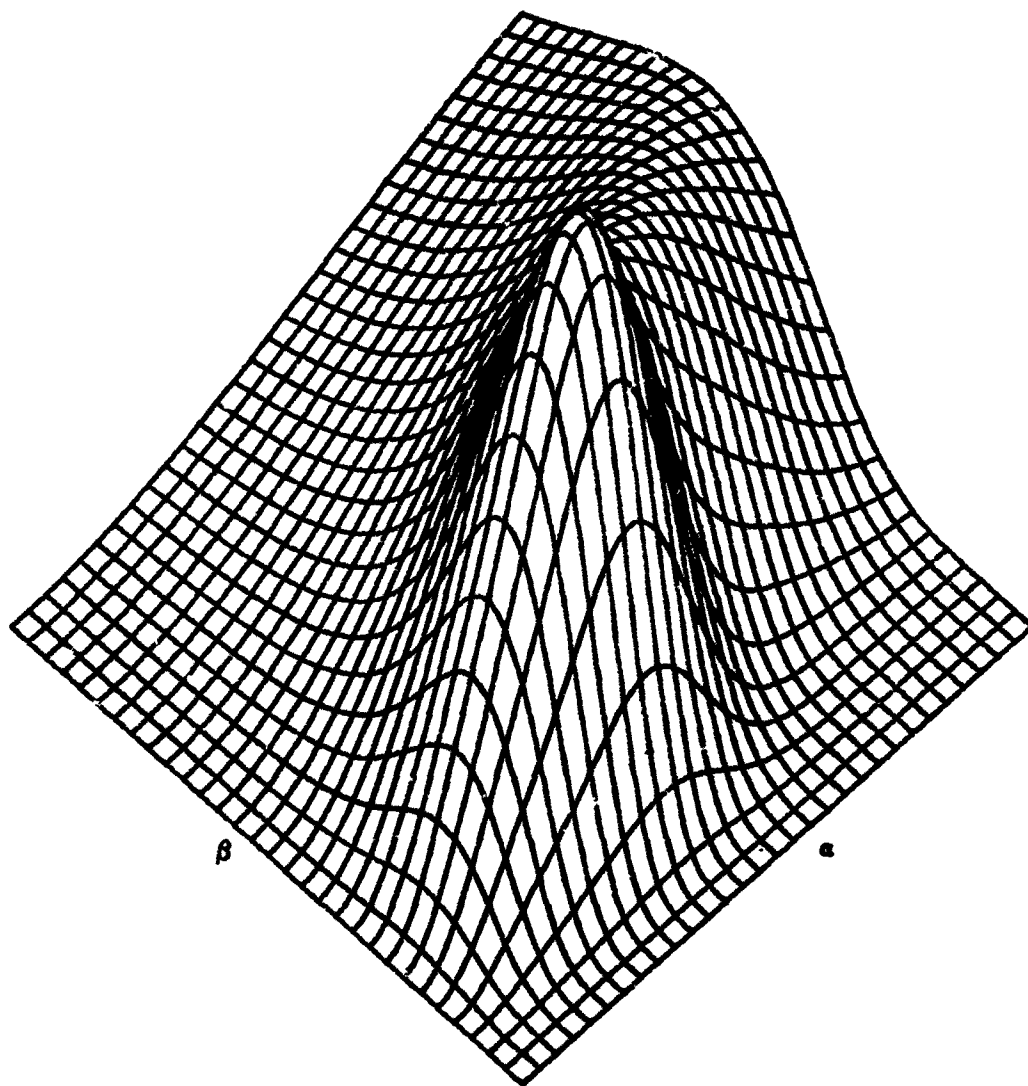
Fig. 33 - V_0 for Gaussianly Modulated Bessel Function Spatial Correlation, Q = 4
$\left(V_0 = .249 \cdot 10^{-1} \text{ at } \alpha = 7\,2/3, \beta = 1.6\right)$
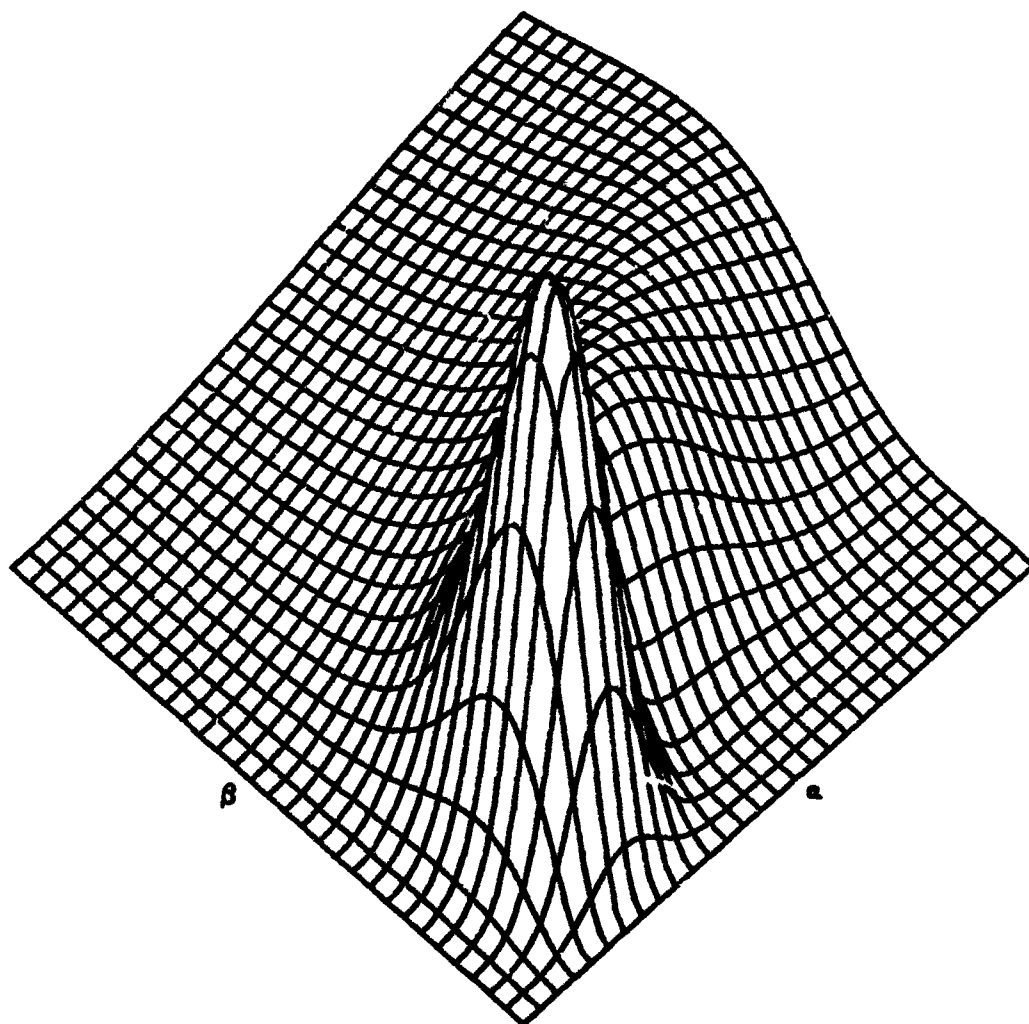
Fig. 34 - V_1 for Gaussianly Modulated Bessel Function Spatial Correlation, $Q = 4$
$\left(V_1 = .398 \cdot 10^{-1} \text{ at } \alpha = 4\,2/3,\ \beta = 1.1 \right)$
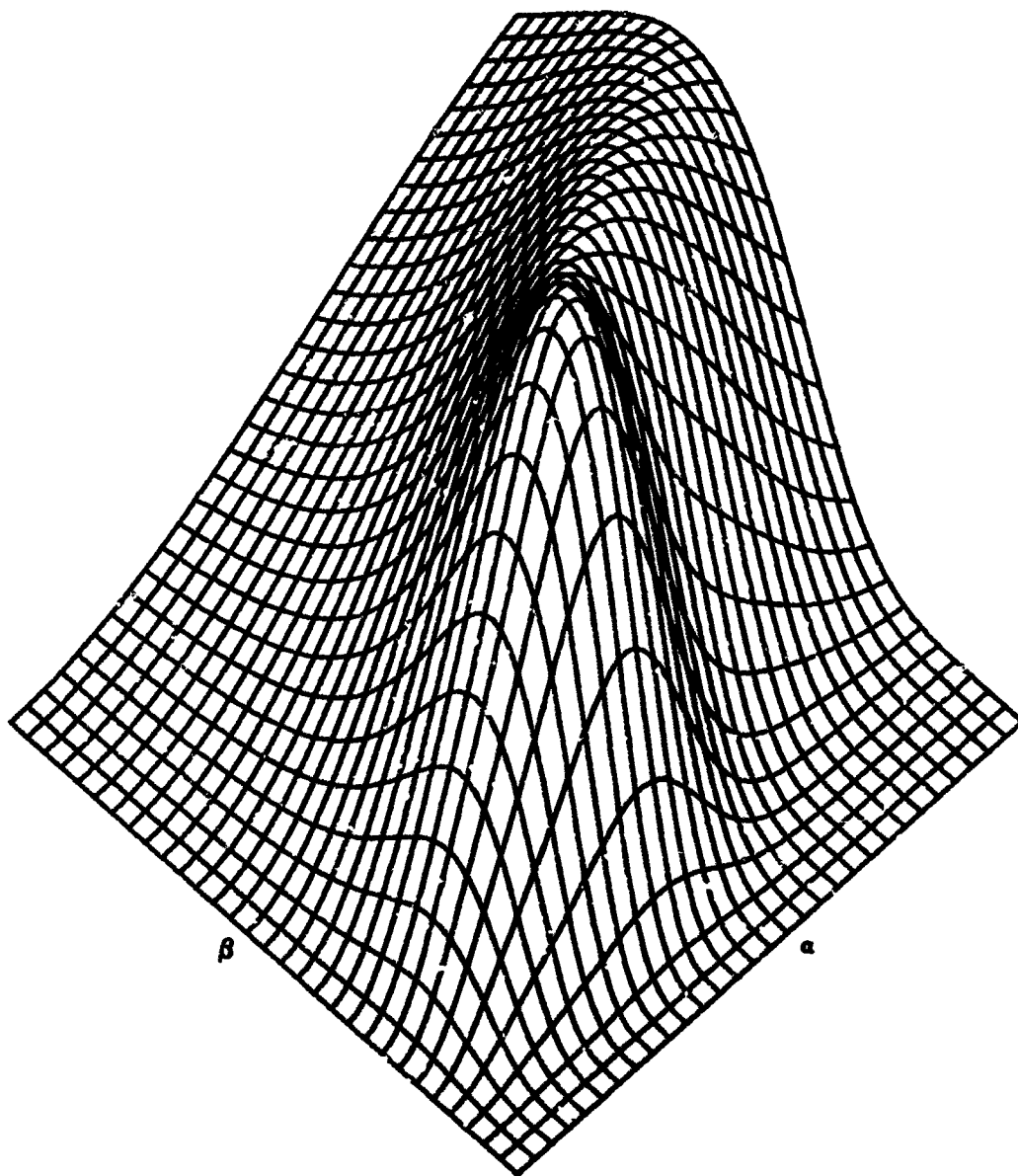
Fig. 35 - V_2 for Gaussianly Modulated Bessel Function Spatial Correlation, $Q = 4$
$\left(V_2 = .141 \cdot 10^{-1} \text{ at } a = 8, \beta = 1.8\right)$
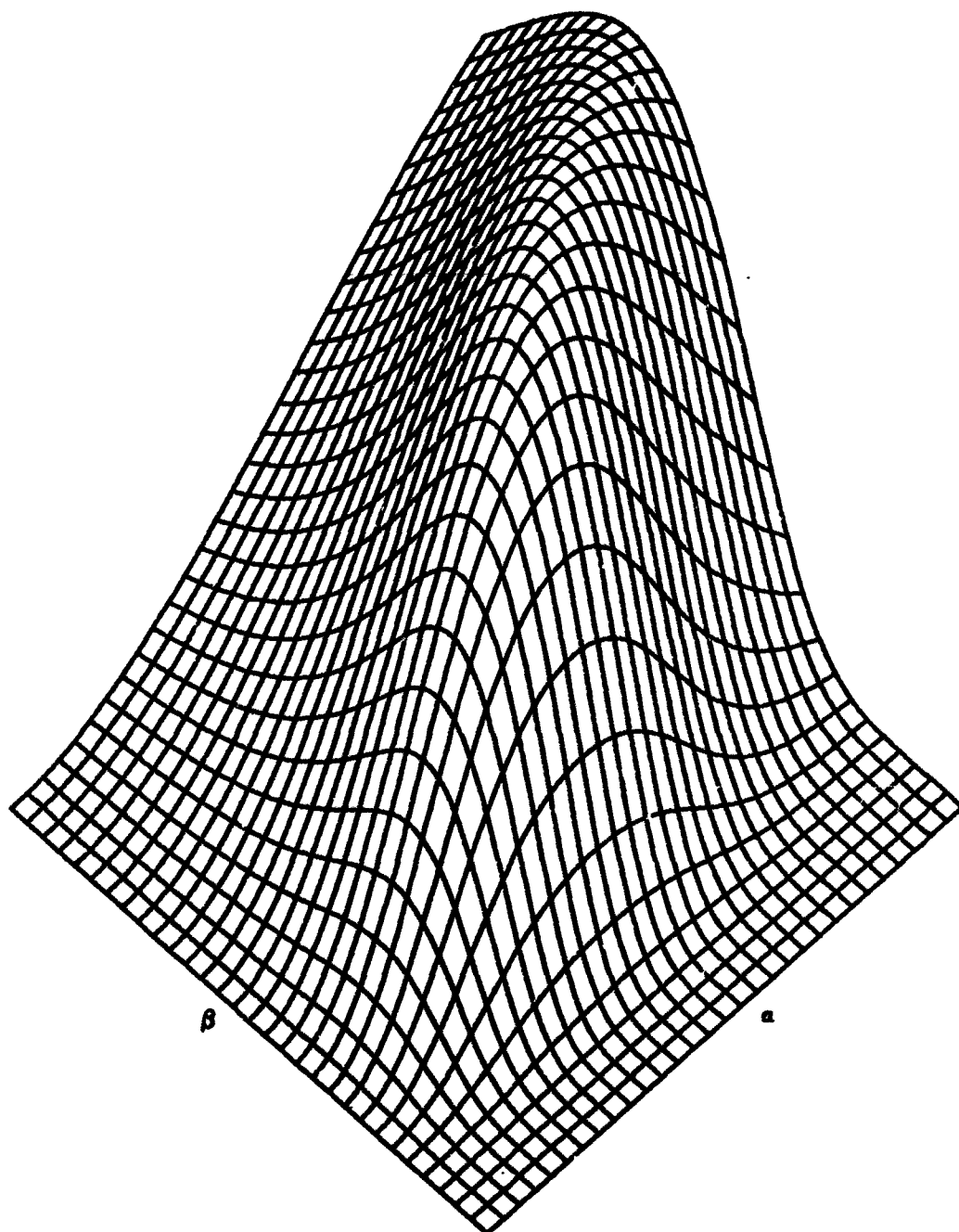
Fig. 36 - V_3 for Gaussianly Modulated Bessel Function Spatial Correlation, $Q = 4$,
$\left(V_3 = .90? \cdot 10^{-2} \text{ at } \alpha = 13 \, 1/3, \, \beta = 3.1\right)$
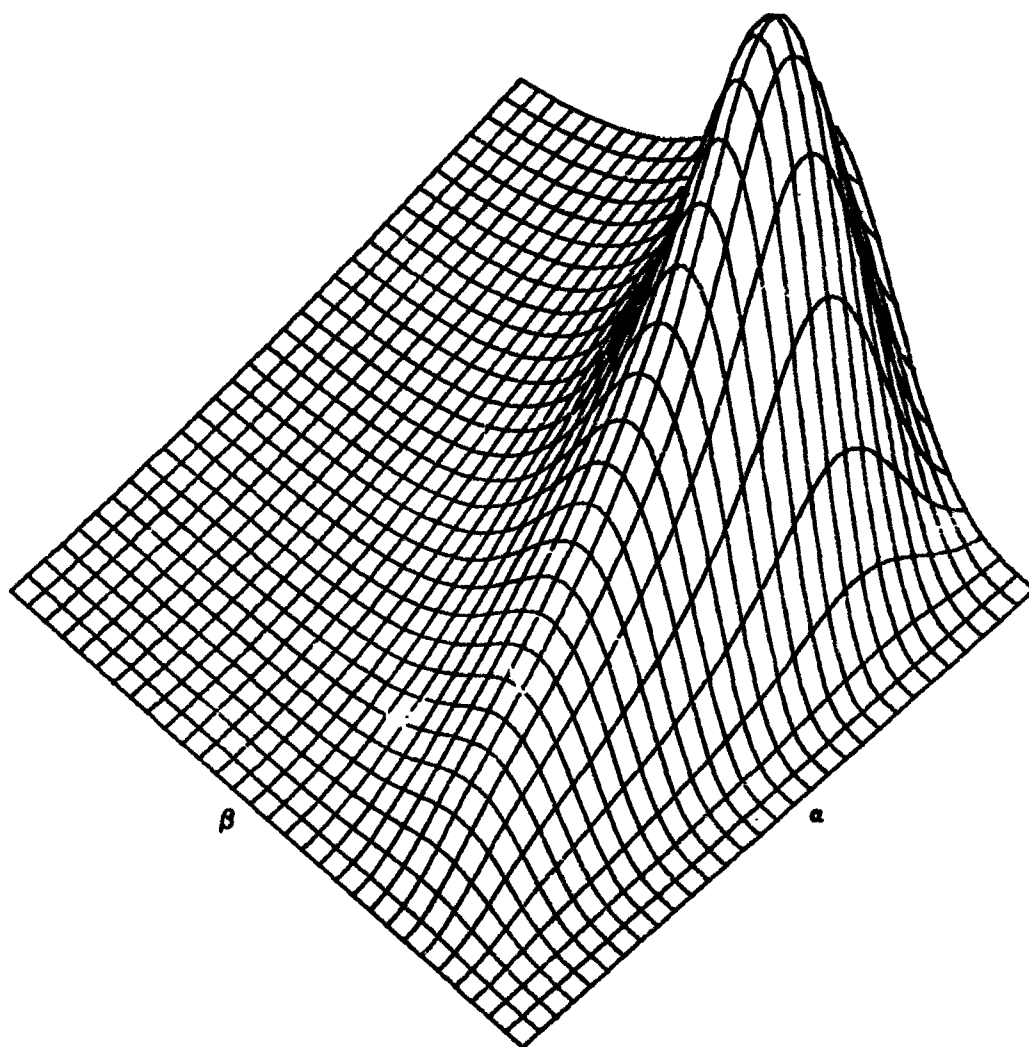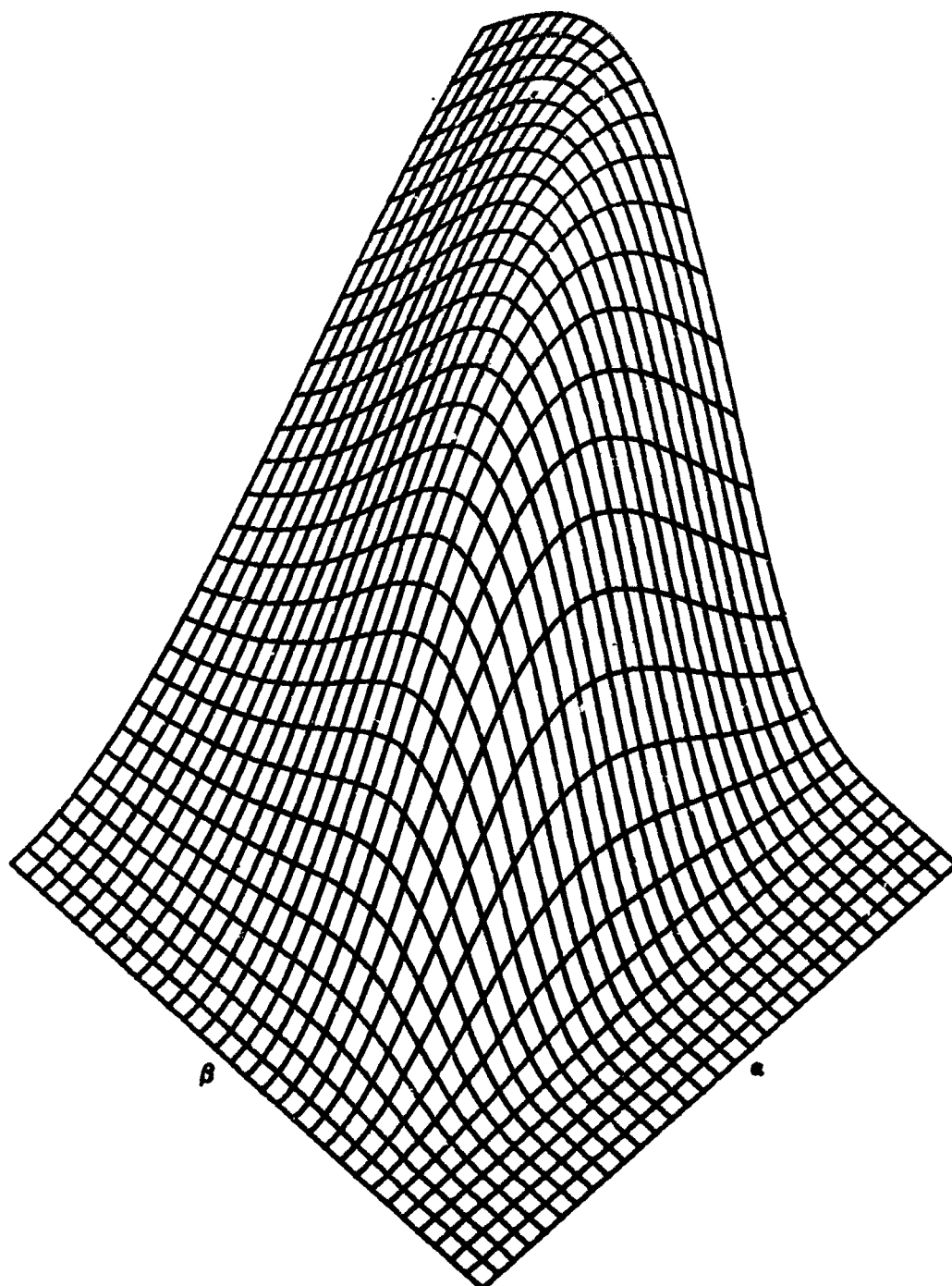
Fig. 37 - V_4 for Gaussianly Modulated Bessel Function Spatial Correlation, $Q = 4$
$(V_4 = .690 \cdot 10^{-2}$ at $\alpha = 18, \beta = 4.1)$

68

Fig. 38 - V_0 for Gaussian Spatial Correlation
$\left(V_0 = .210 \cdot 10^{-1} \text{ at } \alpha = 3, \beta = 1.7\right)$

Fig. 39 - V_1 for Gaussian Spatial Correlation
$\left(V_1 = .237 \cdot 10^{-1} \text{ at } \alpha = 2, \beta = 1.1\right)$
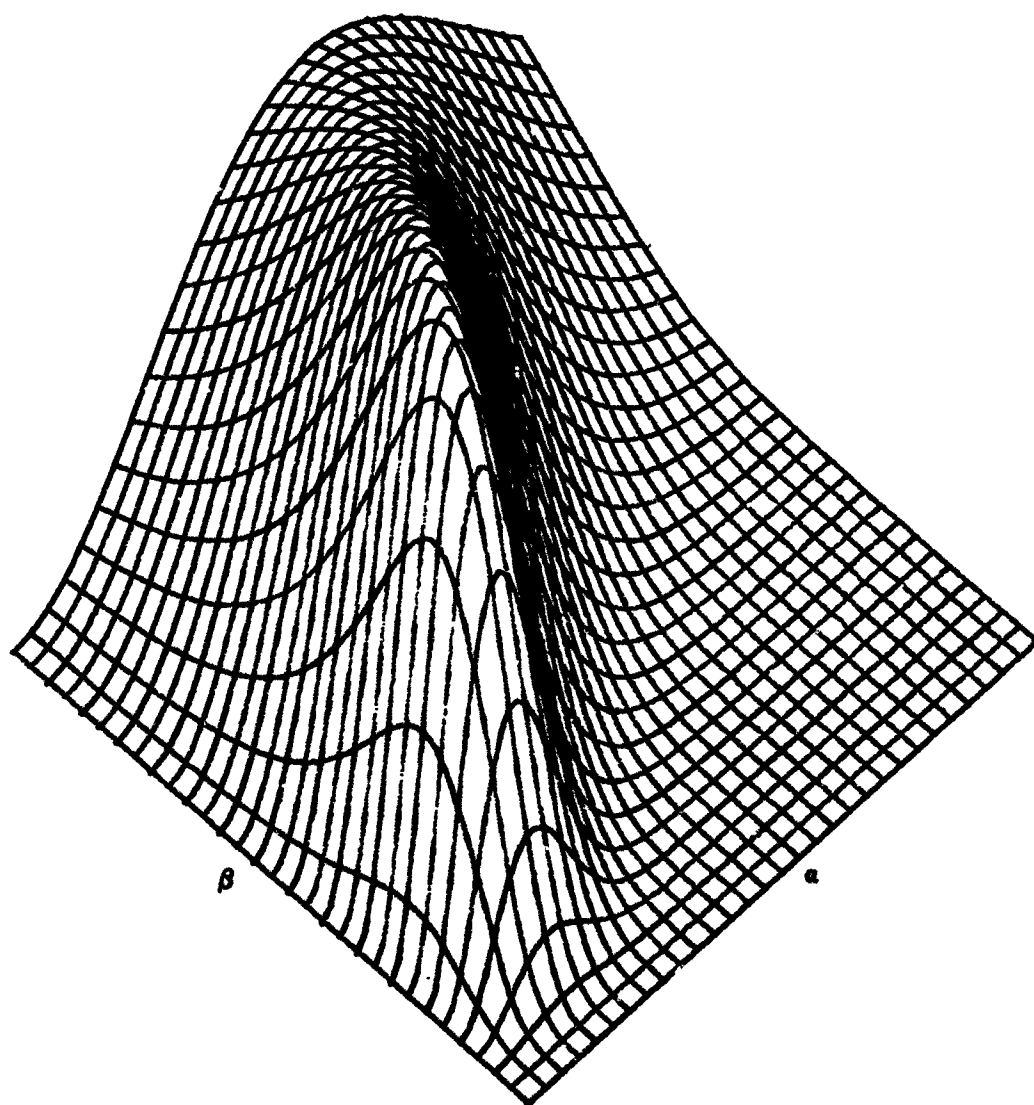
Fig. 40 - V_2 for Gaussian Spatial Correlation
$(V_2 = .125 \cdot 10^{-1}$ at $\alpha = 4, \beta = 2.2)$
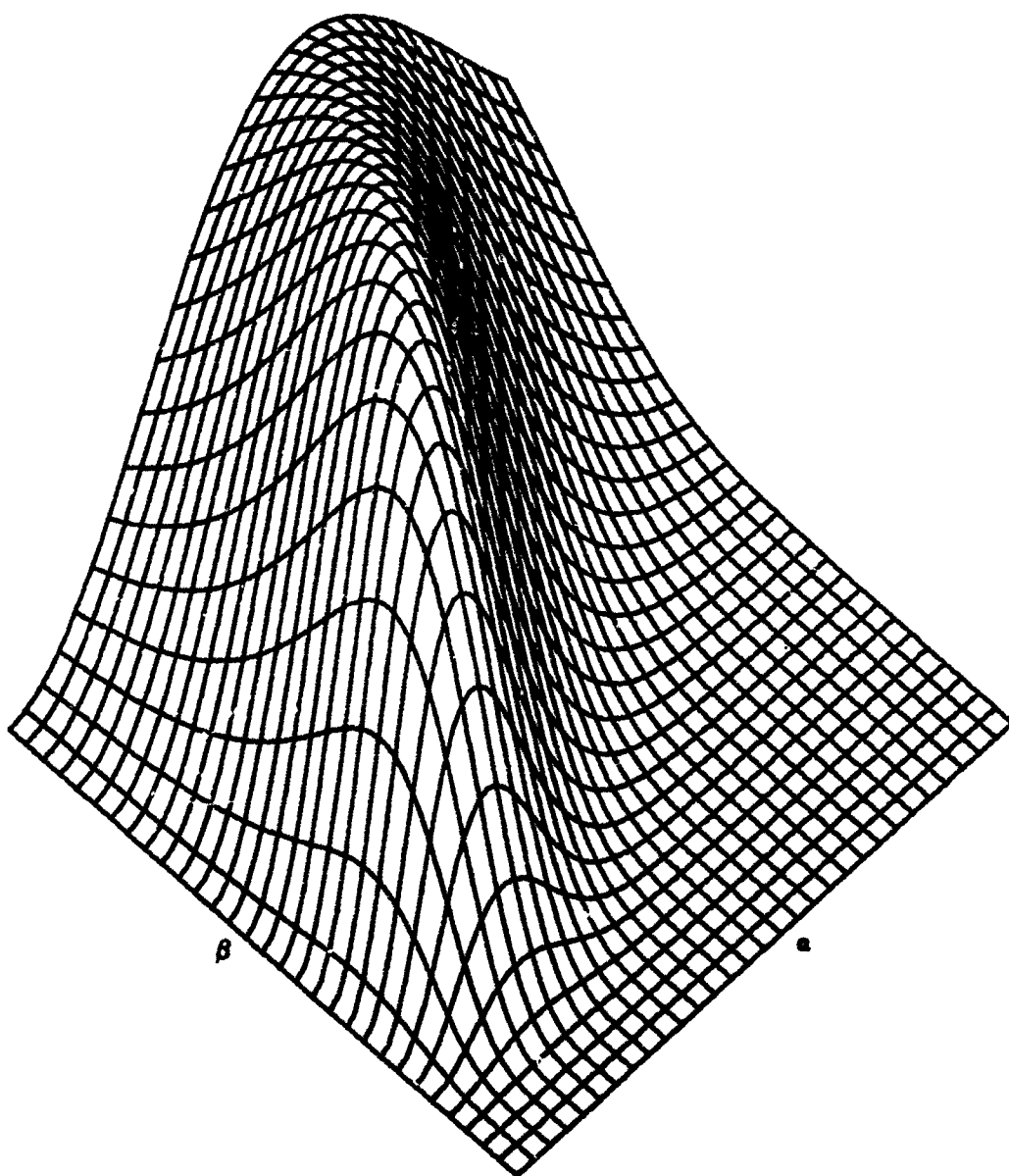
Fig. 41 - V_3 for Gaussian Spatial Correlation
$(V_3 = .886 \cdot 10^{-2}$ at $c = 6 \, 1/3, \beta = 3.3)$
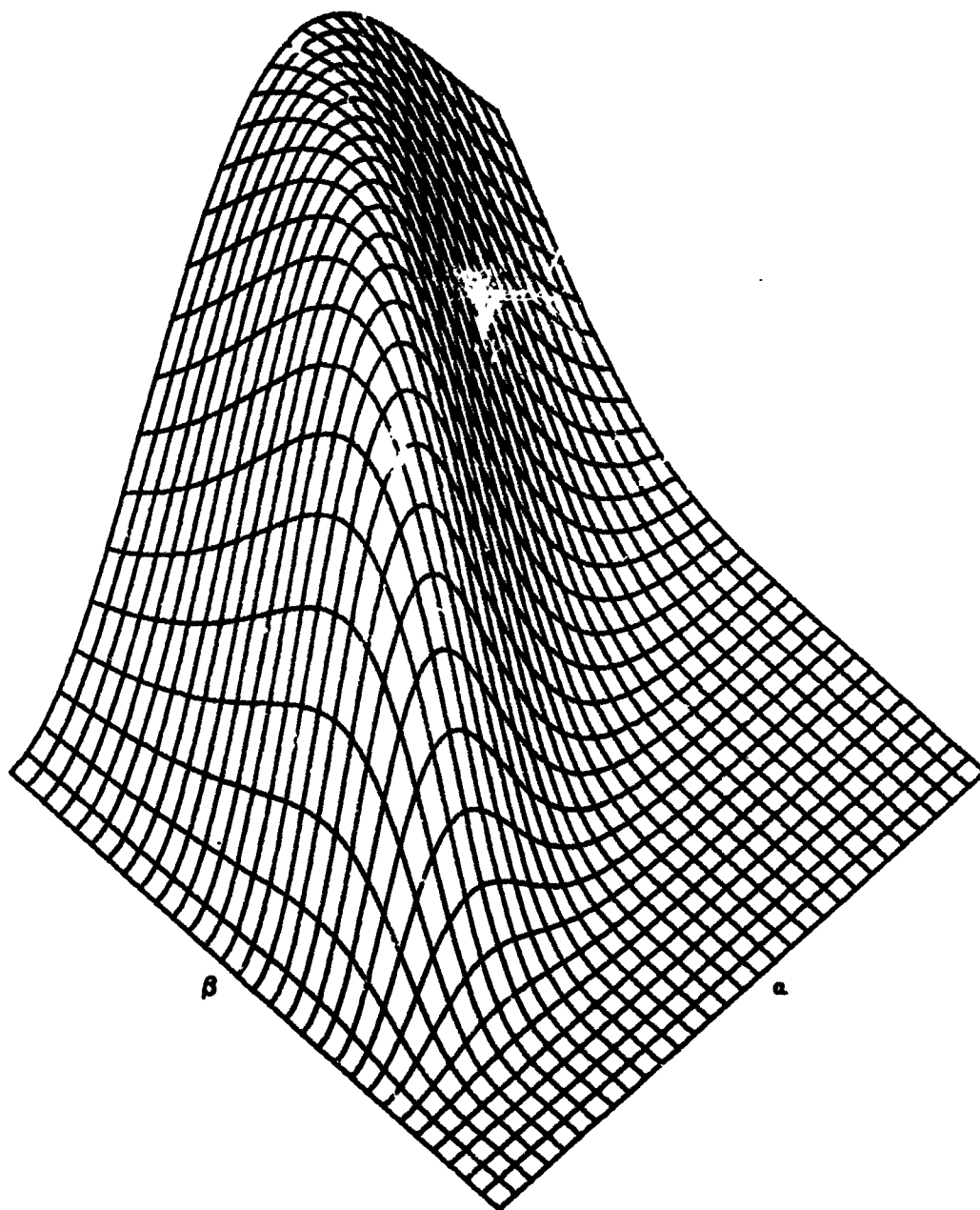
Fig. 42 - V_4 for Gaussian Spatial Correlation
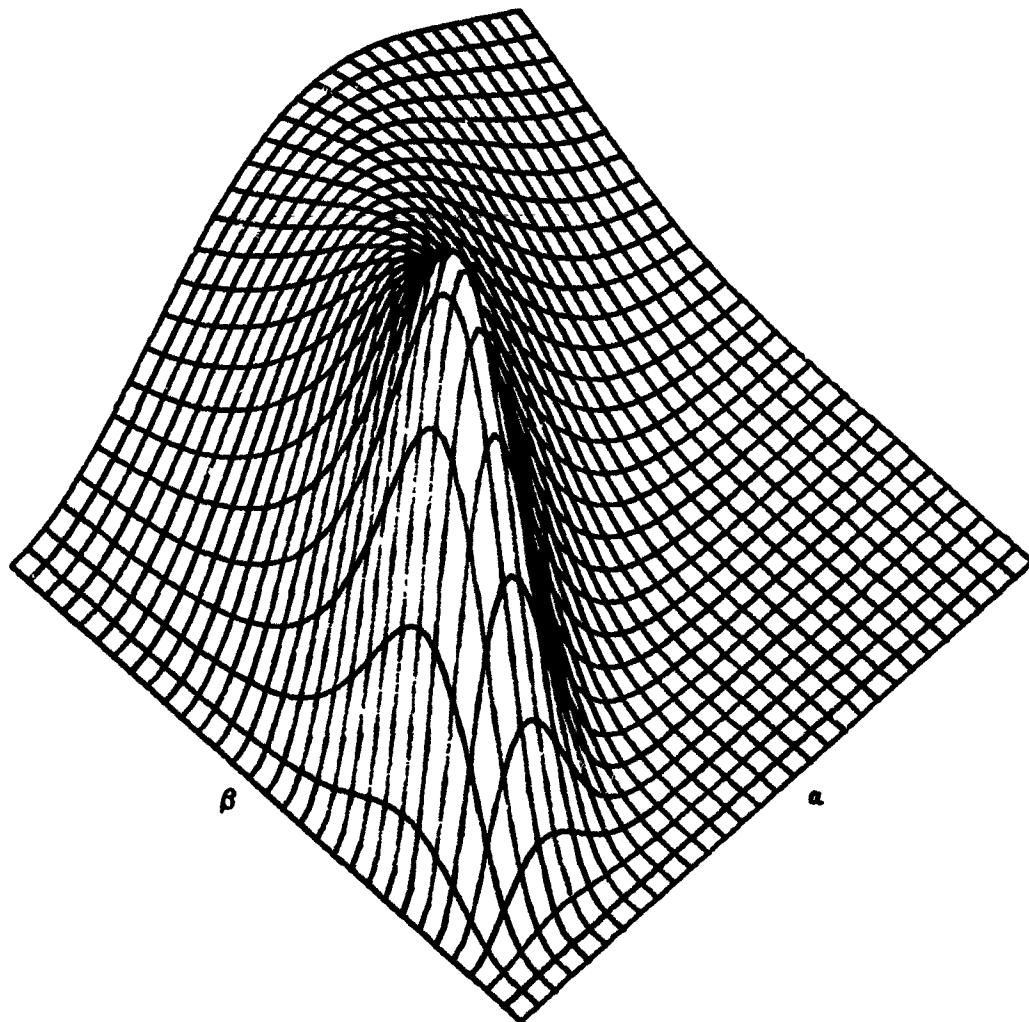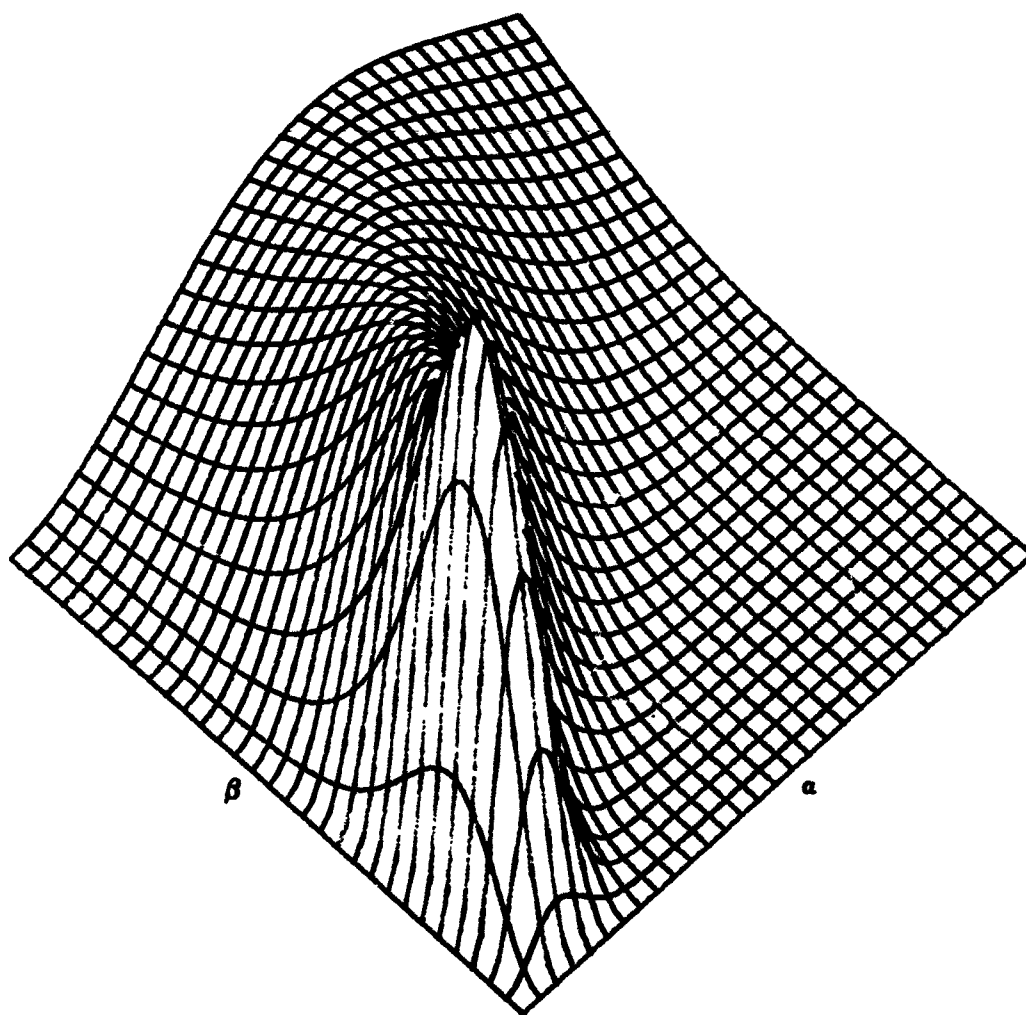
$(V_4 = .683 \cdot 10^{-2}$ at $\alpha = 8, \beta = 4.1)$

power appears in the higher order sidebands. This behavior can occur through either increased β (roughness) or decreased α (correlation distances).

As α approaches zero, for the nonspecular direction, the correlation distances approach zero. For this case, the surface becomes very rough and, in the limit of zero-correlation distances, has the properties of white noise. Although mathematically, for $\alpha = 0$, the amount of scattered energy in the sidebands is zero, the initial assumptions (See Section 1) are violated for small correlation distances; therefore, this portion of the plots does not have physical significance.

Curves of $V_m (\alpha, \beta)$ for $\rho_2 (r) = \exp(-r) \cos(Qr)$, $Q = 1$, were also obtained, but have not been included because they are very similar to the corresponding curves for $\rho_2 (r) = \exp(-r) J_o (Qr)$; in particular, the omitted curves are more peaked than $\exp(-r)$, but not as peaked as $\exp(-r) J_o (4r)$. Similarly, curves of $V_m (\alpha, \beta)$ for $\rho_2 (r) = \exp(-r^2) \cdot \cos(Qr)$, $Q = 1.8482777$,[10] were also obtained and exhibited behavior intermediate to that of $\exp(-r^2)$ and $\exp(-r^2) J_o (4r)$.

Let us now compare the exponentially modulated Bessel function plots with those of the Gaussian modulated Bessel function plots. For large β, the Gaussian case has more power in a given sideband than that of the corresponding exponential case. This behavior is similar to that of the U_m curves in Figs. 7 through 12. For $Q = 0$, the corresponding exponential and Gaussian plots are somewhat dissimilar. However, for $Q = 4$, the corresponding curves of the exponential case are more nearly similar to those of the Gaussian case, whereas for $Q = 8$, the two sets of curves are almost identical. Thus, for small Q, the envelope of the spatial correlation of the heights is the controlling factor, but as Q increases, the number of oscillations per given distance of $J_o (Qr)$ increases, and $J_o (Qr)$ becomes the controlling factor in spatial correlation.

6. DISCUSSION

In summary, an analysis was made of a time-varying random surface statistically stationary in both space and time. The reflected

---

[10]These choices of Q are the largest possible consistent with a nonnegative surface-height spectrum; see Subsection 4.3.

acoustic spectrum was obtained in terms of the first- and second-order characteristic functions of the surface-height variation. For the special case of a Gaussian distribution of surface heights, a narrow-band surface spectrum, and a surface spatial-temporal correlation function that is stationary in the wide sense, the mathematical equation for the received acoustic spectrum showed that the scatter spectrum is composed of spectral lobes, or sidebands, centered at frequencies equal to the acoustic frequency plus multiples of the surface-center frequency (See (47) and (48)). For the special case of a surface spatial correlation that has elliptical contours, the evaluation of the complete spectrum can be expressed as a Fourier transform of a single integral. The complete spectrum was not numerically evaluated in this report, but should be obtained in future work. In addition, the restriction to a symmetric directional wave spectrum, (82), should be eliminated. For example, received spectra for hemispherical directional wave spectra should be computed; this will yield unequal scattered sideband powers.

The power in each sideband was evaluated for a variety of conditions and spatial correlations. It was found that the zeroth and second-order sideband powers had a very similar behavior with surface roughness, whereas the other sidebands had a somewhat different dependence. It has been assumed that there is not an appreciable overlap of the sidebands; for large surface roughness, there would be an appreciable overlap of sidelobes, and the complete spectrum would have to be obtained for this case.

It is worthwhile to discuss the difference between the surface treated in this report and the fixed-amplitude sinusoidal surface considered by Roderick and Cron [7]. We have considered a narrow-band spectrum for the height variation at a point on the surface, and assumed the joint probability density of the surface heights to be Gaussian. As the bandwidth of the surface variation decreases and approaches zero, the properties of this surface process do not approach the fixed-amplitude sinusoidal surface case. For example, the distribution of heights remains Gaussian and is, therefore, different from the probability density associated with a sinusoid. The scattered powers in the sidebands, as given by the narrow-band Gaussian theory, are different from those of the single-frequency sinusoidal theory.

In mathematical terms, the first-order-characteristic function of a fixed-amplitude sinusoid is a Bessel function. If we average this Bessel function with the Rayleigh distribution of sine wave amplitudes, we obtain the Gaussian first-order-characteristic function. Thus, our results can be viewed as a particular average over the sinusoidal surface case.

However, a narrow-band time function with center frequency f_s and bandwidth W resembles a sine wave of frequency f_s over a short period of time, but will differ from a sine wave over a longer period of time. The difference will show up on the order of W^{-1} sec. Thus, if we obtain a short sample of the reflected signal from a narrow-band surface, and determine the received acoustic spectrum from it, the single-frequency theory (with the current surface-height amplitude) should accurately predict that spectrum. However, for a long-time average over the statistical properties of the surface, the narrow-band Gaussian theory, not the fixed-amplitude single-frequency theory, must be used to predict the expected behavior of the spectrum.

This report has concentrated on the spectral quantities of the reflected signal. However, the probability distributions of the envelope of the individual sidebands can also be obtained in at least one important case. If the area of insonification is much larger than the correlation area of the surface (product of correlation distances), we can appeal to the Central Limit Theorem and state that the envelope and phase distributions of the mth component of the received scatter pressure field are Rayleigh and uniform, respectively, for $m \neq 0$. For $m = 0$, the scatter component combined with the coherent component results in a Beckmann distribution [2, Chapter 7]. (Of course, as the coherent component tends to zero, the Beckmann distribution tends to the Rayleigh distribution.) It should be noted that the assumption of Gaussian surface statistics, i.e., $\zeta(x, y, t)$ Gaussian, does not necessarily imply that the received pressure is Gaussian, because the received pressure is obtained via a nonlinear transformation on ζ (See (3)); rather, it is the assumption of a large number of independently reflecting surface portions that yields the Gaussian behavior.

LIST OF REFERENCES

1. C. Eckart, "The Scattering of Sound from the Sea Surface," Journal of the Acoustical Society of America, vol. 25, no. 3, May 1953, pp. 566-570.

2. P. Beckmann and A. Spizzichino, The Scattering of Electromagnetic Waves from Rough Surfaces, The MacMillan Co., New York, 1963.

3. E. O. LaCasce and P. Tamarkin, "Underwater Sound Reflection from a Corrugated Surface," Journal of Applied Physics, vol. 27, 1956, pp. 138-148.

4. C. W. Horton and T. G. Muir, "Theoretical Studies of the Scattering of Acoustic Waves from a Rough Surface," Journal of the Acoustical Society of America, vol. 41, no. 3, March 1967, pp. 627-634.

5. R. J. Wagner, "Shadowing of Randomly Rough Surfaces," Journal of the Acoustical Society of America, vol. 41, no. 1, January 1967, pp. 138-147.

6. H. W. Marsh, "Exact Solution of Wave Scattering by Irregular Surfaces," Journal of the Acoustical Society of America, vol. 33, no. 3, March 1961, pp. 330-333.

7. W. I. Roderick and B. F. Cron, "Frequency Spectra of Forward-Scattered Sound from the Ocean Surface," NUSL* Report No. 1010, 1 July 1969. (Accepted for publication in the September 1970 issue of the Journal of the Acoustical Society of America.)

8. B. E. Parkins, "Scattering from the Time-Varying Surface of the Ocean," Journal of the Acoustical Society of America, vol. 42, no. 6, December 1967, pp. 1262-1267.

9. I. Tolstoy and C. S. Clay, Ocean Acoustics, McGraw-Hill Book Co., New York, 1966.

10. B. Kinsman, Wind Waves, Prentice-Hall, Inc., New York, 1965.

11. I. S. Gradshteyn and I. W. Ryzhik, Table of Integrals, Series, and Products, Academic Press, New York, 1965.

---

*Reports prepared by the New London Laboratory prior to 1 July 1970 bear the Laboratory's earlier acronym NUSL.

12. W. B. Davenport and W. L. Root, _An Introduction to the Theory of Random Signals and Noise_, McGraw-Hill Book Co., New York, 1958.

13. W. J. Pierson, Jr. (editor), _Meteorological Papers_, vol. 2, no. 6, New York University, 1960.

14. W. Magnus and F. Oberhettinger, _Functions of Mathematical Physics_, Chelsea Publishing Co., New York, 1954.

15. Y. L. Luke, _Integrals of Bessel Functions_, McGraw-Hill Book Co., New York, 1962.

16. _Handbook of Mathematical Functions_, U. S. Department of Commerce, National Bureau of Standards, Applied Mathematics Series 55, June 1964.

17. Y. P. Lysanov, "Average Decay Law in a Surface Sound Channel with an Uneven Boundary," _Soviet Physics — Acoustics_, vol. 12, 1967, pp. 425-427.

18. M. Schulkin, _The Propagation of Sound in Imperfect Ocean Surface Ducts_, NUSL Report No. 1013, 22 April 1969.

19. R. J. Urick, _Principles of Underwater Sound for Engineers_, McGraw-Hill Book Co., New York, 1967.

20. A. Papoulis, _The Fourier Integral and Its Applications_, McGraw-Hill Book Co., New York, 1962.

78

Appendix A

GEOMETRY FACTOR

The factor B in (3) is given different values by different authors. For example, the values for B given by Parkins[A1] and Beckmann and Spizzichino,[A2] using the notation in this report, are

$$B = \frac{1 + \vec{u}_Q \cdot \vec{u}_A}{c} = \frac{1 + a_Q a_A + b_Q b_A + c_Q c_A}{c_Q + c_A} \; , \tag{A-1}$$

whereas Eckart[A3] gives the following value for B:

$$B = \frac{c}{2} = \frac{c_Q + c_A}{2} \; . \tag{A-2}$$

Beckmann and Spizzichino[A4] attribute the discrepancy to the replacement of the normal to the surface by a vector in the z-direction, an approximation that is valid only for surfaces with very gentle slopes.

For the specular direction,

$$a_A = -a_Q, \; b_A = -b_Q, \; c_A = c_Q \; , \tag{A-3}$$

both forms for B above become c_Q. Thus, there is no difference in the specular direction. However, there can be significant differences for other cases. For example, the second form for B depends only on the direction cosines with respect to the z-axis, but the first form depends on all direction cosines. Thus, at normal incidence.

$$a_Q = b_Q = 0, \; c_Q = 1 \; , \tag{A-4}$$

[A1]B. E. Parkins, "Scattering from the Time-Varying Surface of the Ocean," Journal of the Acoustical Society of America, vol. 42, no. 6, December 1967, Eq. (10), p. 1263.

[A2]P. Beckmann and A. Spizzichino, The Scattering of Electromagnetic Waves from Rough Surfaces, The Macmillan Co., New York, 1963, Eqs. (11) and (12), p. 27, and Eqs. (29) and (32), pp. 22-23.

[A3]C. Eckart, "The Scattering of Sound from the Sea Surface," Journal of the Acoustical Society of America, vol. 25, no. 3, May 1953, Eq. (6), p. 567.

[A4]Beckmann and Spizzichino, Appendix A, op. cit.

and the two forms for B become

$$1 \text{ and } \tfrac{1}{2}(1+c_A) \quad , \qquad\qquad\qquad (A-5)$$

respectively. For an observation point near grazing, these terms differ by a factor of 2 in pressure.

Rather than attempt to resolve the differences in the scale factor, we have expressed all our quantities in terms of the general symbol B and leave it to the reader to make his choice as to the correct factor. For a fixed geometry, so far as the relative spectral content of the received acoustic waveform is concerned, the exact geometric factor is not important under the assumptions of the present theory.

Appendix B

CORRELATION PROPERTIES OF SINGLE-SIDED PROCESS

Suppose $x(t)$ is a wide-sense stationary single-sided[B1] (complex) process with no dc component. Let

$$x(t) = x_r(t) + i x_i(t) \quad , \qquad (B-1)$$

where

$$x_r(t) = \tfrac{1}{2}[x(t) + x^*(t)] \quad ,$$

$$x_i(t) = \frac{1}{2i}[x(t) - x^*(t)] \quad . \qquad (B-2)$$

Denoting the Hilbert transform by $\mathcal{H}\{\ \}$, we have

$$\mathcal{H}\{x_r(t)\} = \tfrac{1}{2}[\mathcal{H}\{x(t)\} + \mathcal{H}\{x^*(t)\}]$$

$$= \tfrac{1}{2}[-i x(t) + i x^*(t)] = x_i(t) \quad , \qquad (B-3)$$

where the single-sided character of $x(t)$ and its lack of dc has been utilized. The Hilbert transform is represented by a linear network with transfer function $-i\,\mathrm{sgn}(f)$. Therefore, the transformation between $x_r(t)$ and $x_i(t)$ can be represented as in Fig. B-1.
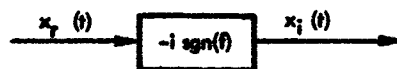
Fig. B-1 - Hilbert Transform

Thus, we have derived the fact that the imaginary part of a wide-sense stationary single-sided process is the Hilbert transform of the real part.[B2] When the properties of linear networks are used, it follows from Fig. B-1 that

---

[B1] Single-sided means that the power density spectrum is confined to positive frequencies.

[B2] This is the converse of the usual situation where a waveform plus i times its Hilbert transform is shown to be single-sided.

81

$$\overline{x_i(t)\, x_i(t-\tau)} = \overline{x_r(t)\, x_r(t-\tau)} \quad,$$

$$\overline{x_r(t)\, x_i(t-\tau)} = \overline{-x_i(t)\, x_r(t-\tau)} \quad. \tag{B-4}$$

Combining these properties, we find that

$$\overline{x(t)\, x(t-\tau)} = 0 \text{ for all } \tau \quad. \tag{B-5}$$

Of course, $\overline{x(t)\, x^*(t-\tau)} \neq 0$.

Appendix C

SCATTERING COEFFICIENT AND SCATTERING STRENGTH

The received (complex) pressure $p(t)$ at the observation point was given in (3). The scatter component $p_s(t)$ was defined in (11), and the mean-square value of $p_s(t)$ was evaluated in (18) and (20). In this appendix, we will relate the scattering coefficient and scattering strength to these quantities.

The average scatter intensity (power/unit area) at the receiver for a real sinusoidal signal transmittal is

$$I_s = \frac{\overline{|p_s(t)|^2}/2}{\rho v} , \qquad (C-1)$$

where ρ is the density of the fluid and v is the propagation velocity.[C1] If the receiver at A subtends a solid angle Ω, as seen from origin O in Fig. 1, the average received scatter power is

$$I_s R_o^2 \Omega , \qquad (C-2)$$

and the average received scatter power per steradian is

$$I_s R_o^2 = \frac{1}{2\rho v} \overline{|p_s(t)|^2} R_o^2 . \qquad (C-3)$$

Since the incident pressure on the surface at x,y is $\hat{p}_i(x, y)$ (See (3)), the incident intensity at x, y is

$$\frac{1}{2\rho v} |\hat{p}_i(x,y)|^2 . \qquad (C-4)$$

Therefore, the total incident power on the surface is

$$c_Q \iint dx\, dy \frac{1}{2\rho v} |\hat{p}_i(x,y)|^2 = \frac{c_Q}{2\rho v} J(0,0) , \qquad (C-5)$$

using (16).

The scattering coefficient or scattering cross section σ_s is defined by Eckart[C2] as

---

[C1] The factor of 1/2 follows in a manner similar to that in (5) and (6).

[C2] C. Eckart, "The Scattering of Sound from the Sea Surface," Journal of the Acoustical Society of America, vol. 25, no. 3, May 1953, Eq. (18), p. 568, and Eq. (10), p. 567.

$$\sigma_s = \frac{\overline{|P_s(t)|^2} \, R_o^2}{J(0,0)} \quad, \tag{C-6}$$

which can be manipulated into the forms

$$\sigma_s = \frac{\overline{|P_s(t)|^2} \, R_o^2}{\iint dx\, dy \, |\hat{p}_i(x,y)|^2} = \frac{I_s R_o^2}{\iint dx\, dy \, \frac{1}{2\rho v} |\hat{p}_i(x,y)|^2}$$

$$= \frac{\text{average received scatter power per steradian}}{\text{incident power on surface} \, / \, c_Q} \quad, \tag{C-7}$$

where we have used (16), (C-3), and (C-5).

For purposes of this report, the "scattering strength" S is defined as[C3]

$$S = \frac{I_{scat}}{I_{inc}} \quad, \tag{C-8}$$

where I_{scat} is the average scatter intensity at the receiver due to unit scattering area, referred to unit distance, and I_{inc} is the average incident intensity on the surface. If we let A_{eff} be the effective area of insonification in the x, y plane (e.g.,

$$A_{eff} = \iint dx\, dy \left| \frac{\hat{p}_i(x,y)}{\hat{p}_i(0,0)} \right|^2 \Big) \quad, \tag{C-9}$$

then

$$I_{scat} = \frac{I_s}{A_{eff}} \, R_o^2 = \frac{\overline{|P_s(t)|^2} \, R_o^2}{2\rho v \, A_{eff}} \quad, \tag{C-10}$$

using (C-1). Also,

$$I_{inc} = \frac{\text{incident power on the surface}}{A_{eff}}$$

$$= \frac{c_Q \, J(0,0)}{2\rho v \, A_{eff}} \quad, \tag{C-11}$$

using (C-5). Taking the ratio of (C-10) and (C-11), we note that the scattering strength becomes

$$S = \frac{\overline{|P_s(t)|^2} \, R_o^2}{c_Q \, J(0,0)} = \frac{\sigma_s}{c_Q} \quad, \tag{C-12}$$

[C3] R. J. Urick, Principles of Underwater Sound for Engineers, McGraw-Hill Book Co., New York, 1967, p. 188, Section 8.2. Actually, Urick has a decibel ratio rather than a linear power ratio.

using (C-6). Thus, the scattering strength equals the scattering coefficient divided by the direction cosine of the incident pressure with respect to the normal to the surface. This latter quantity, σ_s / c_Q, which is exactly what has been recommended by some authors[C4] as preferable to σ_s alone, has been adopted in this report.

Notice that the exact definition of A_{eff} did not enter into S because it cancelled in the ratio (C-8); therefore, (C-9) is merely one possible definition of this quantity. An alternate definition of S, which avoids this quantity altogether, is available upon substitution of (C-7) into (C-12):

$$S = \frac{\text{average received scatter power per steradian}}{\text{incident power on surface}} \quad . \quad (C-13)$$

[C4]C. W. Horton, Sr., and T. G. Muir, "Theoretical Studies of the Scattering Acoustic Waves from a Rough Surface," Journal of the Acoustical Society of America, vol. 41, no. 3, March 1967, Section II.C., p. 630.

Appendix D

COMPLEX ENVELOPE REPRESENTATION OF
NARROW-BAND, SURFACE-HEIGHT-CORRELATION FUNCTION

From (40), the surface-height correlation is

$$\sigma^2 \rho(u, v, \tau) = \overline{\zeta(x, y, t) \; \zeta(x-u, y-v, t-\tau)} \quad . \tag{D-1}$$

These are all real quantities. When the homogeneity and stationarity of the surface is utilized, there follows

$$\rho(-u, -v, -\tau) = \rho(u, v, \tau) \quad . \tag{D-2}$$

We define a normalized cross-spectrum g as the Fourier transform of ρ:

$$g(u, v, f) = \int d\tau \exp(-i2\pi f \tau) \, \rho(u, v, \tau) \quad . \tag{D-3}$$

It is a function of position differences u, v, as well as frequency f, and is neither real nor even in f; however, it is narrow-band. Let us now define the single-sided spectrum as

$$g_+(u, v, f) = \begin{Bmatrix} 2g(u, v, f), \; f > 0 \\ 0, \; f < 0 \end{Bmatrix} \quad , \tag{D-4}$$

and the center frequency of surface variations at a point as

$$f_s = \frac{\int df \, f \, g_+(0, 0, f)}{\int df \, g_+(0, 0, f)} = \frac{\int_0^\infty df \, f \, g(0, 0, f)}{\int_0^\infty df \, g(0, 0, f)} \quad . \tag{D-5}$$

The expression g(0, 0, f) is proportional to the surface-height spectrum at a point; it is real and even because $\rho(0, 0, \tau)$ is real and even. We now shift the single-sided spectrum g_+ down by f_s to get a low-pass spectrum $\underline{g}$ centered about zero frequency:

$$\underline{g}(u, v, f) = g_+(u, v, f + f_s) \quad . \tag{D-6}$$

Then, the Fourier transform of $\underline{g}$ is defined as the complex envelope ϱ:

$$\varrho(u, v, \tau) = \int df \exp(i2\pi f \tau) \, \underline{g}(u, v, \tau)$$

$$= \rho_+(u, v, \tau) \exp(-i2\pi f_s \tau) \quad , \tag{D-7}$$

where we have used (D-6) and defined ρ_+ as the Fourier transform of g_+. Now, using the Fourier transform of the unit step,[D1]

$$\int_0^\infty df \exp(i2\pi f t) = \frac{1}{2}\delta(t) + \frac{i}{2\pi t} \quad , \tag{D-8}$$

[D1]A. Papoulis, The Fourier Integral and Its Applications, McGraw-Hill Book Co., New York, 1962, Eq. (3-13).

ρ_+ can be evaluated from (D-4) as

$$\rho_+(u, v, \tau) = \rho(u, v, \tau) + i\rho_H(u, v, \tau) \quad , \tag{D-9}$$

where ρ_H is the Hilbert transform of ρ:

$$\rho_H(u, v, \tau) = \frac{1}{\pi} \int dw \frac{\rho(u, v, w)}{\tau - w} \quad . \tag{D-10}$$

Combining (D-9) and (D-7), we obtain

$$\rho(u, v, \tau) = \text{Re}\{\rho_+(u, v, \tau)\}$$
$$= \text{Re}\{\varrho(u, v, \tau) \exp(i2\pi f_s \tau)\} \quad , \tag{D-11}$$

which is the property desired in (44).

An additional property of complex envelope ϱ that will be necessary is now derived from (D-10):

$$\rho_H(-u, -v, -\tau) = -\rho_H(u, v, \tau) \quad . \tag{D-12}$$

Substituting into (D-9), we note that

$$\rho_+(-u, -v, -\tau) = \rho_+^*(u, v, \tau) \quad , \tag{D-13}$$

and then from (D-7), we get

$$\varrho(-u, -v, -\tau) = \varrho^*(u, v, \tau) \quad . \tag{D-14}$$

For the special case where $\rho(u, v, \tau)$ is even in τ for all u, v, i.e.,

$$\rho(u, v, -\tau) = \rho(u, v, \tau) \quad , \tag{D-15}$$

$\varrho(u, v, 0)$ is purely real and is given by

$$\varrho(u, v, 0) = \rho(u, v, 0) \quad . \tag{D-16}$$

This may be seen as follows: From (D-10), using the evenness of ρ,

$$\rho_H(u, v, 0) = 0. \tag{D-17}$$

Then, using (D-9) and (D-7), (D-16) follows.

Appendix E

NUMERICAL EVALUATION OF EQ. (112)

In (112), the surface-height spectrum was given in terms of an integral:

$$\hat{\Phi}(x) = |x|^3 \int_0^\infty dt \, t \exp(-t^2) \cos(qt) \, J_0(x^2 t) \quad , \tag{E-1}$$

where $q = Q/R$. To evaluate this integral, we expand $\cos(qt)$ in a power series in t and obtain

$$\hat{\Phi}(x) = |x|^3 \sum_{n=0}^\infty (-1)^n \frac{q^{2n}}{(2n)!} \int_0^\infty dt \, t^{2n+1} \exp(-t^2) \, J_0(x^2 t) \quad . \tag{E-2}$$

The integral in (E-2), from Gradshteyn and Ryzhik,[E1] is

$$\tfrac{1}{2} n! \exp(-x^4/4) \, L_n(x^4/4) \quad , \tag{E-3}$$

where L_n is a Laguerre polynomial. Ther ..ore,

$$\hat{\Phi}(x) = \tfrac{1}{2} |x|^3 \exp(-x^4/4) \sum_{n=0}^\infty (-q^2)^n \frac{n!}{(2n)!} L_n(x^4/4) \quad . \tag{E-4}$$

This series, which can be easily evaluated by using rec·rrence relations on the Laguerre polynomials, is plotted in Fig. 5.

For x near zero, $\hat{\Phi}(x)$ becomes negative if q is made too large. From (E-1), it may be seen that the largest value of q allowed is when

$$\int_0^\infty dt \, t \exp(-t^2) \cos(qt) = 0 \quad . \tag{E-5}$$

That is, from Gradshteyn and Ryzhik,[E2]

$$\tfrac{1}{2} \, _1F_1(1; \tfrac{1}{2}; -\tfrac{1}{4}q^2) = 0 \quad . \tag{E-6}$$

The solution for the smallest value of q satisfying (E-6) is

$$q = \frac{Q}{R} = 1.8482777 \quad . \tag{E-7}$$

Therefore, (112) has been plotted only for Q/R less than this value.

[E1] I. S. Gradshteyn and I. W. Ryzhik, Table of Integrals, Series, and Products, Academic Press, New York, 1965, Eq. 6.631 10.

[E2] Ibid., Eq. 3.952 8.

Appendix F

ERROR ANALYSIS OF EQS. (61) AND (63)

The infinite integral of (61) must be approximated by a finite integral, up to value L, say. In order to determine how large L must be for negligible error, we note that for small x

$$I_m(x) - \delta_{om} \sim \begin{cases} (x/2)^2 & , \quad m = 0 \\[2mm] \quad . \\[2mm] \dfrac{(x/2)^m}{(m!)^2} & , \quad m \geq 1 \end{cases} \quad . \tag{F-1}$$

Therefore, for large values of r,

$$I_m(\beta^2 \rho_2(r)) - \delta_{om} \sim \begin{cases} [\tfrac{1}{2}\beta^2 \rho_2(r)]^2 & , \quad m = 0 \\[2mm] [\tfrac{1}{2}\beta^2 \rho_2(r)]^m \dfrac{1}{(m!)^2} & , \quad m \geq 1 \end{cases} \quad . \tag{F-2}$$

The slowest decaying order is $m = 1$; therefore, the largest error in terminating the integral (61) at L is approximately

$$E = (2\pi)^{-1} \exp(-\beta^2) \int_L^\infty dr \; r \tfrac{1}{2}\beta^2 \rho_2(r) \quad . \tag{F-3}$$

When spatial correlation ρ_2 is an exponential modulation of either a cosine or a Bessel function,

$$\rho_2(r) = \exp(-r) \cos(Qr) \text{ or } \exp(-r) J_o(Qr) \quad , \tag{F-4}$$

(F-3) is upper-bounded by

$$E \leq (2\pi)^{-1} \exp(-\beta^2) \tfrac{1}{2}\beta^2 \int_L^\infty dr \; r \exp(-r)$$

$$= (4\pi)^{-1} \beta^2 \exp(-\beta^2) (L+1) \exp(-L) \quad . \tag{F-5}$$

The largest value of $\beta^2 \exp(-\beta^2)$ occurs at $\beta = 1$, yielding

$$E \leq (4\pi e)^{-1} (L+1) \exp(-L) \quad . \tag{F-6}$$

For $L = 25$, $E \leq 10^{-11}$. The limit 25 was used in evaluating (61) for the exponentially modulated spatial correlation; all the values of U_m in Figs. 7, 8, and 9 are much larger than 10^{-11}.

For a Gaussianly modulated spatial correlation,

$$\rho_2(r) = \exp(-r^2) \cos(Qr) \text{ or } \exp(-r^2) J_o(Qr) \quad ; \tag{F-7}$$

the bound corresponding to (F-6) is

$$E \leq (8\pi e)^{-1} \exp(-L^2) \quad . \tag{F-8}$$

For $L = 5$, $E \leq 2 \times 10^{-13}$. The limit of 5 was used in evaluating (61) for the Gaussianly modulated spatial correlation; all the values of U_m in Figs. 10, 11, and 12 are much larger than 2×10^{-13}.

For integral (63), we can upper-bound the integrand by replacing the Bessel function by unity. The slowest decaying order is again $m = 1$. An analysis similar to that in (F-1) through (F-3) yields, for exponential modulation, the upper bound on the error

$$E \leq (4\pi e)^{-1} a^2 (L+1) \exp(-L) \quad , \tag{F-9}$$

whereas, for Gaussian modulation, the upper bound on the error is given by

$$E \leq (8\pi e)^{-1} a^2 \exp(-L^2) \quad . \tag{F-10}$$

For $L = 25$, (F-9) yields $10^{-11}a^2$; for $L = 5$, (F-10) yields $2 \times 10^{-13}a^2$.

The interval $(0, L)$, used in evaluating (61) and (63), was repeatedly cut in half and evaluated by Simpson's rule until insignificant change occurred in the sum.

DOCUMENT CONTROL DATA - R & D

(Security classification of title, body of abstract a' ' indexing annotation must be entered when the overall report is classified)

1 ORIGINATING ACTIVITY *(Corporate author)*	2a. REPORT SECURITY CLASSIFICATION
New London Laboratory Naval Underwater Systems Center New London, Connecticut 06320	UNCLASSIFIED
	2b GROUP

3 REPORT TITLE

SPECTRUM OF A SIGNAL REFLECTED FROM A TIME-VARYING RANDOM SURFACE

4. DESCRIPTIVE NOTES *(Type of report and inclusive dates)*

Research Report

5 AUTHOR(S) *(First name, middle initial, last name)*

Albert H. Nuttall
Benjamin F. Cron

6 REPORT DATE	7a. TOTAL NO OF PAGES	7b. NO. OF REFS
25 August 1970	103	20

8a. CONTRACT OR GRANT NO.	9a. ORIGINATOR'S REPORT NUMBER(S)
A-041-00-00	
b. PROJECT NO A-055-00-00	NL-3013
ZF XX 112 001	
c. ZR 011 01 01	9b. OTHER REPORT NO(S) *(Any other numbers that may be assigned this report)*
d.	

10 DISTRIBUTION STATEMENT

This document has been approved for public release and sale; its distribution
is unlimited.

11. SUPPLEMENTARY NOTES	12. SPONSORING MILITARY ACTIVITY
	Department of the Navy

13 ABSTRACT

The power density spectrum of the received acoustic waveform after reflection off
the time-varying random sea surface is evaluated at an arbitrary observation point in
the farfield. For a monochromatic transmitted signal and a narrow-band Gaussian
surface-height variation, the received acoustic spectrum is shown to consist of an
impulse at the transmitted acoustic frequency plus sidelobes centered at frequencies
separated from the transmitted frequency by multiples of the surface center frequency.
The powers in the coherent component and scattered sideband components of the
received pressure waveform are evaluated in terms of the surface roughness and
spatial-temporal correlation function of the surface. For the special case of elliptical
contours of iso-correlation at zero time delay, the sideband powers and scattering
strengths are evaluated in terms of two fundamental parameters that include the
geometry of the experiment, the incident acoustic frequency, the root mean square
(rms) surface height, and the surface correlation distances.

The rms bandwidths of the sideband scatter components are evaluated for small
surface roughness and shown to be approximately proportional to the square root of
the sideband number. Numerous examples of sideband scattering strengths for a
variety of spatial correlation functions, including exponential and Gaussian decay as
special cases, are given.

DD FORM 1473 (PAGE 1)
1 NOV 66

S/N 0102-014-6600

14 KEY WORDS	LINK A		LINK B		LINK C	
	ROLE	WT	ROLE	WT	ROLE	WT
Exponentially Modulated Bessel Function Spatial Correlation						
Exponentially Modulated Cosine Spatial Correlation						
Gaussianly Modulated Bessel Function Spatial Correlation						
Gaussianly Modulated Cosine Spatial Correlation						
Monochromatic Transmitted Signal						
Time-Varying Random Surface						

DD FORM 1473 (BACK)
(PAGE 2)